NAVAL POSTGRADUATE SCHOOL
Monterey, California

THESIS

RANDOM WAVE ANALYSIS OF SHIP/RAMP/BARGE
RESPONSE

by

Dimitrios S. Konstantinou

September 2000

Thesis Advisor: Fotis A. Papoulias

Approved for public release; distribution is unlimited.

REPORT DOCUMENTATION PAGE		*Form Approved* *OMB No. 0704-0188*

Public reporting burden for this collection of information is estimated to average 1 hour per response, including the time for reviewing instruction, searching existing data sources, gathering and maintaining the data needed, and completing and reviewing the collection of information. Send comments regarding this burden estimate or any other aspect of this collection of information, including suggestions for reducing this burden, to Washington headquarters Services, Directorate for Information Operations and Reports, 1215 Jefferson Davis Highway, Suite 1204, Arlington, VA 22202-4302, and to the Office of Management and Budget, Paperwork Reduction Project (0704-0188) Washington DC 20503.

1. AGENCY USE ONLY *(Leave blank)*	2. REPORT DATE September 2000	3. REPORT TYPE AND DATES COVERED Master's Thesis	
4. TITLE AND SUBTITLE: RANDOM WAVE ANALYSIS OF SHIP/RAMP/BARGE RESPONSE		5. FUNDING NUMBERS	
6. AUTHOR(S) **Dimitrios Konstantinou**			
7. PERFORMING ORGANIZATION NAME(S) AND ADDRESS(ES) Naval Postgraduate School Monterey, CA 93943-5000		8. PERFORMING ORGANIZATION REPORT NUMBER	
9. SPONSORING / MONITORING AGENCY NAME(S) AND ADDRESS(ES) N/A		10. SPONSORING /MONITORING AGENCY REPORT NUMBER	

11. SUPPLEMENTARY NOTES
The views expressed in this thesis are those of the author and do not reflect the official policy or position of the Department of Defense or the U.S. Government.

12a. DISTRIBUTION / AVAILABILITY STATEMENT Approved for public release; distribution is unlimited.	12b. DISTRIBUTION CODE

13. ABSTRACT *(maximum 200 words)*

A mathematical model describing the fundamental physics of a ship/ramp/barge system, including a passive isolator, is developed. The model properly accounts for hydrodynamic proximity effects and structural coupling between the bodies. A standard second order model is used, for demonstration purposes, in order to model the frequency response properties of the connecting body. Parametric studies of the response amplitude operator of the ramp motion are performed for varying wave directions and isolator stiffness and damping. These are utilized for the random wave analysis in standard fully developed seas. The results indicate that rational selection of isolator properties can result in significant reduction of motions and stress levels in the connecting ramp.

14. SUBJECT TERMS Hydrodynamic Modeling, Roll-On, Roll-Off, Hydrodynamic Interactions, Wamit Program Solver.			15. NUMBER OF PAGES 142
			16. PRICE CODE
17. SECURITY CLASSIFICATION OF REPORT Unclassified	18. SECURITY CLASSIFICATION OF THIS PAGE Unclassified	19. SECURITY CLASSIFICATION OF ABSTRACT Unclassified	20. LIMITATION OF ABSTRACT UL

NSN 7540-01-280-5500

Standard Form 298 (Rev. 2-89)
Prescribed by ANSI Std. 239-18

THIS PAGE INTENTIONALLY LEFT BLANK

RANDOM WAVE ANALYSIS OF SHIP/RAMP/BARGE RESPONSE

Dimitrios S. Konstantinou
Lieutenant, Hellenic Navy
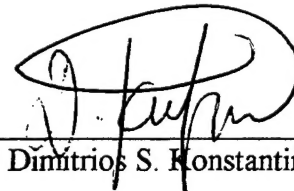Hellenic Naval Academy, 1989

Submitted in partial fulfillment of the
requirements for the degree of

MASTER OF SCIENCE IN MECHANICAL ENGINEERING

from the
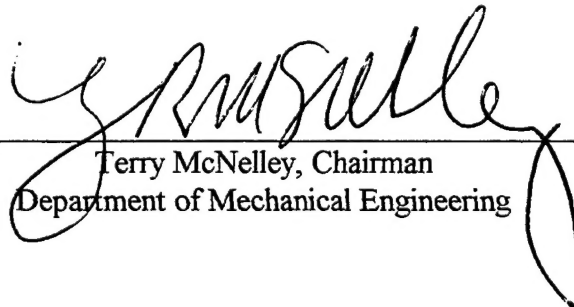
NAVAL POSTGRADUATE SCHOOL
September 2000

Author: _____
Dimitrios S. Konstantinou

Approved by: _____
Fotis A. Papoulias, Thesis Advisor

_____
Terry McNelley, Chairman
Department of Mechanical Engineering

iii

THIS PAGE INTENTIONALLY LEFT BLANK

ABSTRACT

A mathematical model describing the fundamental physics of a ship/ramp/barge system, including a passive isolator, is developed. The model properly accounts for hydrodynamic proximity effects and structural coupling between the bodies. A standard second order model is used, for demonstration purposes, in order to model the frequency response properties of the connecting body. Parametric studies of the response amplitude operator of the ramp motion are performed for varying wave directions and isolator stiffness and damping. These are utilized for the random wave analysis in standard fully developed seas. The results indicate that rational selection of isolator properties can result in significant reduction of motions and stress levels in the connecting ramp.

THIS PAGE INTENTIONALLY LEFT BLANK

TABLE OF CONTENTS

THIS PAGE INTENTIONALLY LEFT BLANK

ACKNOWLEDGMENTS

The author would like to thank Professor Fotis A. Papoulias for all of his guidance, patience and assistance while this thesis was completed. The author would also like to thank his wife Dora, and his little daughter Efremia-Georgia for all of their patience and understanding.

THIS PAGE INTENTIONALLY LEFT BLANK

I. INTRODUCTION

Over the past several years, the types of missions faced by the military have changed dramatically. Although the possibility of large, long-term military operations in a particular area still exists, the emphasis of modern military missions is on the rapid deployment of large numbers of troops and equipment for relatively short periods. These developments have led to an increased need of providing portable warehouse capability that can be pre-positioned and/or be moved to a particular location quickly. Therefore, it is becoming more important to be able to discharge supplies from ships to the shore without a readily available port facility. In order to accomplish this, it is desired that cargo and equipment be able to transfer quickly between oceangoing cargo ships and a floating base (barge), and between the base and military vessels involved in the mission, sometimes in undesirable weather and sea conditions.

The increased use of cargo ships with roll on / roll off (RO/RO) cargo handling capability through the use of ramps has become a common means of rapidly transferring cargo. However, the procedure of loading and unloading cargo from a ship to a roll on /roll off discharge facility (RRDF) through a ramp in the open sea is not a simple one since it is often subject to overloading of the pinned connections, used to mount the ramp on the ship and barge, beyond their design limitations. In order to be able to come up with a method to minimize the forces acting on these connections sufficiently, first of all we have to accurately model the motions of the two vessels floating in proximity (ship & barge), and the hydrodynamic forces acting on them.

1

The Linearized Equations of Motion for both vessels were developed after defining the governing equations of motion for a single unrestrained vessel in sinusoidal waves, as presented in detail in [Ref 1]. These are six coupled, linear equations for the six unknown complex amplitudes.

The previous work done is included in [Ref 3] through [Ref 5]. The main observations made there were the following:

1. Ship motion is practically unaffected by the barge and therefore can be considered uncoupled.

2. Large number of panels may be required to avoid numerical high frequency oscillations.

3. A 2-D program solver based on strip theory can be utilized to model the ship hydrodynamics.

4. Strong port/starboard asymmetry was observed on barge motions due to ship sheltering.

These observations provided the starting ground for the current work.

In Chapter II, we formulate the problem of the two vessels floating in proximity and being connected through a ramp. Seakeeping equations of motions are typically written in the frequency domain. Added mass, damping matrices, and exciting force/moment vectors are based on WAMIT, a 3-D analysis program (Wave Analysis MIT) based on potential theory. Matching conditions between ship/RRDF and the ramp are based on the frequency response characteristics of the ramp (synthesis model). Passive isolator properties are to be selected based on a minimization criterion in random seas.

2

In Chapter III, we present the Regular Wave Results in terms of the absolute vertical motion at the Ramp/Barge connection point. Other responses, such as ramp relative motion or induced mid-point stress, can be employed. The Response Amplitude Operator (RAO) is parametrized in terms of isolator properties. A simple second order model is used for demonstration purposes to model the structural rigidity of the ramp.

In Chapter IV, after a short description of the seaway and a brief discussion about the statistical properties of random waves and the fully developed Pierson-Moscowitz seas, we present the random wave results in terms of normalized significant amplitudes. Finally, conclusions from this thesis and some recommendations for further work are given in Chapter V.

THIS PAGE INTENTIONALLY LEFT BLANK

II.   PROBLEM FORMULATION

A.   OUTLINE

The connection between the ship and the barge is accomplished through a ramp. There are two connection points mounting the ramp to the ship and barge. These points where the ramp is attached to the ship and barge exhibit induced forces on the corresponding locations. In the case of a very narrow ramp, modeled as a beam, there is one connection point for the ship and one for the barge. If the ramp is modeled as a plate, there are a total of four independent connection points and forces. The purpose of this chapter is to develop an efficient and accurate model for the prediction of these forces and their effect on ship motions.

B.   SHIP MOTIONS IN WAVES

A subject of great concern is the effect suffered by a ship in the presence of sea waves. The most common responses of concern are ship motions and structural loading. In the simplest case it may be assumed that the waves incident upon the body are plane progressive waves of small amplitude, with sinusoidal time dependence. Ship motions are assumed to be sufficiently small so that linear theory holds. The results that are obtained in regular sea waves are not without physical interest. However, their practical value might be questioned given the highly irregular nature of actual waves in the sea. Fortunately, the statistical description of the seaway, which will be explained in more detail in the next chapter, makes the study of ship motions in irregular seas a rather straight forward extension of the regular waves case.

In the problem to be formulated here, a single vessel (rigid floating body) will move in response to the sea waves, in general, with six degrees of freedom. The motions are defined in terms of a right-hand coordinate system, with x forward, y to port, and z upward. The origin can be somewhat arbitrary, but in order to keep things simple we will use a point in the waterline (z=0), on centerline at the longitudinal center of gravity (which is also the longitudinal center of buoyancy for a freely floating body) as the origin. We define three translational motions parallel to x, y, z directions as *surge, sway,* and *heave,* and three rotational motions about the same axes as *roll, pitch,* and *yaw* respectively. The six modes of motion are therefore:

η_1 = surge = translation in x-direction

η_2 = sway = translation in y-direction

η_3 = heave = translation in z-direction

η_4 = roll = rotation about x-axis

η_5 = pitch = rotation about y-axis

η_6 = yaw = rotation about z-axis.

Accepting that in general, the hydrodynamic properties of a rigid floating body are modeled as a spring-mass-damper system, the equations of motion for the vessel are written as six simultaneous linear equations in the frequency domain:

$$\sum_{k=1}^{6}\left[-\omega_e^2\ M_{jk}+A_{jk}\ +i\omega_e B_{jk}+C_{jk}\right]\overline{\eta}_k = F_j^H \qquad (1)$$

The A_{jk} terms are called hydrodynamic added mass. These terms are in phase with vertical accelerations, and physically A_{jk} represents the force component in the j-th mode of

6

motion due to the acceleration in the k-th mode of motion. The B_{jk} terms correspond to hydrodynamic damping in phase with vertical velocity, and physically B_{jk} represents the force component in the j-th mode of motion due to the velocity in the k-th mode of motion. Terms involving the coefficients C_{jk} are the restoring forces and moments representing the net hydrostatic buoyancy effects of the ship motions and similarly. C_{jk} is the hydrostatic restoring force coefficient in j-th direction due to k-th motion. The F_j^H terms represent the hydrodynamic wave exciting forces and moments and are usually subdivided into two components according to the following equation:

$$F_j^H = F_j^I + F_j^D \qquad (2)$$

The F_j^I terms are the complex amplitudes of the wave exciting forces and moments due to incident waves, also known as *Froude-Krylov* excitations. The Froude-Krylov excitations represent the integration of the pressure over the body surface that would exist in the incident wave system if the body were not present. The F_j^D terms are the complex amplitudes of the wave exciting forces and moments due to diffracted waves. The diffraction exciting forces and moments are caused by the diffraction or modification of the incident waves due to the presence of the vessel. The Froude-Krylov forces and moments are sometimes used to approximate the total exciting forces, and this is a considerably simpler task than diffraction force computations. This is a good approximation if the wavelength is much larger than the vessel length, such as in the case of a small underwater vehicle in waves. For shorter wavelengths the approximation is

7

increasingly inaccurate because the diffraction force becomes significant. For short waves the diffraction force may become approximately one-half of the total exciting force.

The determination of the above coefficients and exciting forces and moments amplitudes represents the major problem in ship motion calculations. The problem can be simplified by utilizing advanced computational techniques such as strip theory or full three-dimensional (WAMIT) program solvers. In this study we utilized results obtained from WAMIT, an extensive comparison between 3-D and 2-D solvers has been presented in [Ref 5] and will not be discussed here.

In matrix form, equations (1) become:

$$\left[C - \omega^2 \; M + A \; + i\omega B \right] \eta = F \tag{3}$$

where C is the hydrostatic coefficient matrix, M is the mass/inertia matrix, A is the hydrodynamic added mass/inertia matrix, B is the hydrodynamic damping matrix, F is the hydrodynamic excitation force/moment vector, and η is the solution (motion) vector.

According to linear theory, the harmonic responses of the vessel $\eta_j(t)$ will be proportional to the amplitude of the exciting forces and at the same frequency ω. Consequently, the ship motions will have the form:

$$\eta_j(t) = \overline{\eta}_j e^{i\omega t}$$

$$\dot{\eta}_j(t) = i\omega \overline{\eta}_j e^{i\omega t} \; , \qquad j = 1,2,\ldots,6 \tag{4}$$

$$\ddot{\eta}_j(t) = -\omega^2 \overline{\eta}_j e^{i\omega t} ,$$

where $\overline{\eta}_j$ is the corresponding complex response amplitude.

The three principal motions that affect vertical motions are heave, roll, and pitch only (ie. $j = 3,4,5$). Solving equations (1) for the three relevant motions to this problem, the equations of motion can be written as:

$$Heave: \quad \overline{A}_{33}\overline{\eta}_3 + \overline{A}_{35}\overline{\eta}_5 = F_3^H \tag{5}$$

$$Roll: \quad \overline{A}_{44}\overline{\eta}_4 = F_4^H \tag{6}$$

$$Pitch: \quad \overline{A}_{53}\overline{\eta}_3 + \overline{A}_{55}\overline{\eta}_5 = F_5^H \tag{7}$$

where the $\overline{A}_{jk}$ terms correspond to the hydrodynamic effects of the ship on to itself, the $\overline{\eta}$ terms denote the complex amplitudes in heave, roll, and pitch, and the F_j^H terms denote the complex amplitudes of the corresponding wave excitation forces and moments. The $\overline{A}_{jk}$ terms are given by the following set of equations:

$$\overline{A}_{33} = -\omega^2(m + A_{33}) + i\omega B_{33} + C_{33} \tag{8}$$

$$\overline{A}_{35} = -\omega^2(-mx_G + A_{35}) + i\omega B_{35} + C_{35} \tag{9}$$

$$\overline{A}_{44} = -\omega^2(I_{44} + A_{44}) + i\omega B_{44} + C_{44} \tag{10}$$

$$\overline{A}_{53} = -\omega^2(-mx_G + A_{53}) + i\omega B_{53} + C_{53} \tag{11}$$

$$\overline{A}_{55} = -\omega^2(I_{55} + A_{55}) + i\omega B_{55} + C_{55} \tag{12}$$

where A_{jk} are the hydrodynamic added mass terms, B_{jk} are the hydrodynamic damping terms, C_{jk} are the hydrostatic restoring terms, and ω is the frequency of the incoming wave. All of these parameters are functions of the frequency of motion ω. This frequency is the same as the wave excitation frequency. Frequency shifting (i.e., Doppler) effects are not considered since both bodies are at rest.

9

Since we are considering vertical plane motions only, the main effect upon the vessel movement would be in the vertical direction. Therefore, the absolute vertical motion of the vessel at a given point is:

$$\xi = \overline{\eta_3} + \overline{\eta_4}y - \overline{\eta_5}x \qquad (13)$$

where ξ is the complex local amplitude of the vertical motion of the given point and x and y are its coordinates on the body fixed frame.

C.   SHIP AND BARGE EQUATIONS OF MOTION

Equations (5), (6), (7) hold for a single floating body in the open sea, without the existence of any other objects in the close vicinity. In our case, the ship and barge are floating close to one another and therefore there will exist a radiative effect between them. This results from waves striking one vessel, bouncing off its hull and then striking the other vessel alongside. These reflected waves affect heave, roll, and pitch of the adjacent vessel. These hydrodynamic proximity effects can be modeled by modifying the hydrodynamic added mass and damping coefficients, and by utilizing hydrodynamic influence coefficients. These represent the force on one body due to a unit acceleration or velocity of the neighboring body. If we also take into account the ramp connection forces, the equations of motion for the ship and barge will be of the form:

1. Ship Equations of Motion

$$\textit{Heave:} \quad \overline{A}_{33,S}\overline{\eta}_{3,S} + \overline{A}_{35,S}\overline{\eta}_{5,S} + \overline{B}_{33,B}\overline{\eta}_{3,B} + \overline{B}_{34,B}\overline{\eta}_{4,B} + \overline{B}_{35,B}\overline{\eta}_{5,B} = F_{3,S}^{H} + f_S \qquad (14)$$

$$\textit{Roll:} \quad \overline{A}_{44,S}\overline{\eta}_{4,S} + \overline{B}_{43,B}\overline{\eta}_{3,B} + \overline{B}_{44,B}\overline{\eta}_{4,B} + \overline{B}_{45,B}\overline{\eta}_{5,B} = F_{4,S}^{H} + f_S y_S \qquad (15)$$

$$\textit{Pitch:} \quad \overline{A}_{53,S}\overline{\eta}_{3,S} + \overline{A}_{55,S}\overline{\eta}_{5,S} + \overline{B}_{53,B}\overline{\eta}_{3,B} + \overline{B}_{54,B}\overline{\eta}_{4,B} + \overline{B}_{55,B}\overline{\eta}_{5,B} = F_{5,S}^{H} - f_S x_S \qquad (16)$$

10

The above equations are written in standard sea-keeping convention where index 3 corresponds to heave (vertical motion), 4 to roll (rotational with respect to the ship's longitudinal axis), and 5 to pitch (rotational with respect to the ship's lateral axis). Subscript S corresponds to the ship and B to the barge. The $\bar{\eta}$ terms denote the complex amplitudes in heave, roll, and pitch of the ship; ie.,

$$\text{Heave:} \qquad \eta_3(t) = \bar{\eta}_3 e^{i\omega t} \tag{17}$$

$$\text{Roll:} \qquad \eta_4(t) = \bar{\eta}_4 e^{i\omega t} \tag{18}$$

$$\text{Pitch:} \qquad \eta_5(t) = \bar{\eta}_5 e^{i\omega t} \tag{19}$$

where ω is the frequency of the incoming wave. The $\bar{A}$ terms correspond to the hydrodynamic effects of the ship onto itself, while the $\bar{B}$ terms model the influence of the barge onto the ship due to the fact that they are floating in close proximity to one another. The f_S term represents the ship-ramp connection force, and the terms x_S and y_S are the coordinates of the ship-ramp connection point with respect to the ship's midpoint.

Since the ship is significantly larger than the barge, we can neglect the hydrodynamic influence coefficients as well as the connection force f_S on ship motions. In such a case the equations of motion for the ship can be reduced to:

$$\text{Heave:} \quad \bar{A}_{33,S}\bar{\eta}_{3,S} + \bar{A}_{35,S}\bar{\eta}_{5,S} = F_{3,S}^H \tag{20}$$

$$\text{Roll:} \quad \bar{A}_{44,S}\bar{\eta}_{4,S} = F_{4,S}^H \tag{21}$$

$$\text{Pitch:} \quad \bar{A}_{53,S}\bar{\eta}_{3,S} + \bar{A}_{55,S}\bar{\eta}_{5,S} = F_{5,S}^H \tag{22}$$

11

The validity of this approach has been confirmed repeatedly, and typical results are presented in [Ref 5].

We can then solve the above equations for the $\overline{\eta}$ terms for the ship and get:

$$\overline{\eta}_{3,S} = \frac{F_{3,S}^H \overline{A}_{55,S} - F_{5,S}^H \overline{A}_{35,S}}{\overline{A}_{33,S} \overline{A}_{55,S} - \overline{A}_{35,S} \overline{A}_{53,S}} \tag{23}$$

$$\overline{\eta}_{4,S} = \frac{F_{4,S}^H}{\overline{A}_{44,S}} \tag{24}$$

$$\overline{\eta}_{5,S} = \frac{F_{5,S}^H - \overline{A}_{53,S} \overline{\eta}_{3,S}}{\overline{A}_{55,S}} \tag{25}$$

Once the $\overline{\eta}$ terms for the ship are found, the vertical displacement at the ship-ramp connection point (ξ_S) can be determined from the equation:

$$\xi_S = \overline{\eta}_{3,S} + y_S \overline{\eta}_{4,S} - x_S \overline{\eta}_{5,S} \tag{26}$$

2. Barge Equations of Motion

Similarly to the ship, the equations of motion for the barge will be written as:

Heave: $\overline{A}_{33,B} \overline{\eta}_{3,B} + \overline{A}_{35,B} \overline{\eta}_{5,B} + \overline{B}_{33,S} \overline{\eta}_{3,S} + \overline{B}_{34,S} \overline{\eta}_{4,S} + \overline{B}_{35,S} \overline{\eta}_{5,S} = F_{3,B}^H + f_B$ (27)

Roll: $\overline{A}_{44,B} \overline{\eta}_{4,B} + \overline{B}_{43,S} \overline{\eta}_{3,S} + \overline{B}_{44,S} \overline{\eta}_{4,S} + \overline{B}_{45,S} \overline{\eta}_{5,S} = F_{4,B}^H + y_B f_B$ (28)

Pitch: $\overline{A}_{53,B} \overline{\eta}_{3,B} + \overline{A}_{55,B} \overline{\eta}_{5,B} + \overline{B}_{53,S} \overline{\eta}_{3,S} + \overline{B}_{54,S} \overline{\eta}_{4,S} + \overline{B}_{55,S} \overline{\eta}_{5,S} = F_{5,B}^H - x_B f_B$ (29)

The $\overline{A}$ terms correspond to the hydrodynamic effects of the barge onto itself, while the $\overline{B}$ terms model the influence of the ship onto the barge due to the fact that they are floating in close proximity to one another. The influence terms $\overline{B}$ here cannot be neglected and are given from:

12

$$\overline{B}_{ij} = -\omega^2 D_{ij} + i\omega E_{ij} \qquad (30)$$

where D_{ij} are the hydrodynamic added mass influence coefficients, and E_{ij} are the hydrodynamic damping influence coefficients. These parameters, like the A_{jk}, and the B_{jk} parameters, are functions of the frequency of motion ω. The $\overline{\eta}$ terms here denote the complex amplitudes in heave, roll and pitch of the barge. The right hand side of the barge equations of motion contains the hydrodynamic wave exciting forces and moments $F_{j,B}^H$ and the barge-ramp connection force f_B. The terms x_B and y_B are the coordinates of the barge-ramp connection point with respect to the barge midpoint. The hydrodynamic forces F_j^H, both for the ship and barge, are computed as functions of ω and the wave direction (heading). All of the $\overline{\eta}$ terms in the above equations as well as the f_B term are unknown.

The vertical displacement at the barge-ramp connection point (ξ_B) can similarly be defined from the equation:

$$\xi_B = \overline{\eta}_{3,B} + y_B \overline{\eta}_{4,B} - x_B \overline{\eta}_{5,B} \qquad (31)$$

Solving then the hydrodynamic equations of motion for the barge ((27) through (29)) for $\overline{\eta}_{3,B}$, $\overline{\eta}_{4,B}$, and $\overline{\eta}_{5,B}$, and utilizing equation (31), we can express ξ_B in terms of the ramp-barge connection force f_B as:

$$\xi_B = \xi_{B_o} + \xi_{B_f} f_B \qquad (32)$$

where the coefficients ξ_{B_o} and ξ_{B_f} can separately be determined using the principle of superposition as follows:

13

(i) Determination of ξ_{B_o}:

Assuming that $f_B = 0$ and defining the following coefficients as:

$$F_{3,B} = F_{3,B}^H - \overline{B}_{33,S}\,\overline{\eta}_{3,S} - \overline{B}_{34,S}\,\overline{\eta}_{4,S} - \overline{B}_{35,S}\,\overline{\eta}_{5,S} \qquad (33)$$

$$F_{4,B} = F_{4,B}^H - \overline{B}_{43,S}\,\overline{\eta}_{3,S} - \overline{B}_{44,S}\,\overline{\eta}_{4,S} - \overline{B}_{45,S}\,\overline{\eta}_{5,S} \qquad (34)$$

$$F_{5,B} = F_{5,B}^H - \overline{B}_{53,S}\,\overline{\eta}_{3,S} - \overline{B}_{54,S}\,\overline{\eta}_{4,S} - \overline{B}_{55,S}\,\overline{\eta}_{5,S} \qquad (35)$$

the equations of motion for the barge become:

$$\overline{A}_{33,B}\,\overline{\eta}_{3,B} + \overline{A}_{35,B}\,\overline{\eta}_{5,B} = F_{3,B} \qquad (36)$$

$$\overline{A}_{44,B}\,\overline{\eta}_{4,B} = F_{4,B} \qquad (37)$$

$$\overline{A}_{53,B}\,\overline{\eta}_{3,B} + \overline{A}_{55,B}\,\overline{\eta}_{5,B} = F_{5,B} \qquad (38)$$

Solving the above for the $\overline{\eta}$ terms we get:

$$\overline{\eta}_{3,B} = \frac{F_{3,B}\,\overline{A}_{55,B} - F_{5,B}\,\overline{A}_{35,B}}{\overline{A}_{33,B}\,\overline{A}_{55,B} - \overline{A}_{35,B}\,\overline{A}_{53,B}} \qquad (39)$$

$$\overline{\eta}_{4,B} = \frac{F_{4,B}}{\overline{A}_{44,B}} \qquad (40)$$

$$\overline{\eta}_{5,B} = \frac{F_{5,B} - \overline{A}_{53,B}\,\overline{\eta}_{3,B}}{\overline{A}_{5,B}} \qquad (41)$$

Then substituting in equation (31):

$$\xi_{B_o} = \overline{\eta}_{3,B} + y_B\,\overline{\eta}_{4,B} - x_B\,\overline{\eta}_{5,B} \qquad (42)$$

14

(ii) Determination of ξ_{B_f}:

Assuming now that $f_B = 1$ and neglecting the hydrodynamic forces and moments as well as the ship influence, the equations of motion for the barge become:

$$\overline{A}_{33,B}\overline{\eta}_{3,B} + \overline{A}_{35,B}\overline{\eta}_{5,B} = 1 \tag{43}$$

$$\overline{A}_{44,B}\overline{\eta}_{4,B} = y_B \tag{44}$$

$$\overline{A}_{53,B}\overline{\eta}_{3,B} + \overline{A}_{55,B}\overline{\eta}_{5,B} = -x_B \tag{45}$$

Solving again for the $\overline{\eta}$ terms we get:

$$\overline{\eta}_{3,B} = \frac{\overline{A}_{55,B} + x_B \overline{A}_{35,B}}{\overline{A}_{33,B}\overline{A}_{55,B} - \overline{A}_{35,B}\overline{A}_{53,B}} \tag{46}$$

$$\overline{\eta}_{4,B} = \frac{y_B}{\overline{A}_{44,B}} \tag{47}$$

$$\overline{\eta}_{5,B} = -\frac{x_B + \overline{A}_{53,B}\overline{\eta}_{3,B}}{\overline{A}_{55,B}} \tag{48}$$

Then substituting again in equation (31):

$$\xi_{B_f} = \overline{\eta}_{3,B} + y_B\overline{\eta}_{4,B} - x_B\overline{\eta}_{5,B} \tag{49}$$

D.   RAMP MODELING

After defining the governing equations that would model the motion of each vessel, a free-body diagram was produced of the ramp. In this diagram we assumed that there is one simple pinned connection mounting the ramp to the ship and we modeled the other connection between the ramp and the barge as a spring-damper connection.

15

Each connection produces a vertical displacement defined as ξ_S and ξ_B respectively. Consider the ramp as a simply supported beam of total mass m_b and uniform properties through its length. A concentrated mass M is located at mid-span and ξ_l is the vertical displacement at that end of the ramp where the ramp-barge connection is located. The vertical displacements at the two ends of the ramp, ξ_S and ξ_l, can be modeled as the input and the response respectively of a typical system described in the frequency domain by the following equation:

$$\xi_l = G(S)\xi_S \qquad (50)$$

Here G represents the transfer function between the input ξ_S and the output ξ_l. As an example, in the case of a standard second order system, we have [Ref 6]:

$$G(S) = \frac{\omega_n^2}{S^2 + 2\zeta\omega_n S + \omega_n^2} \qquad (51)$$

where ζ is the damping ratio of the system, and ω_n the natural frequency:

$$\omega_n = \sqrt{\frac{48EI}{l^3(M + 0.4857m_b)}} \qquad (52)$$

where l is the length of the beam.

The above consideration of a concentrated mass M at the middle of the ramp, corresponds to an envisioned worse case scenario of one tank breaking down in the middle of the ramp and a second one providing assistance during a military equipment and machinery transfer from the ship to the barge through the connected ramp system.

16

E.   MATCHING CONDITIONS

It was stated previously that the connection mounting the ramp on the barge is a spring-damper connection. If k and c are the spring and damper coefficients respectively, then the connection force f_B will be:

$$f_B(t) = k(\xi_l - \xi_B) + c(\dot{\xi}_l - \dot{\xi}_B) \tag{53}$$

where ξ_l is the vertical displacement at that end of the ramp where the ramp-barge connection is. The above equation is defined in the time domain. Taking the Laplace transform at both sides we can define f_B in the frequency domain:

$$f_B = (k + cs)(\xi_l - \xi_B) \tag{54}$$

where $s = j\omega$.

Combining then equations (32), (50) and (54) we get:

$$f_B = (k + cs)(G\xi_S - \xi_{B_o} - \xi_{B_f} f_B) \tag{55}$$

Solving equation (55) for the connection force f_B we finally get:

$$f_B = \frac{(k + cs)(G\xi_S - \xi_{B_o})}{1 + (k + cs)\xi_{B_f}} \tag{56}$$

Once the ramp-barge connection force is found, the corresponding vertical displacement ξ_B can be determined from equation (32).

F.   EXTENSION TO PLATE MODEL

In the above analysis we considered the ramp connecting the two vessels (ship and barge) as a simply supported beam. At this point we want to extend this assumption and

17

further model the ramp as a simply supported plate with uniform properties throughout its area.

Working on the plate model of the ramp, let's further assume that there are two pinned connection points at the side of the ship and two spring-damper connection points at the side of the barge. Following exactly the same procedure as before, we can write again the equations of motion for both the ship and the barge as follows:

1. Ship Equations of Motion

$$\text{Heave: } \bar{A}_{33,S}\bar{\eta}_{3,S} + \bar{A}_{35,S}\bar{\eta}_{5,S} + \bar{B}_{33,B}\bar{\eta}_{3,B} + \bar{B}_{34,B}\bar{\eta}_{4,B} + \bar{B}_{35,B}\bar{\eta}_{5,B} = F_{3,S}^{H} + f_{S_1} + f_{S_2} \qquad (57)$$

$$\text{Roll: } \bar{A}_{44,S}\bar{\eta}_{4,S} + \bar{B}_{43,B}\bar{\eta}_{3,B} + \bar{B}_{44,B}\bar{\eta}_{4,B} + \bar{B}_{45,B}\bar{\eta}_{5,B} = F_{4,S}^{H} + f_{S_1}y_{S_1} + f_{S_2}y_{S_2} \qquad (58)$$

$$\text{Pitch: } \bar{A}_{53,S}\bar{\eta}_{3,S} + \bar{A}_{55,S}\bar{\eta}_{5,S} + \bar{B}_{53,B}\bar{\eta}_{3,B} + \bar{B}_{54,B}\bar{\eta}_{4,B} + \bar{B}_{55,B}\bar{\eta}_{5,B} = F_{5,S}^{H} - f_{S_1}x_{S_1} - f_{S_2}x_{S_2} \quad (59)$$

Since the ship is much larger than the barge, we can neglect the hydrodynamic influence terms as well as the ship-ramp connection forces f_{S_1} and f_{S_2}. Then the ship equations of motion reduce again to the equations (20), (21), (22), exactly as in the case of the beam model. Solving these equations for the ship's $\bar{\eta}$ terms we find the values described in equations (23), (24), and (25).

Once the $\bar{\eta}$ terms for the ship are found, the vertical displacements at the ship-ramp connection points can be determined from the following equations:

$$\xi_{S_1} = \bar{\eta}_{3,S} + y_{S_1}\bar{\eta}_{4,S} - x_{S_1}\bar{\eta}_{5,S} \qquad (60)$$

$$\xi_{S_2} = \bar{\eta}_{3,S} + y_{S_2}\bar{\eta}_{4,S} - x_{S_2}\bar{\eta}_{5,S} \qquad (61)$$

2. Barge Equations of Motion

Similarly to the ship, the equations of motion for the barge will be written as:

Heave: $\bar{A}_{33,B}\bar{\eta}_{3,B} + \bar{A}_{35,B}\bar{\eta}_{5,B} + \bar{B}_{33,S}\bar{\eta}_{3,S} + \bar{B}_{34,S}\bar{\eta}_{4,S} + \bar{B}_{35,S}\bar{\eta}_{5,S} = F^{H}_{3,B} + f_{B_1} + f_{B_2}$ $\qquad$ (62)

Roll: $\bar{A}_{44,B}\bar{\eta}_{4,B} + \bar{B}_{43,S}\bar{\eta}_{3,S} + \bar{B}_{44,S}\bar{\eta}_{4,S} + \bar{B}_{45,S}\bar{\eta}_{5,S} = F^{H}_{4,B} + f_{B_1}y_{B_1} + f_{B_2}y_{B_2}$ $\qquad$ (63)

Pitch: $\bar{A}_{53,B}\bar{\eta}_{3,B} + \bar{A}_{55,B}\bar{\eta}_{5,B} + \bar{B}_{53,S}\bar{\eta}_{3,S} + \bar{B}_{54,S}\bar{\eta}_{4,S} + \bar{B}_{55,S}\bar{\eta}_{5,S} = F^{H}_{5,S} - f_{B_1}x_{B_1} - f_{B_2}x_{B_2}$ (64)

The vertical displacements at the barge-ramp connection points can similarly be defined from the equations:

$$\xi_{B_1} = \bar{\eta}_{3,B} + y_{B_1}\bar{\eta}_{4,B} - x_{B_1}\bar{\eta}_{5,B} \qquad\qquad (65)$$

$$\xi_{B_2} = \bar{\eta}_{3,B} + y_{B_2}\bar{\eta}_{4,B} - x_{B_2}\bar{\eta}_{5,B} \qquad\qquad (66)$$

Solving then the hydrodynamic equations of motion for the barge (62) through (64) for $\bar{\eta}_{3,B}$, $\bar{\eta}_{4,B}$, and $\bar{\eta}_{5,B}$, and utilizing equations (65) and (66), we can express ξ_{B_1} and ξ_{B_2} in terms of the ramp-barge connection forces f_{B_1} and f_{B_2} as:

$$\xi_{B_1} = \xi_{B_{10}} + \xi_{B_{11}}f_{B_1} + \xi_{B_{12}}f_{B_2} \qquad\qquad (67)$$

$$\xi_{B_2} = \xi_{B_{20}} + \xi_{B_{21}}f_{B_1} + \xi_{B_{22}}f_{B_2} \qquad\qquad (68)$$

where the coefficients $\xi_{B_{10}}$, $\xi_{B_{20}}$, $\xi_{B_{11}}$, $\xi_{B_{21}}$, $\xi_{B_{12}}$ and $\xi_{B_{22}}$ can separately be determined using the principle of superposition as follows:

19

(i) Determination of $\xi_{B_{10}}$, $\xi_{B_{20}}$:

Assuming that $f_{B_1} = f_{B_2} = 0$, the motion of the barge is described by equations (36), (37), (38) of the beam case. The $\overline{\eta}$ terms are given by equations (39), (40), and (41). Then the ξ_{B_0} terms can be determined from equations:

$$\xi_{B_{10}} = \overline{\eta}_{3,B} + y_{B_1}\overline{\eta}_{4,B} - x_{B_1}\overline{\eta}_{5,B} \tag{69}$$

$$\xi_{B_{20}} = \overline{\eta}_{3,B} + y_{B_2}\overline{\eta}_{4,B} - x_{B_2}\overline{\eta}_{5,B} \tag{70}$$

(ii) Determination of $\xi_{B_{11}}$, $\xi_{B_{21}}$:

Assuming now that $f_{B_1} = 1$ and $f_{B_2} = 0$, and neglecting the hydrodynamic forces and moments as well as the ship influence, the barge equations of motion become:

$$\overline{A}_{33,B}\overline{\eta}_{3,B} + \overline{A}_{35,B}\overline{\eta}_{5,B} = 1 \tag{71}$$

$$\overline{A}_{44,B}\overline{\eta}_{4,B} = y_{B_1} \tag{72}$$

$$\overline{A}_{53,B}\overline{\eta}_{3,B} + \overline{A}_{55,B}\overline{\eta}_{5,B} = -x_{B_1} \tag{73}$$

Solving then for the $\overline{\eta}$ terms we get:

$$\overline{\eta}_{3,B} = \frac{\overline{A}_{55,B} + x_{B_1}\overline{A}_{35,B}}{\overline{A}_{33,B}\overline{A}_{55,B} - \overline{A}_{35,B}\overline{A}_{53,B}} \tag{74}$$

$$\overline{\eta}_{4,B} = \frac{y_{B_1}}{\overline{A}_{44,B}} \tag{75}$$

$$\overline{\eta}_{5,B} = -\frac{x_{B_1} + \overline{A}_{53,B}\overline{\eta}_{3,B}}{\overline{A}_{55,B}} \tag{76}$$

Then the ξ_{B_1} terms can be determined from the equations:

$$\xi_{B_{11}} = \overline{\eta}_{3,B} + y_{B_1}\overline{\eta}_{4,B} - x_{B_1}\overline{\eta}_{5,B} \qquad (77)$$

$$\xi_{B_{21}} = \overline{\eta}_{3,B} + y_{B_2}\overline{\eta}_{4,B} - x_{B_2}\overline{\eta}_{5,B} \qquad (78)$$

(iii) Determination of $\xi_{B_{12}}, \xi_{B_{22}}$:

Finally, assuming that $f_{B_1} = 0$ and $f_{B_2} = 1$, and neglecting again the hydrodynamic

coefficients, the barge equations of motion become:

$$\overline{A}_{33,B}\overline{\eta}_{3,B} + \overline{A}_{35,B}\overline{\eta}_{5,B} = 1 \qquad (79)$$

$$\overline{A}_{44,B}\overline{\eta}_{4,B} = y_{B_2} \qquad (80)$$

$$\overline{A}_{53,B}\overline{\eta}_{3,B} + \overline{A}_{55,B}\overline{\eta}_{5,B} = -x_{B_2} \qquad (81)$$

Solving again for the $\overline{\eta}$ terms:

$$\overline{\eta}_{3,B} = \frac{\overline{A}_{55,B} + x_{B_2}\overline{A}_{35,B}}{\overline{A}_{33,B}\overline{A}_{55,B} - \overline{A}_{35,B}\overline{A}_{53,B}} \qquad (82)$$

$$\overline{\eta}_{4,B} = \frac{y_{B_2}}{\overline{A}_{44,B}} \qquad (83)$$

$$\overline{\eta}_{5,B} = -\frac{x_{B_2} + \overline{A}_{53,B}\overline{\eta}_{3,B}}{\overline{A}_{55,B}} \qquad (84)$$

Then, the ξ_{B_2} terms can be determined from:

$$\xi_{B_{12}} = \overline{\eta}_{3,B} + y_{B_1}\overline{\eta}_{4,B} - x_{B_1}\overline{\eta}_{5,B} \qquad (85)$$

$$\xi_{B_{22}} = \overline{\eta}_{3,B} + y_{B_2}\overline{\eta}_{4,B} - x_{B_2}\overline{\eta}_{5,B} \qquad (86)$$

21

3. Matching Conditions

If k_1, k_2 and c_1, c_2 are the spring and damper coefficients of the two ramp-barge connection points, then the corresponding connection forces f_{B_1} and f_{B_2} in the frequency domain, will be:

$$f_{B_1} = (k_1 + c_1 s)(\xi_{l_1} - \xi_{B_1}) \tag{87}$$

$$f_{B_2} = (k_2 + c_2 s)(\xi_{l_2} - \xi_{B_2}) \tag{88}$$

Combining the two above equations with equations (65), (66), we get:

$$f_{B_1} = (k_1 + c_1 s)(\xi_{l_1} - \xi_{B_{10}} - \xi_{B_{11}} f_{B_1} - \xi_{B_{12}} f_{B_2}) \tag{89}$$

$$f_{B_2} = (k_2 + c_2 s)(\xi_{l_2} - \xi_{B_{20}} - \xi_{B_{21}} f_{B_1} - \xi_{B_{22}} f_{B_2}) \tag{90}$$

Similarly to the beam model case for the ramp, the vertical displacements ξ_{l_1} and ξ_{l_2} at the end of the ramp that is connected to the barge can be related to ξ_{S_1} and ξ_{S_2} by the following equation:

$$\begin{bmatrix} \xi_{l_1} \\ \xi_{l_2} \end{bmatrix} = \begin{bmatrix} G_{11} & G_{12} \\ G_{21} & G_{22} \end{bmatrix} \begin{bmatrix} \xi_{S_1} \\ \xi_{S_2} \end{bmatrix} \tag{91}$$

Here, similar to the beam model case, the G_{ij} terms may have the form:

$$G_{ij}(S) = \frac{\omega_{ij}^2}{S^2 + 2\zeta_{ij}\omega_{ij}S + \omega_{ij}^2}, \qquad i, j = 1, 2 \tag{92}$$

where ω_{ij} terms are considered to have values near the natural frequency ω_n used in the beam model case. Introducing for brevity:

$$K_1 = k_1 + c_1 s \tag{93}$$

22

$$K_2 = k_2 + c_2 s \tag{94}$$

and solving (89), (90) for the two ramp-barge connection forces f_{B_1} and f_{B_2}, we get:

$$f_{B_1} = K_1 \frac{(\xi_{l_1} - \xi_{B_{10}})(1+K_2\xi_{B_{22}}) - K_2\xi_{B_{12}}(\xi_{l_2} - \xi_{B_{20}})}{(1+K_1\xi_{B_{11}})(1+K_2\xi_{B_{22}}) - K_1 K_2 \xi_{B_{12}}\xi_{B_{21}}} \tag{95}$$

$$f_{B_2} = \frac{K_1(\xi_{l_1} - \xi_{B_{10}}) - (1+K_1\xi_{B_{11}})f_{B_1}}{K_1\xi_{B_{12}}} \tag{96}$$

Once the ramp-barge connection forces f_{B_1} and f_{B_2} are found, the corresponding vertical displacements ξ_{B_1} and ξ_{B_2} can be determined from (65), (66).

THIS PAGE INTENTIONALLY LEFT BLANK

III.   REGULAR WAVE RESULTS

A.   INTRODUCTION

The coefficients produced as output from the three-dimensional (WAMIT) program solver are in non-dimensional form, as shown in Table 1 and Table 2, with ω (wave frequency), ρ (water density), g (gravitational constant), ζ (wave amplitude), and the ship's reference length L.

Ship/Barge Coefficients	Non-dimensionalization (WAMIT)
Heave Added Mass A_{33}	$A_{33} / \rho L^3$
Heave to Pitch Added Mass A_{35}	$A_{35} / \rho L^4$
Roll Added Mass A_{44}	$A_{44} / \rho L^5$
Pitch to Heave Added Mass A_{53}	$A_{53} / \rho L^4$
Pitch Added Mass A_{55}	$A_{55} / \rho L^5$
Heave Damping B_{33}	$B_{33} / \omega \rho L^3$
Heave to Pitch Damping B_{35}	$B_{35} / \omega \rho L^4$
Roll Damping B_{44}	$B_{44} / \omega \rho L^5$
Pitch to Heave Damping B_{53}	$B_{53} / \omega \rho L^4$

Table 1. Non-dimensionalization of A_{ij} and B_{ij} terms.

Ship/Barge Coefficients	Non-dimensionalization (WAMIT)
Heave Stiffness C_{33}	$C_{33} / \rho g L^2$
Heave to Pitch Stiffness C_{35}	$C_{35} / \rho g L^3$
Roll Stiffness C_{44}	$C_{44} / \rho g L^4$
Pitch to Heave Stiffness C_{53}	$C_{53} / \rho g L^3$
Pitch Stiffness C_{55}	$C_{55} / \rho g L^4$
Heave Excitation Force F_3^H	$F_3^H / \rho g \zeta L^2$
Roll Excitation Moment F_4^H	$F_4^H / \rho g \zeta L^3$
Pitch Excitation Moment F_5^H	$F_5^H / \rho g \zeta L^3$

Table 2. Non-dimensionalization of C_{ij} and F_j^H terms

B. SHIP/BARGE ANALYSIS

Figures 1 through 64 display the results for the regular wave responses (amplitudes and phase angles) for the Ship (LMSR), and the Barge (RRDF), without Ramp Influence. These regular wave responses range from zero degrees (following seas) through 315 degrees at 45-degree intervals. This provides complete 360-degree coverage for regular wave response analysis for both the Ship and the Barge. The irregular oscillatory behavior of the plots at higher frequencies (lower periods) is attributed to artificially generated high frequency interactions due to discretization effects in the three-dimensional (WAMIT) solver. However such high frequencies may rarely be encountered

in open seas. In the results displayed in the above figures, the Barge is modeled as a square platform with shallow draft. The actual dimensions for both the Ship (LMSR), and the Barge (RRDF) are given in Table 3.

Dimension	Ship (LMSR)	Barge (RRDF)
Length (in feet)	894.53	79.2
Beam (in feet)	105.8	72.6
Depth (in feet)	Non Given	4.7
Draft (in feet)	27.5(FWD), 32.27(AFT)	1.3
Displacement	45211 Long Tons	402783 Pounds

Table 3. Applicable Ship and Barge Dimensions.

In the results shown here, the following notation is used:

Ship: Motions for the LMSR.

Barge0: Motions for the RRDF neglecting LMSR and ramp influence.

Barge: Motions for the RRDF neglecting ramp influence.

xiS: Vertical motion at the LMSR/ramp connection point.

xiB00: Vertical motion at the RRDF/ramp connection point neglecting LMSR and ramp influence.

xiB0: Vertical motion at the RRDF/ramp connection point neglecting ramp influence.

Based on these results we can draw the following conclusion: Barge motions are virtually unaffected by the presence of the influence coefficients described in the previous chapter. This results in a significant simplification in the form of the equations of motion;

27

namely direct ship-to-barge feedback terms are not required for accurate modeling. It should be emphasized, however, that this does not mean that there is no influence from the ship to the barge, but rather that such influence can be modeled by properly calculating the barge added mass and damping coefficients, and the wave exciting forces. As has been previously established, such calculations depend heavily on ship/barge proximity effects.
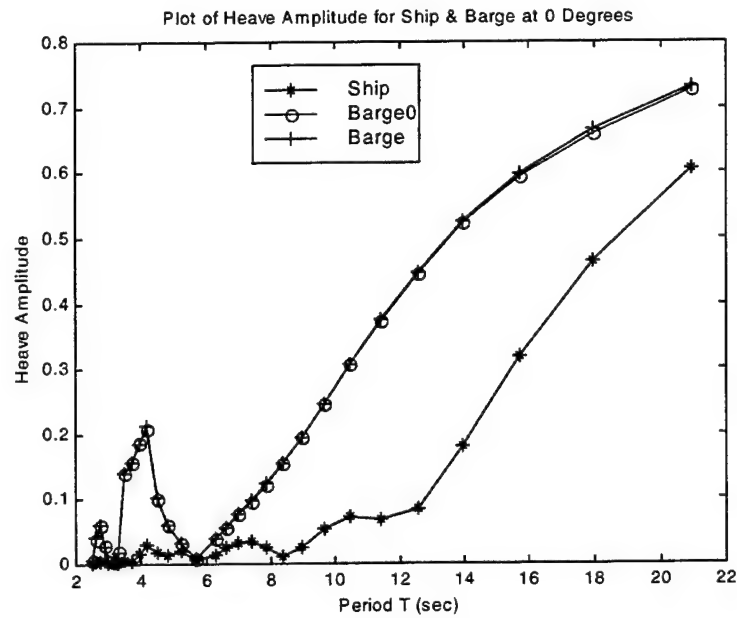
Figure 1. Plot of Heave Amplitude for the Ship, Barge without Ship/Ramp Influence and Barge without Ramp Influence at 0 Degrees Wave Angle.
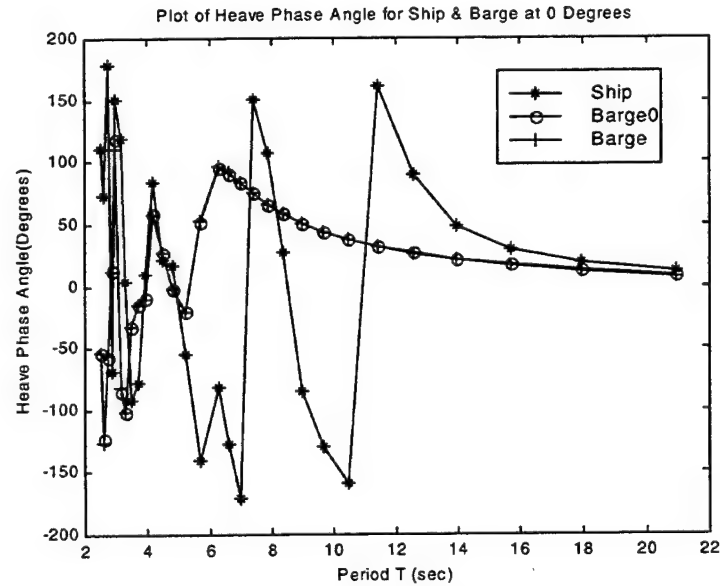
Figure 2. Plot of Heave Phase Angle for the Ship, Barge without Ship/Ramp Influence and Barge without Ramp Influence at 0 Degrees Wave Angle.
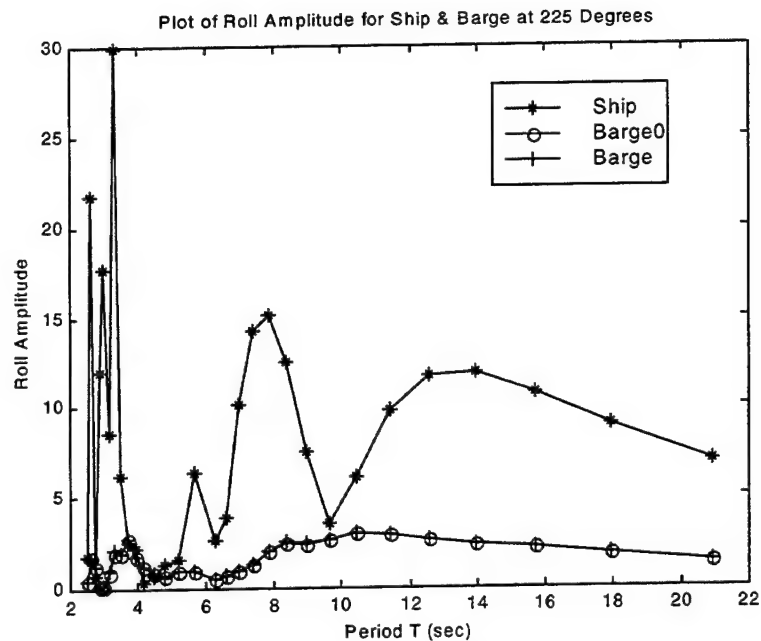
29
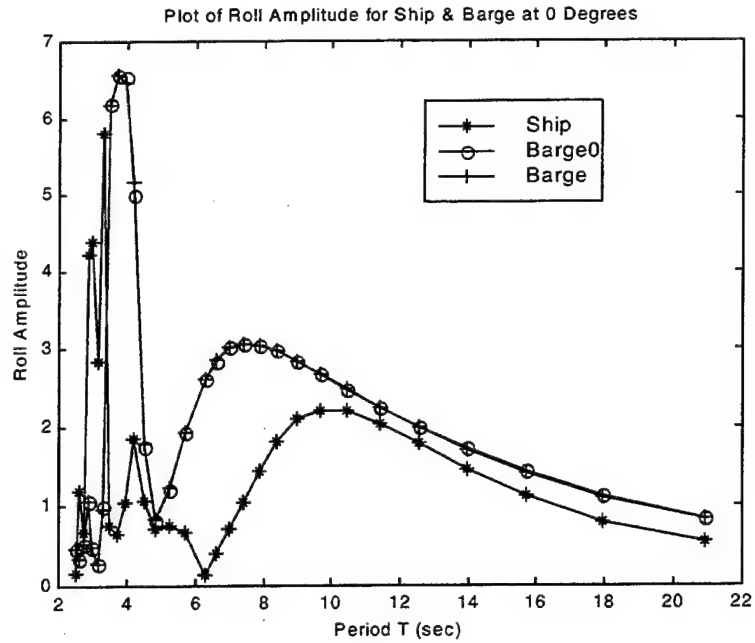
Figure 3. Plot of Roll Amplitude for the Ship, Barge without Ship/Ramp
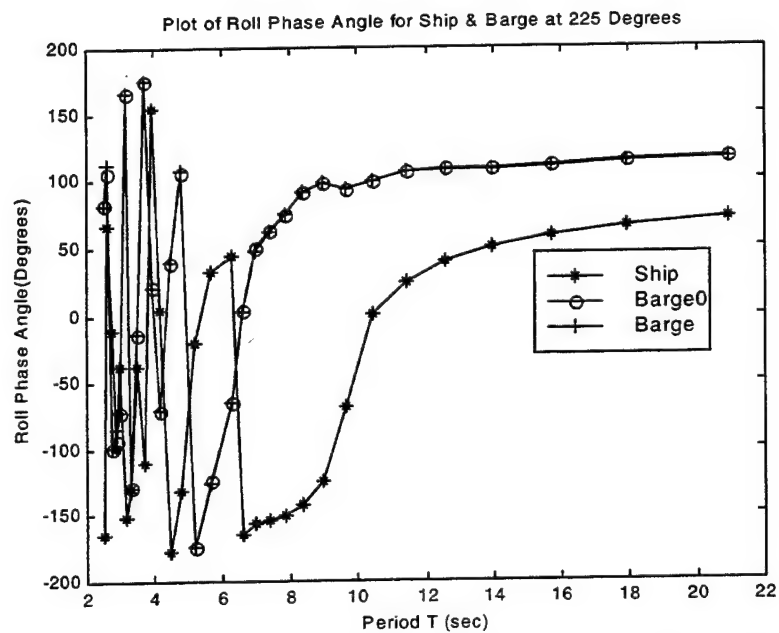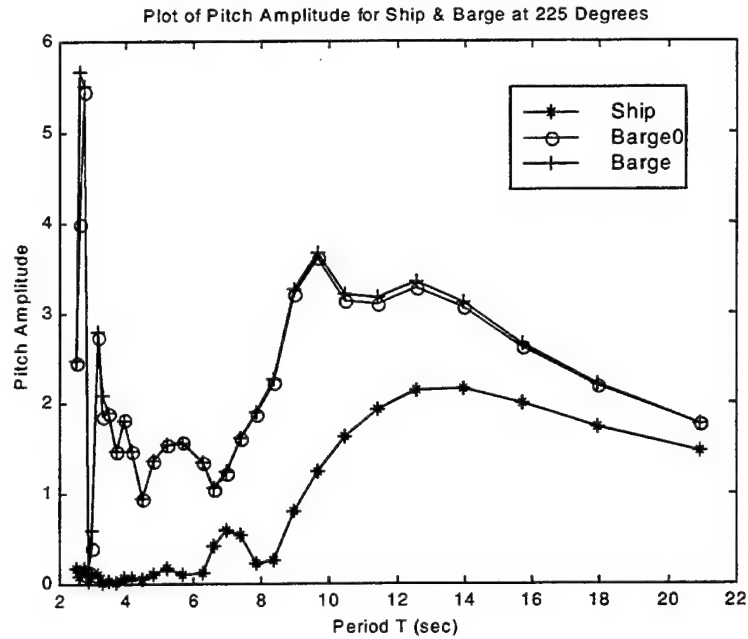Influence, and Barge without Ramp Influence at 0 Degrees Wave Angle.
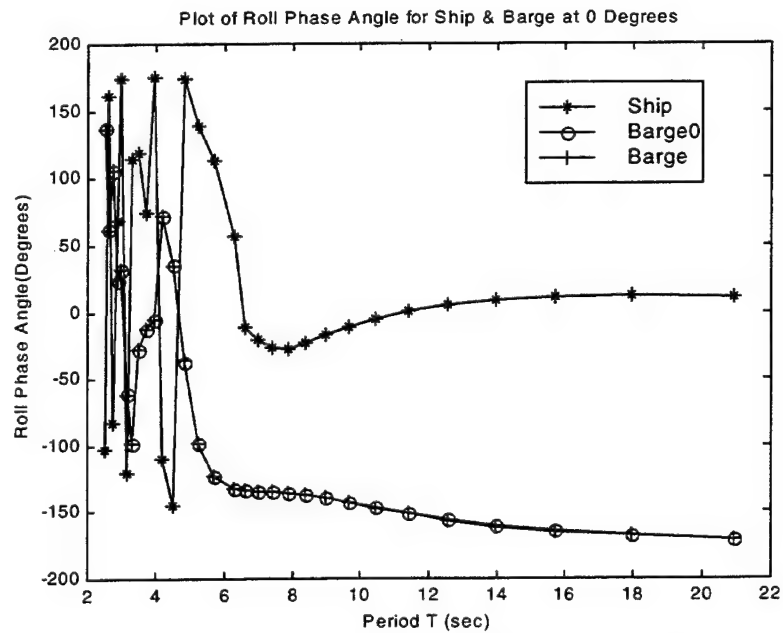
Figure 4. Plot of Roll Phase Angle for the Ship, Barge without Ship/Ramp
Influence, and Barge without Ramp Influence at 0 Degrees Wave Angle.

30
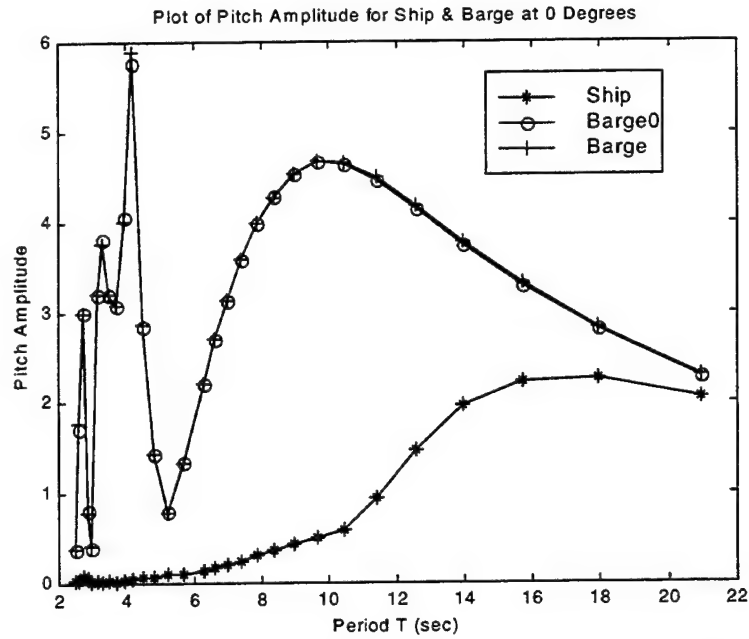
Figure 5. Plot of Pitch Amplitude for the Ship, Barge without Ship/Ramp Influence, and Barge without Ramp Influence at 0 Degrees Wave Angle.
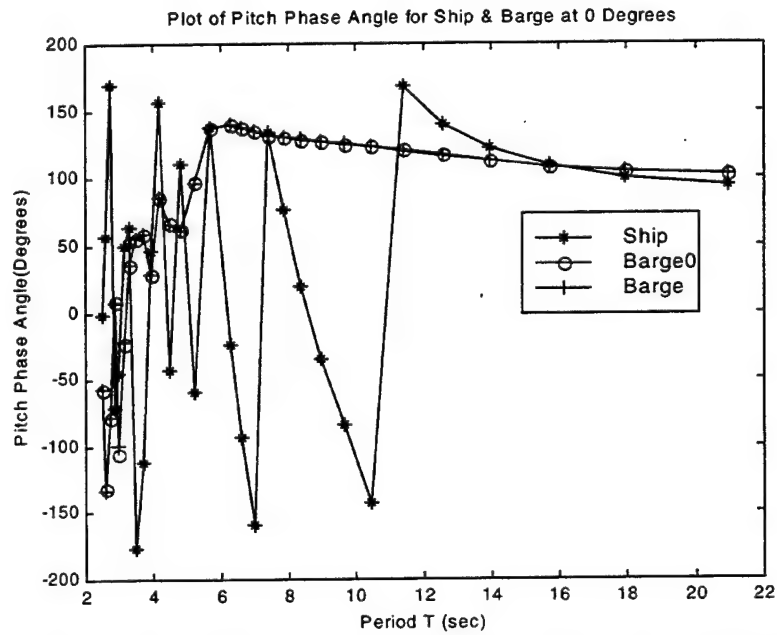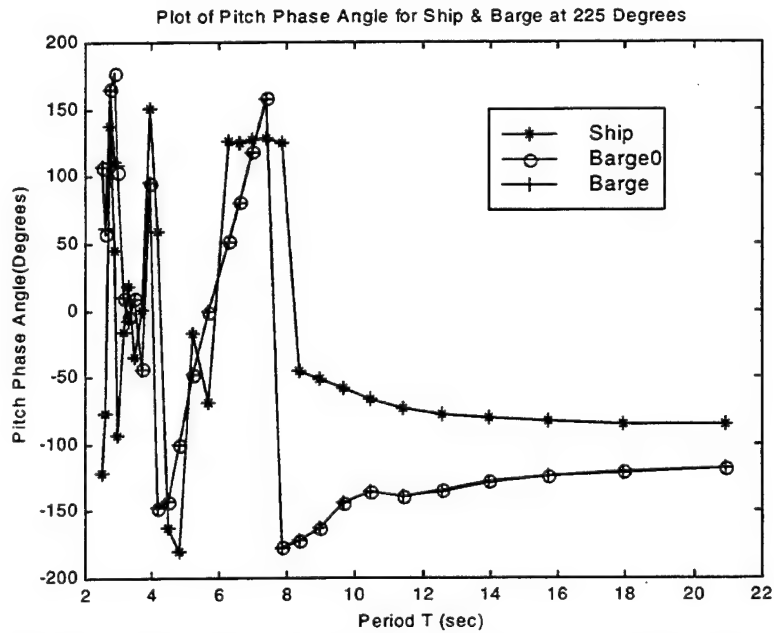

Figure 6. Plot of Pitch Phase Angle for the Ship, Barge without Ship/Ramp Influence, and Barge without Ramp Influence at 0 Degrees Wave Angle.
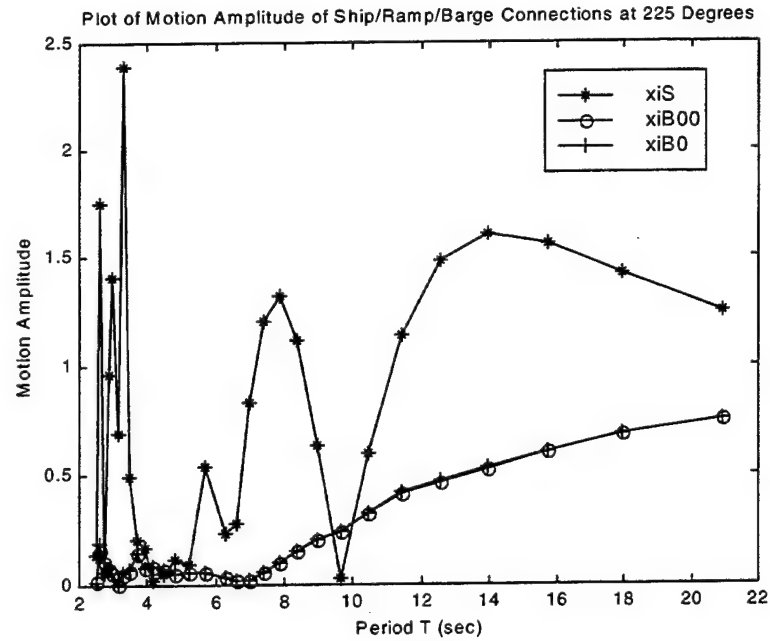
31
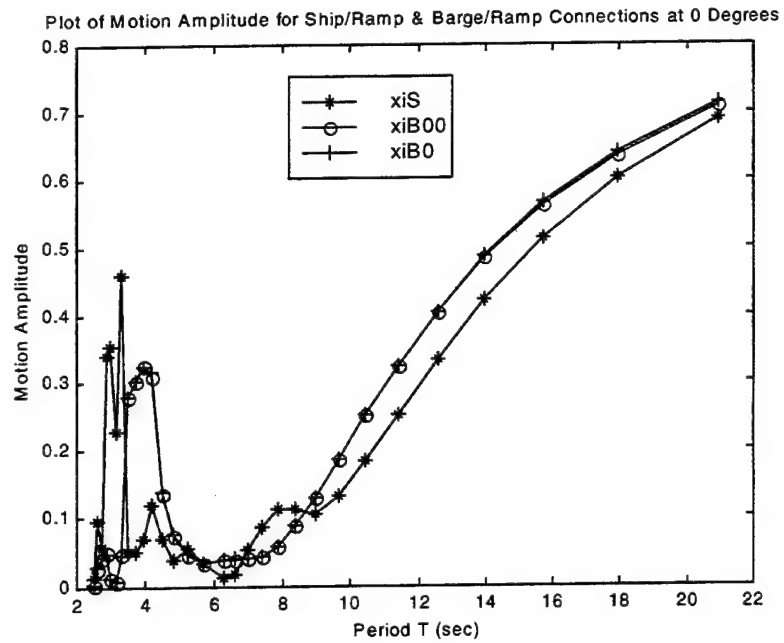
Figure 7. Plot of Vertical Motion Amplitude at the Ship/Ramp/Barge Connection Points without Ramp Influence for the Barge at 0 Degrees Wave Angle.
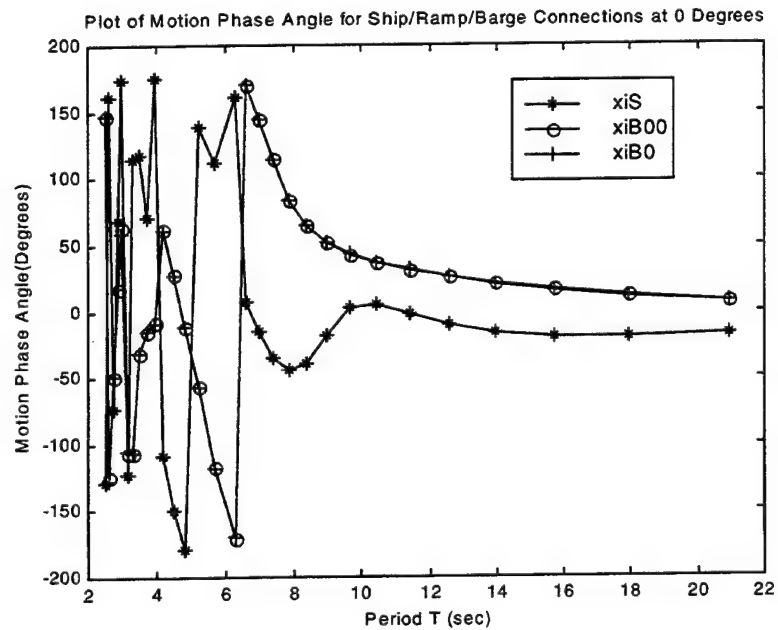
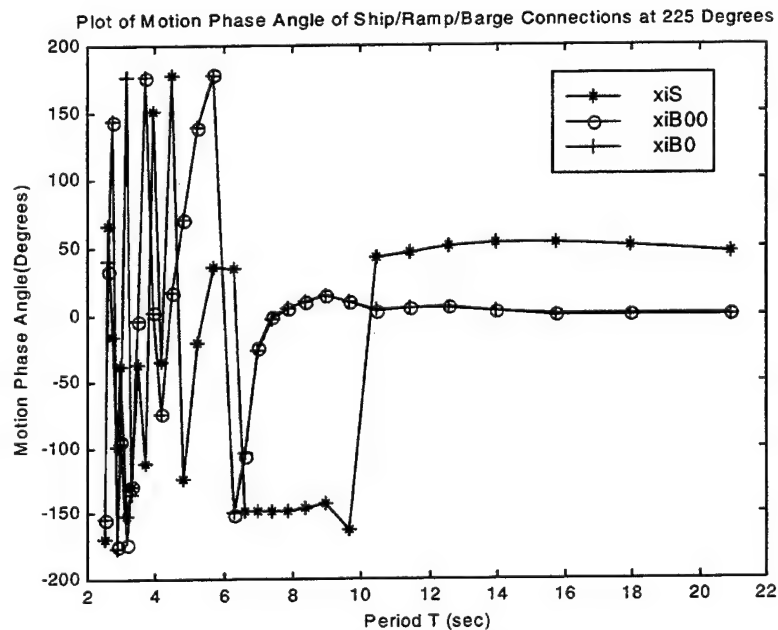
Figure 8. Plot of Vertical Motion Phase Angle at the Ship/Ramp/Barge Connection Points without Ramp Influence for the Barge at 0 Degrees Wave Angle.
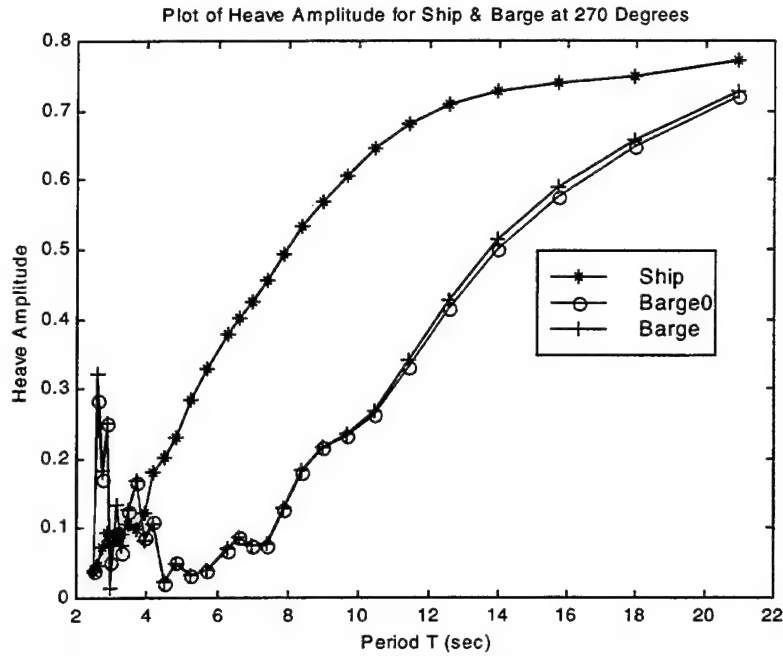
32
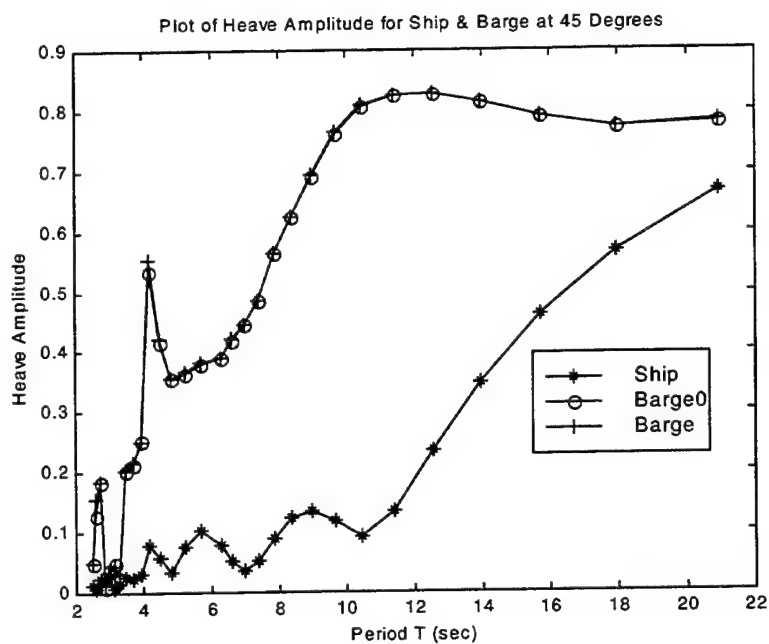
Figure 9. Plot of Heave Amplitude for the Ship, Barge without Ship/Ramp Influence, and Barge without Ramp Influence at 45 Degrees Wave Angle.
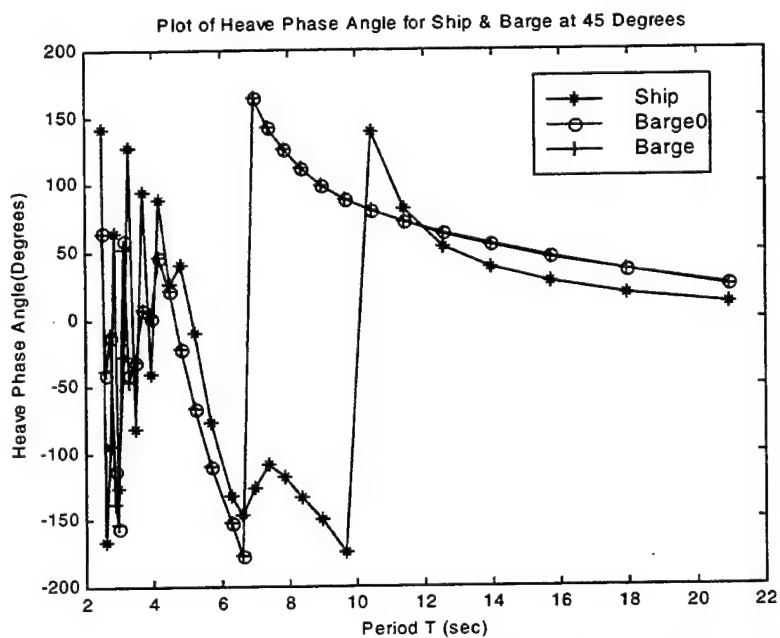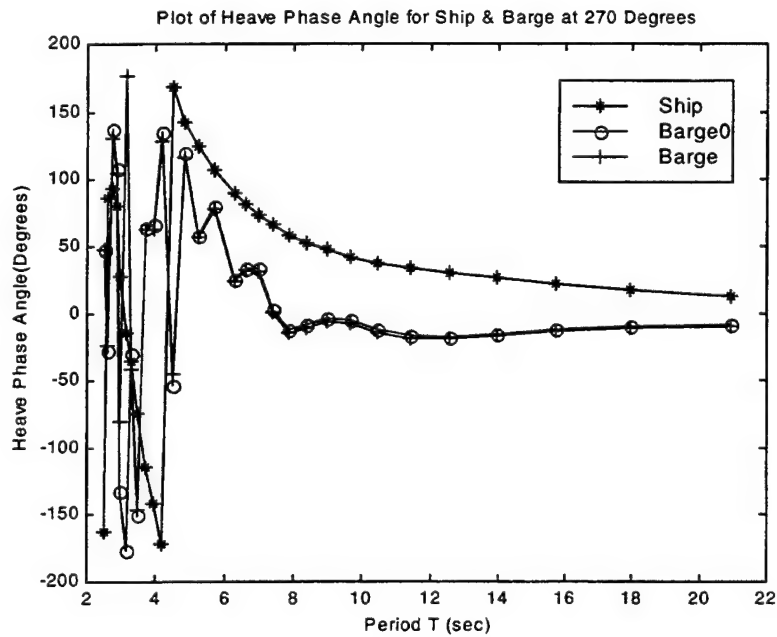

Figure 10. Plot of Heave Phase Angle for the Ship, Barge without Ship/Ramp Influence, and Barge without Ramp Influence at 45 Degrees Wave Angle.
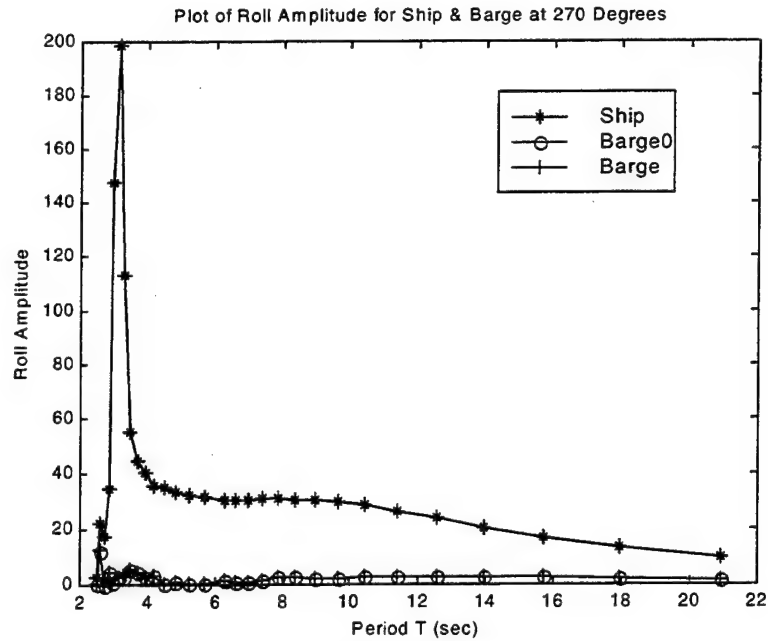
33
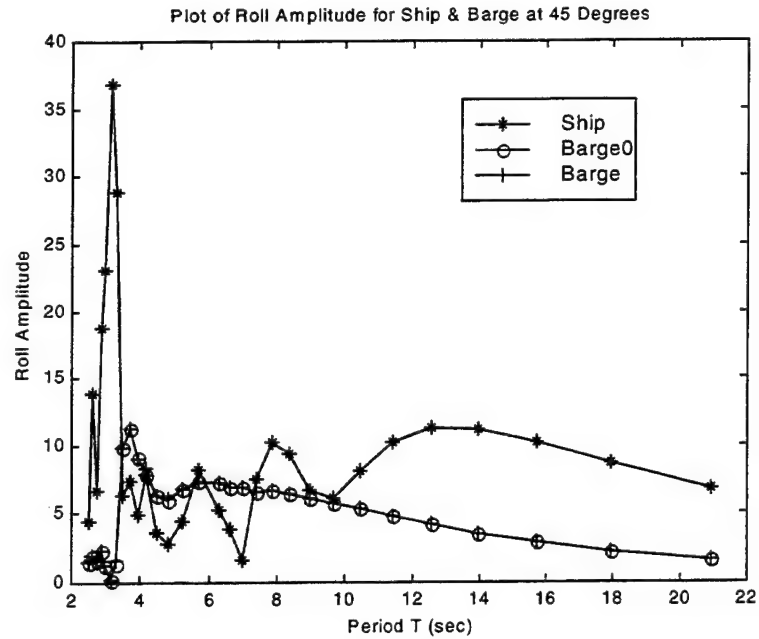
Figure 11. Plot of Roll Amplitude for the Ship, Barge without Ship/Ramp Influence, and Barge without Ramp Influence at 45 Degrees Wave Angle.
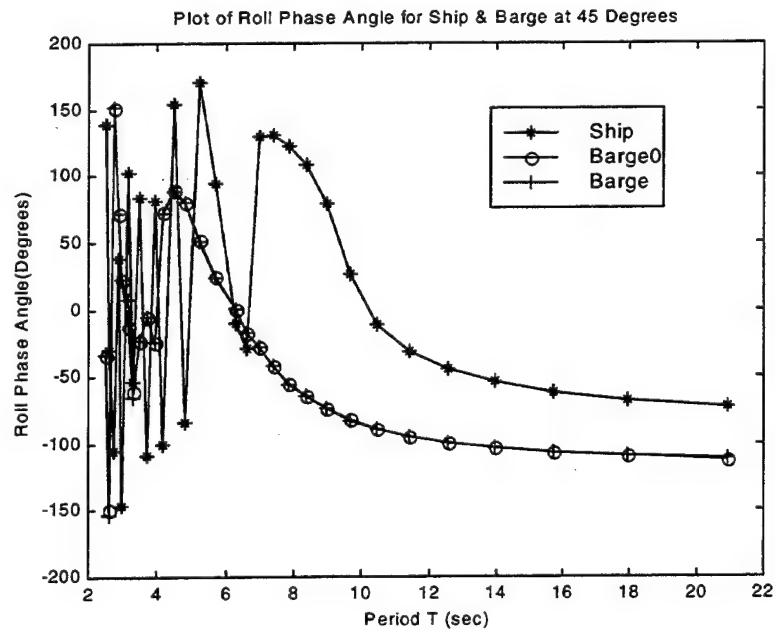
Figure 12. Plot of Roll Phase Angle for the Ship, Barge without Ship/Ramp Influence, and Barge without Ramp Influence at 45 Degrees Wave Angle.

34

Plot of Pitch Amplitude for Ship & Barge at 45 Degrees
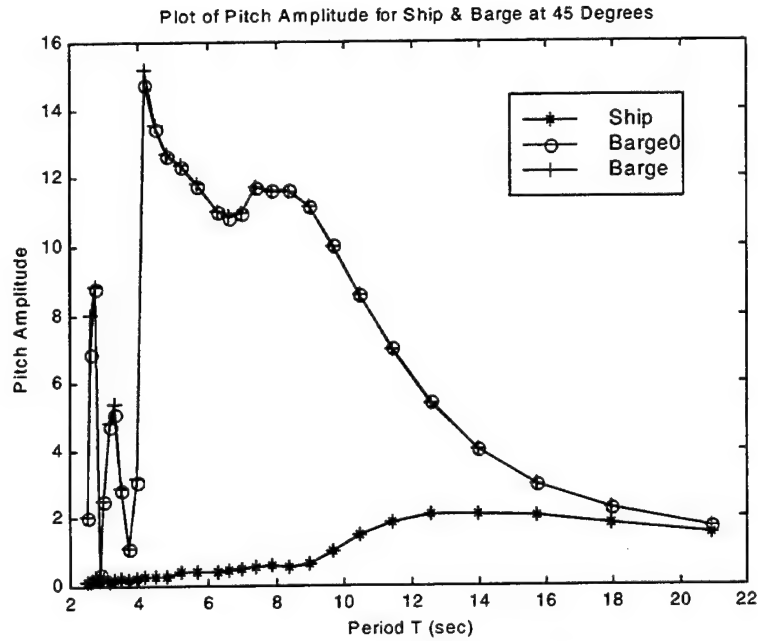
Figure 13. Plot of Pitch Amplitude for the Ship, Barge without Ship/Ramp Influence, and Barge without Ramp Influence at 45 Degrees Wave Angle.

Plot of Pitch Phase Angle for Ship & Barge at 45 Degrees
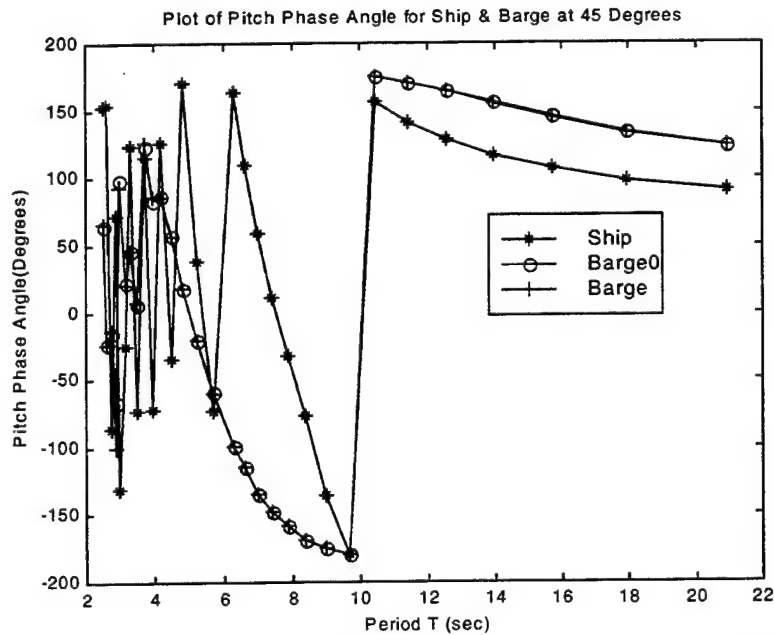
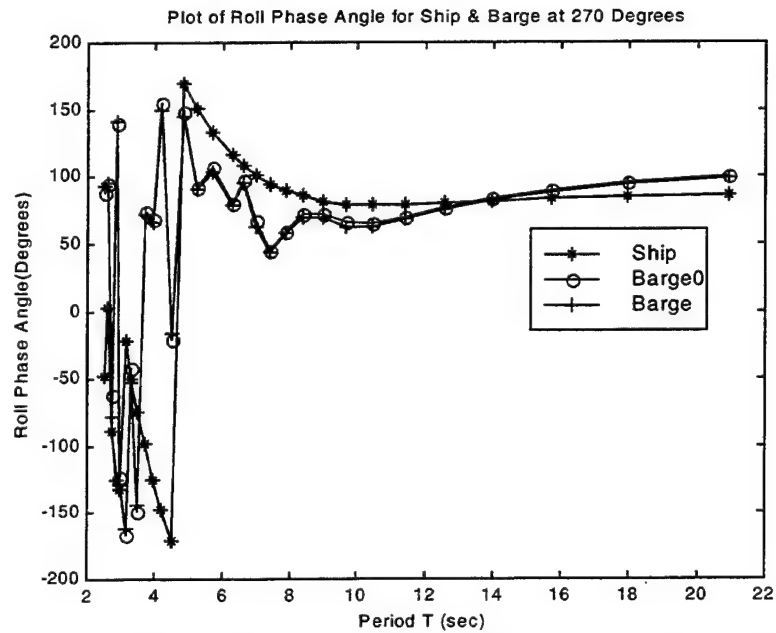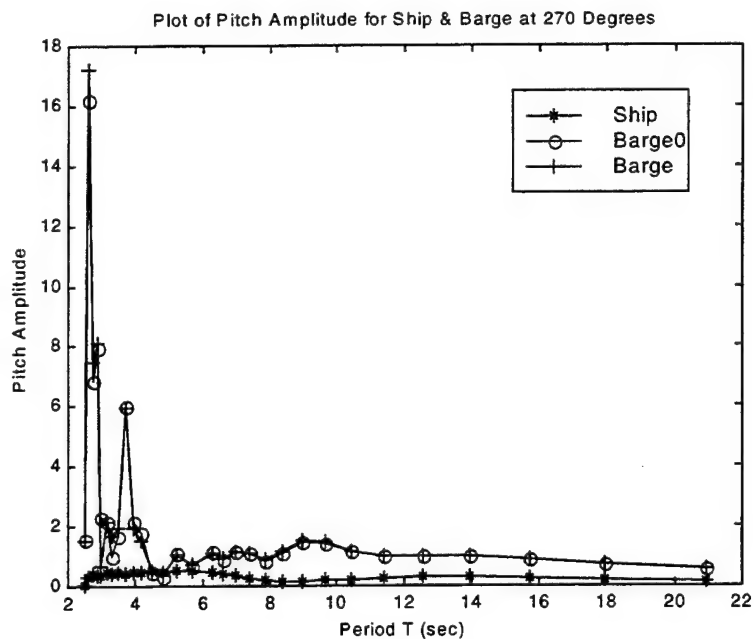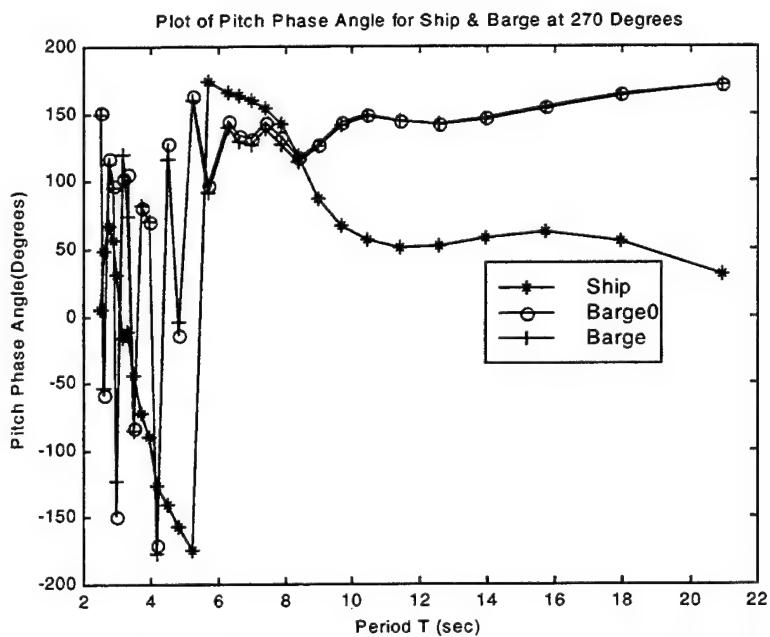
Figure 14. Plot of Pitch Phase Angle for the Ship, Barge without Ship/Ramp Influence, and Barge without Ramp Influence at 45 Degrees Wave Angle.

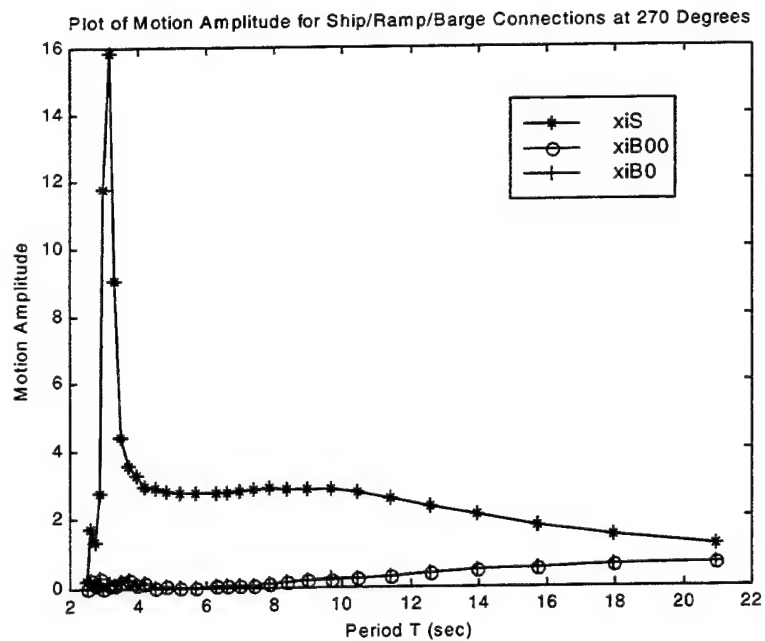Plot of Motion Amplitude for Ship/Ramp/Barge Connections at 45 Degrees
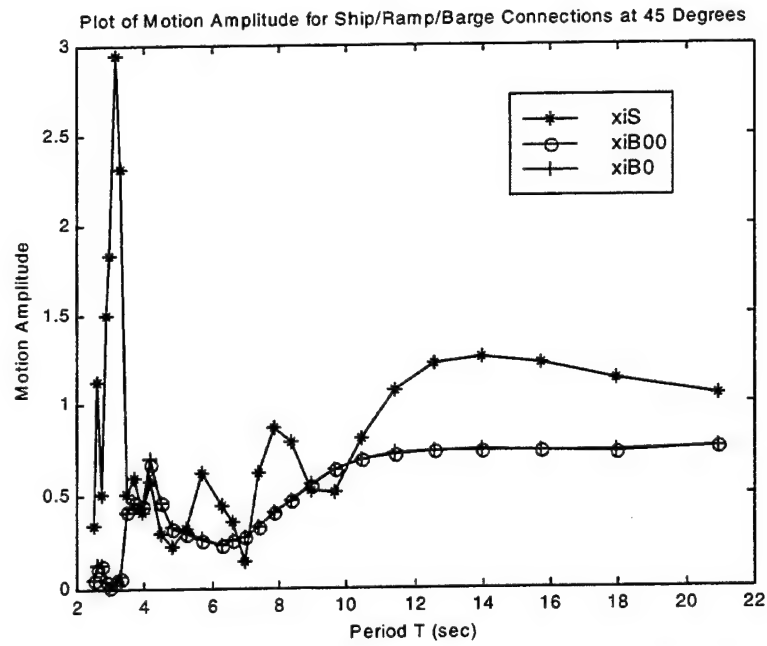
Figure 15. Plot of Vertical Motion Amplitude at the Ship/Ramp/Barge Connection Points, without Ramp Influence for the Barge, at 45 Degrees Wave Angle.

Plot of Motion Phase Angle for Ship/Ramp/Barge Connections at 45 Degrees
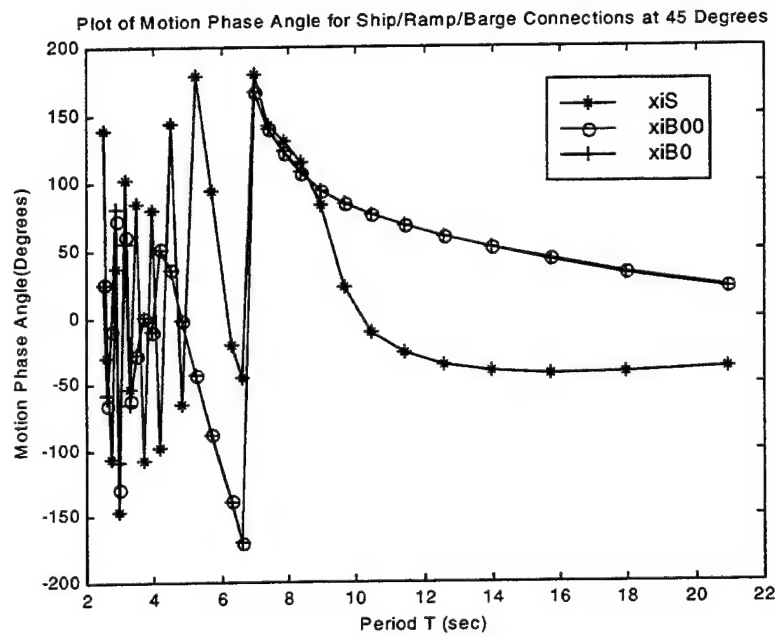
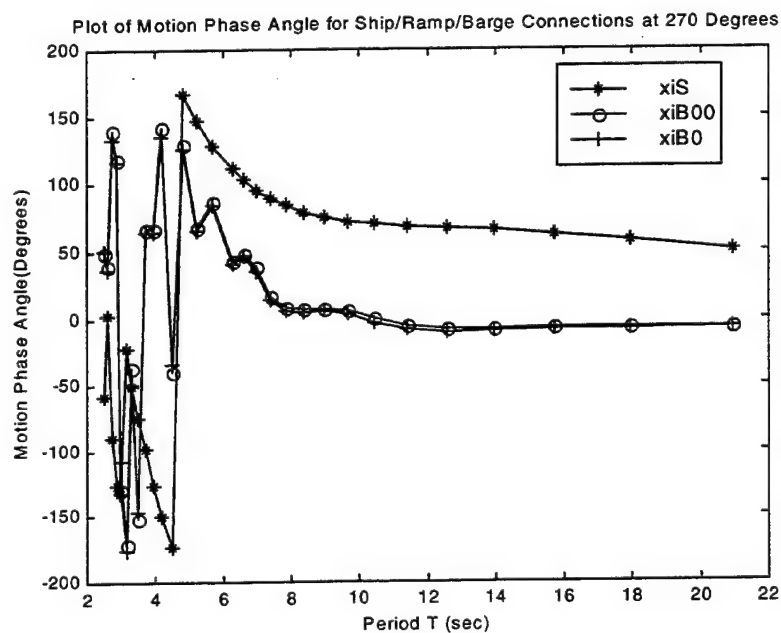
Figure 16. Plot of Vertical Motion Phase Angle at the Ship/Ramp/Barge Connection Points, without Ramp Influence for the Barge, at 45 Degrees Wave Angle.

36
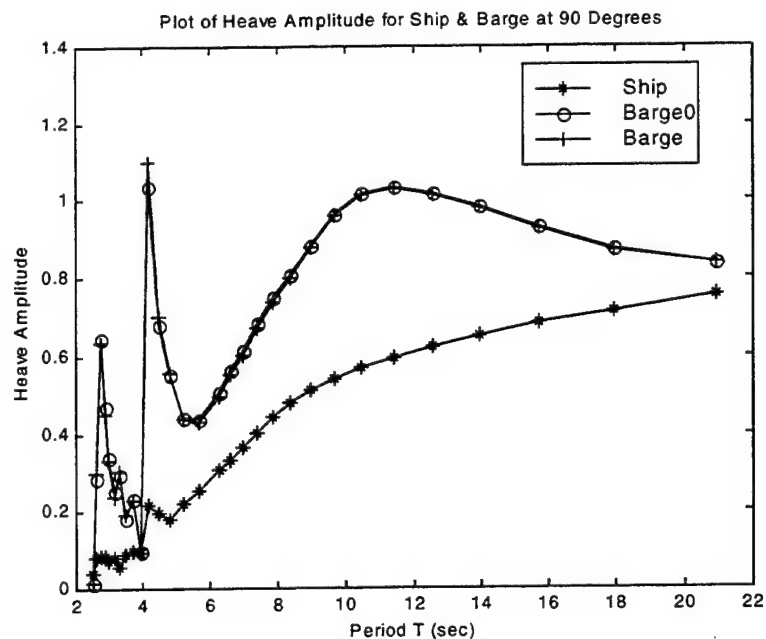
Figure 17. Plot of Heave Amplitude for the Ship, Barge without Ship/Ramp Influence, and Barge without Ramp Influence, at 90 Degrees Wave Angle.
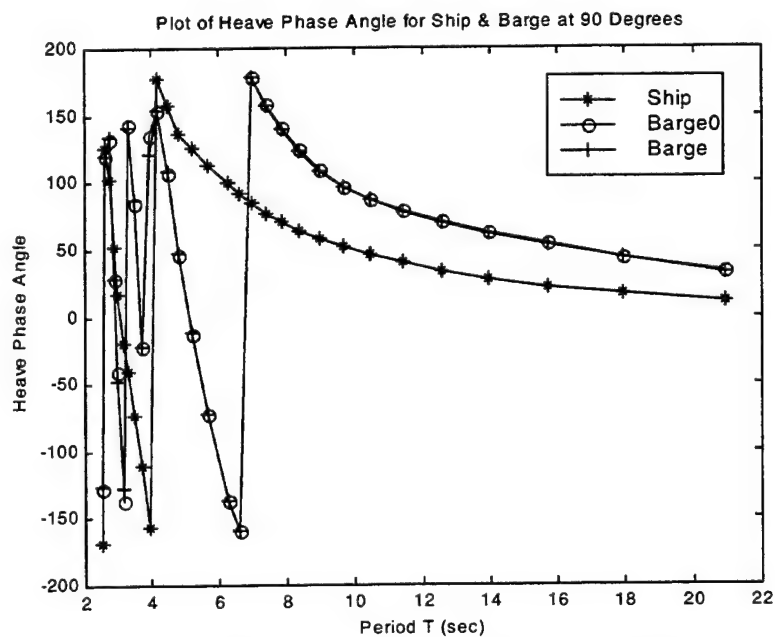
Figure 18. Plot of Heave Phase Angle for the Ship, Barge without Ship/Ramp Influence, and Barge without Ramp Influence, at 90 Degrees Wave Angle.

37
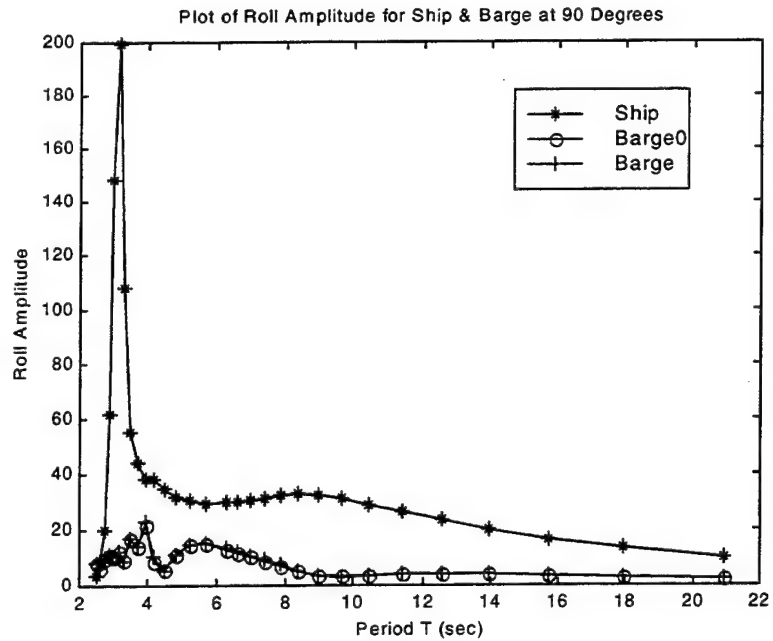
Figure 19. Plot of Roll Amplitude for the Ship, Barge without Ship/Ramp Influence, and Barge without Ramp Influence, at 90 Degrees Wave Angle.
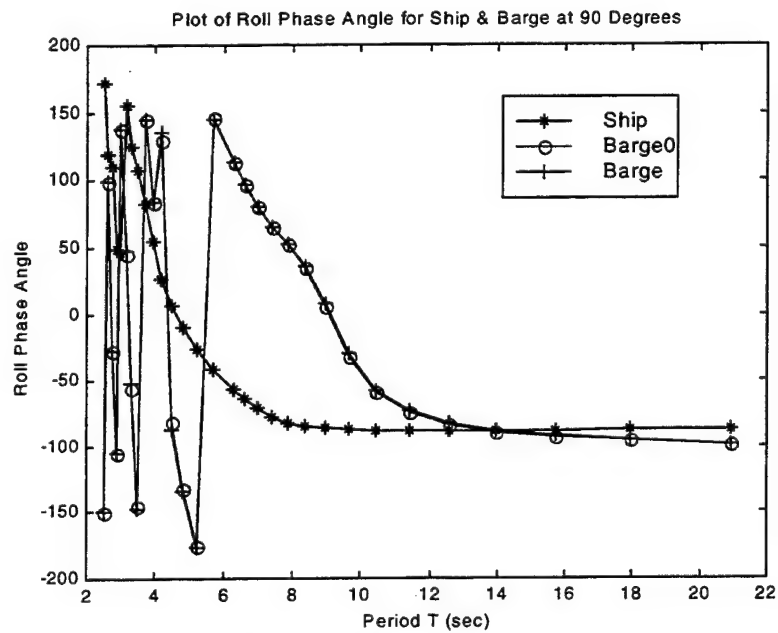
Figure 20. Plot of Roll Phase Angle for the Ship, Barge without Ship/Ramp Influence, and Barge without Ramp Influence, at 90 Degrees Wave Angle.
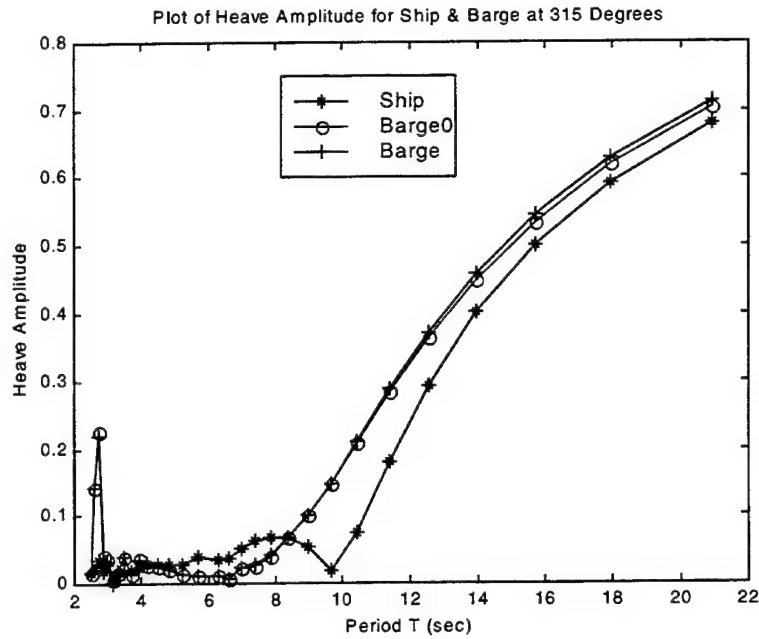
38
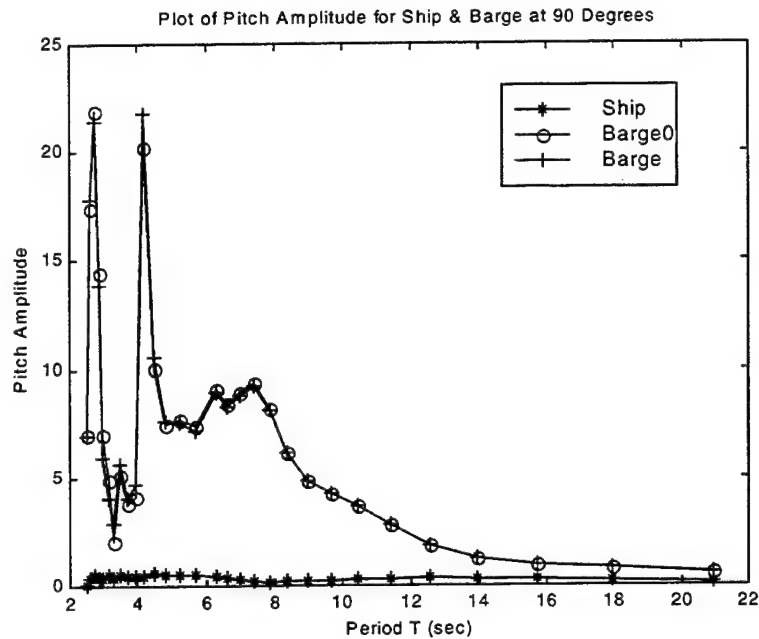
Figure 21. Plot of Pitch Amplitude for the Ship, Barge without Ship/Ramp Influence, and Barge without Ramp Influence, at 90 Degrees Wave Angle.
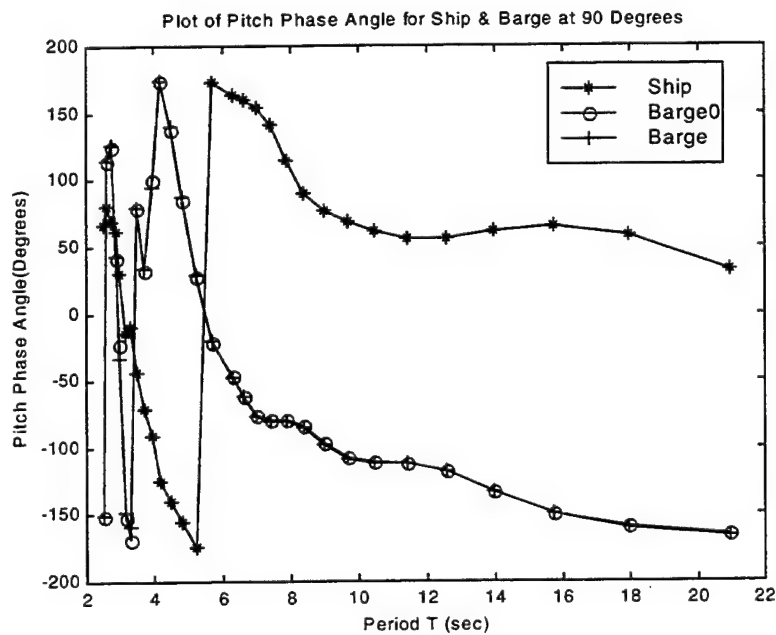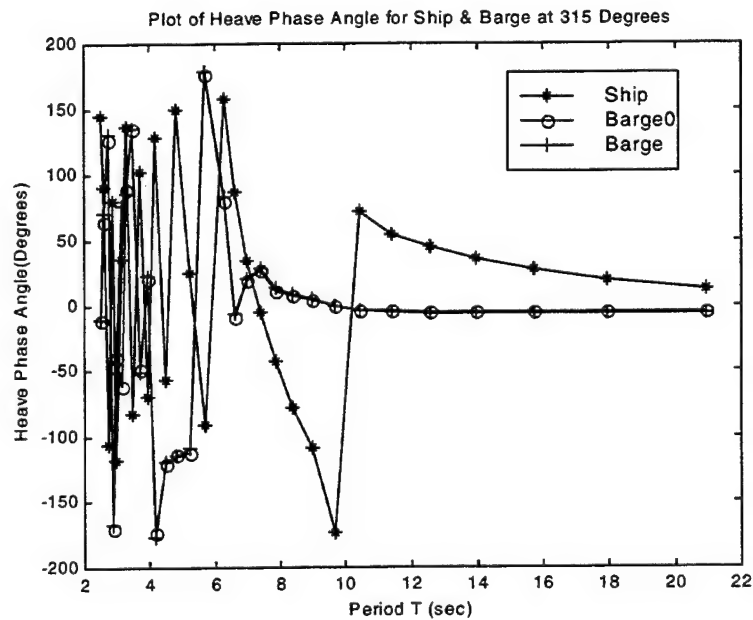

Figure 22. Plot of Pitch Phase Angle for the Ship, Barge without Ship/Ramp Influence, and Barge without Ramp Influence, at 90 Degrees Wave Angle.
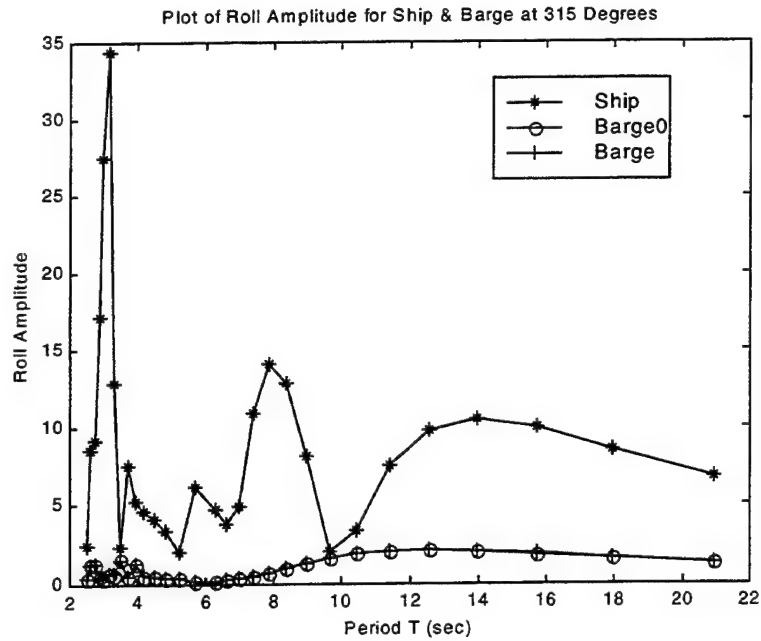
39
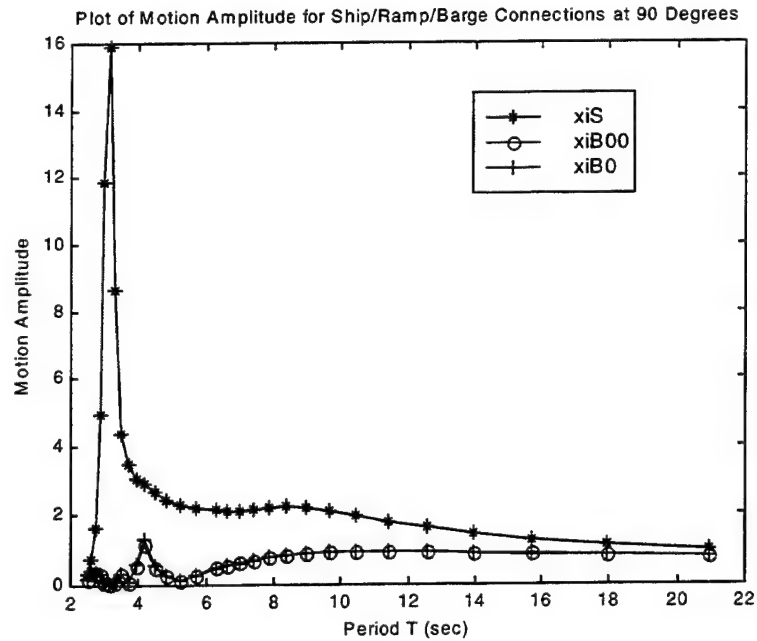
Figure 23. Plot of Vertical Motion Amplitude at the Ship/Ramp/Barge Connection Points, without Ramp Influence for the Barge, at 90 Degrees Wave Angle.
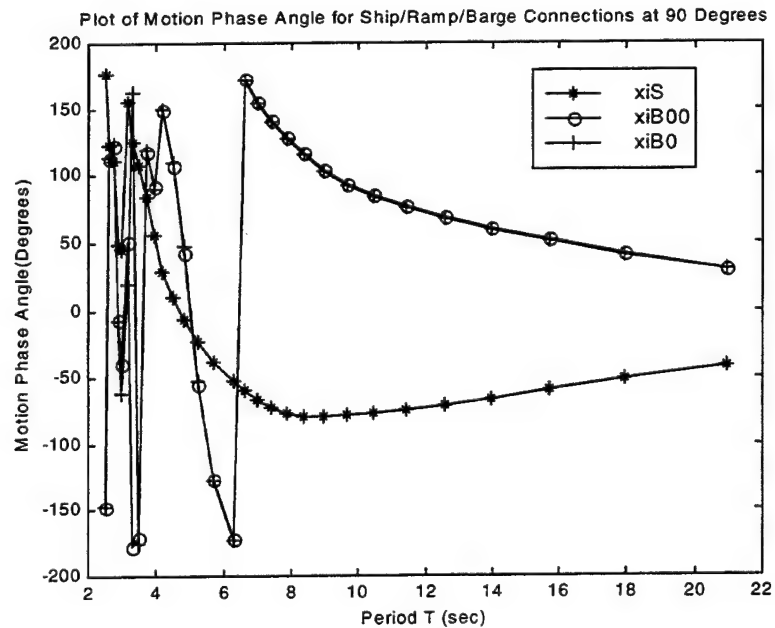
Figure 24. Plot of Vertical Motion Phase Angle at the Ship/Ramp/Barge Connection Points, without Ramp Influence for the Barge, at 90 Degrees Wave Angle.

40
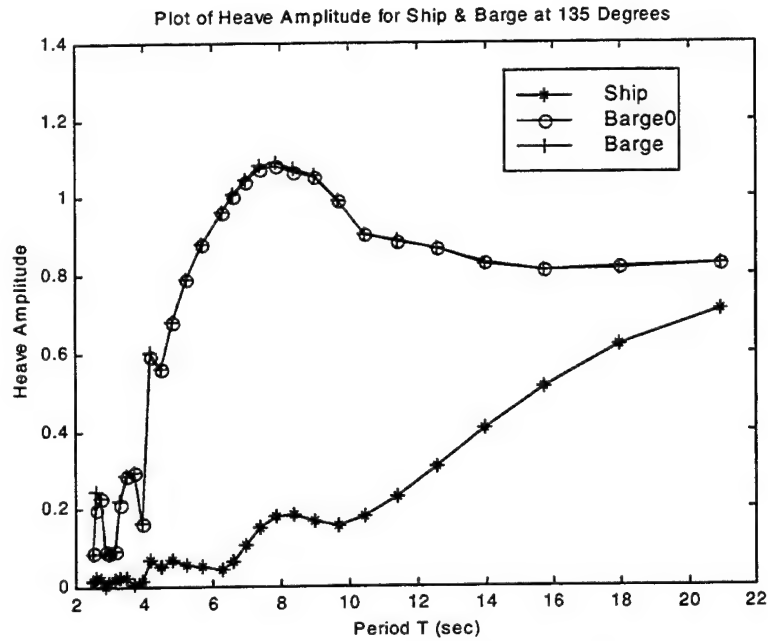
Figure 25. Plot of Heave Amplitude for the Ship, Barge without Ship/Ramp Influence, and Barge without Ramp Influence, at 135 Degrees Wave Angle.
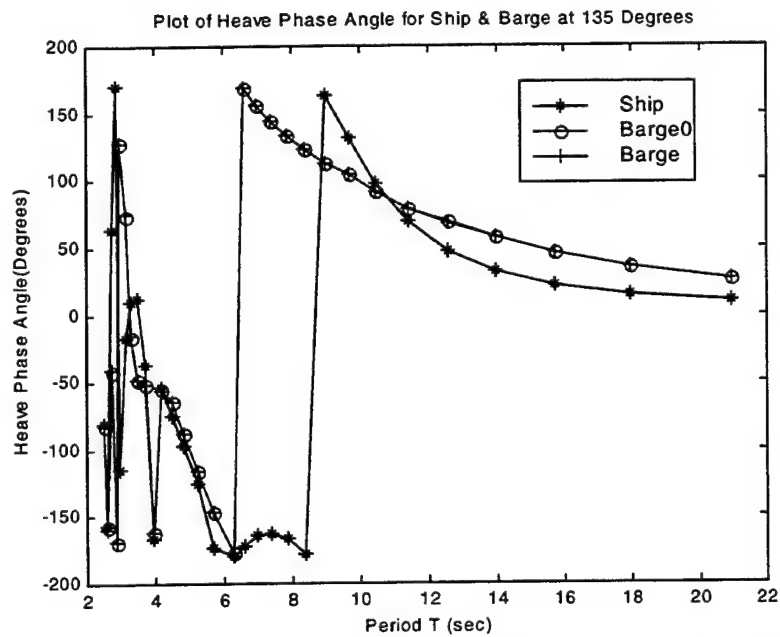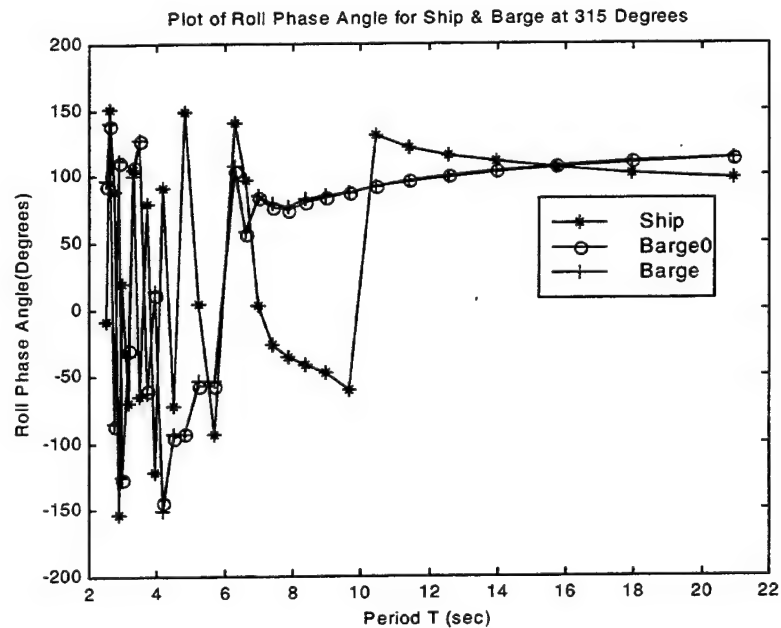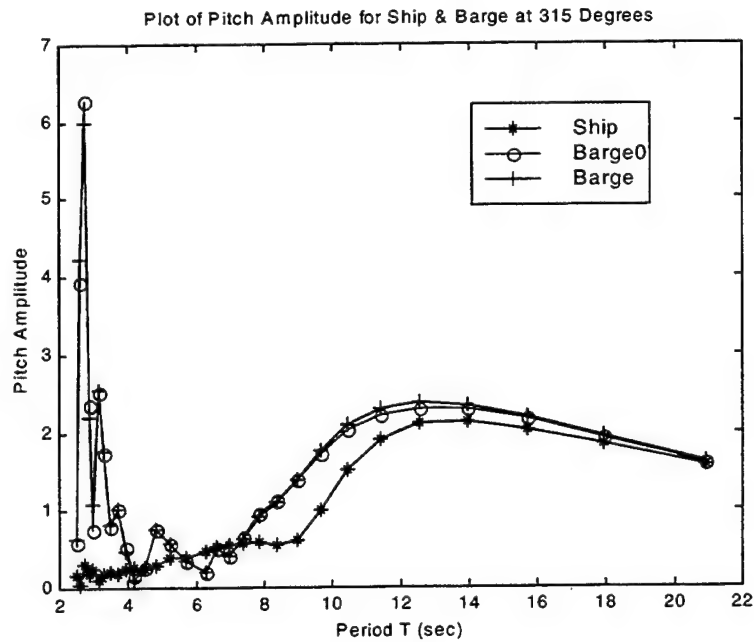

Figure 26. Plot of Heave Phase Angle for the Ship, Barge without Ship/Ramp Influence, and Barge without Ramp Influence, at 135 Degrees Wave Angle.

41
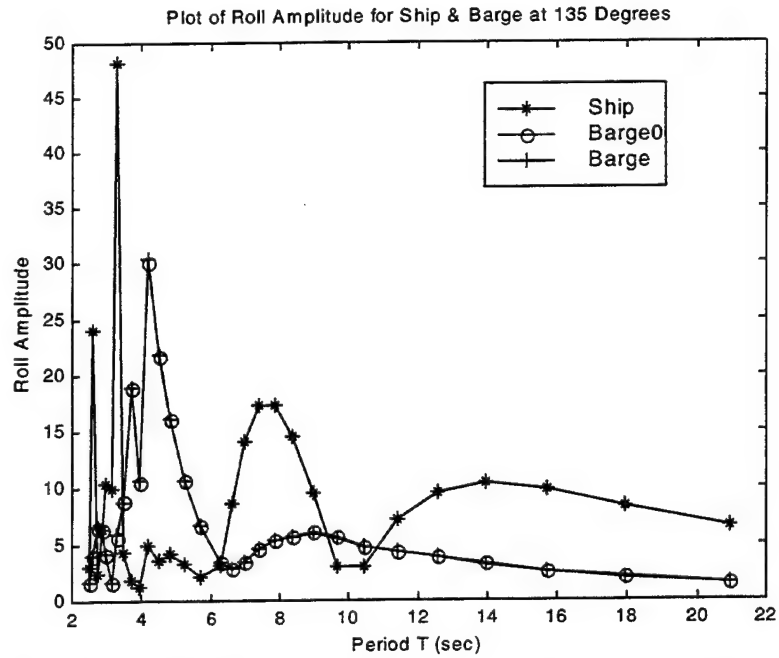
Figure 27. Plot of Roll Amplitude for the Ship, Barge without Ship/Ramp Influence, and Barge without Ramp Influence, at 135 Degrees Wave Angle.
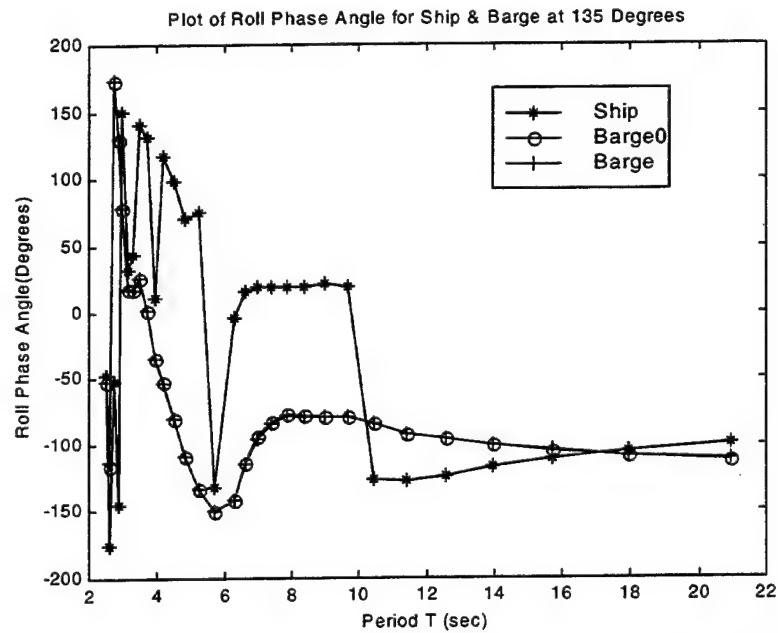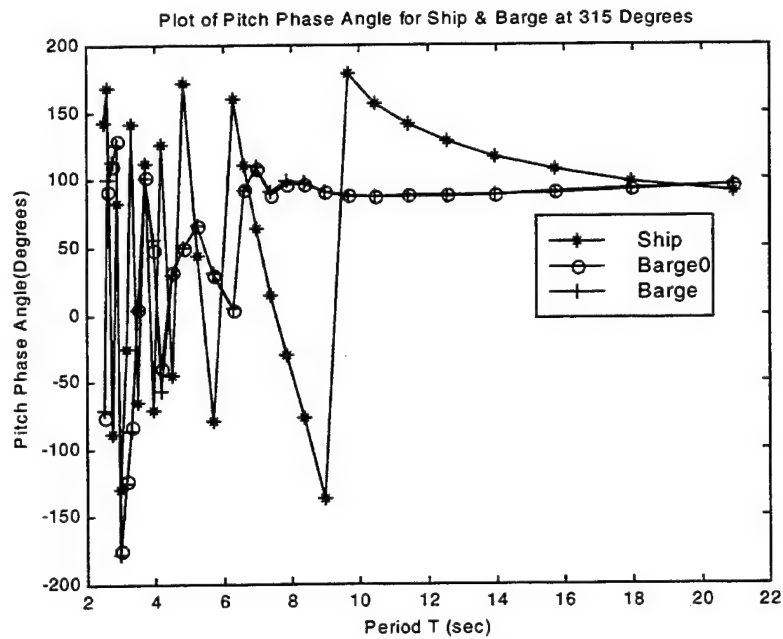

Figure 28. Plot of Roll Phase Angle for the Ship, Barge without Ship/Ramp Influence, and Barge without Ramp Influence, at 135 Degrees Wave Angle.

42
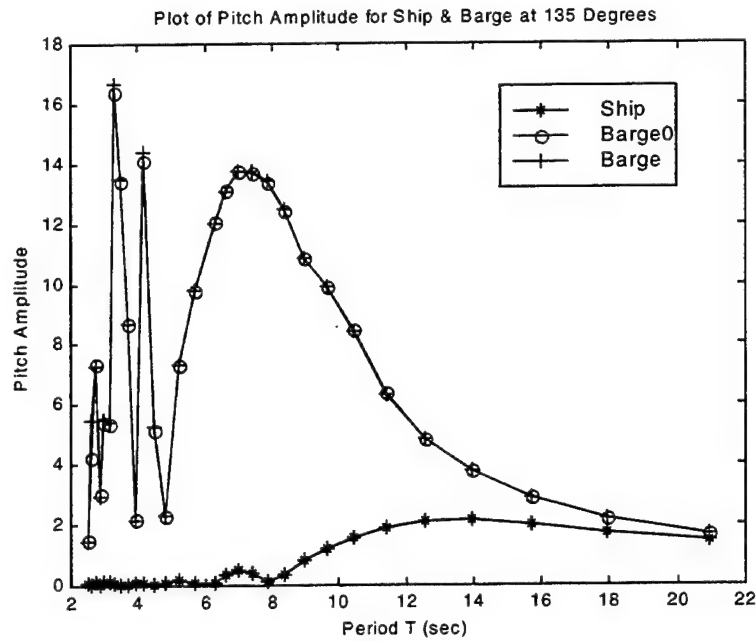
Figure 29. Plot of Pitch Amplitude for the Ship, Barge without Ship/Ramp Influence, and Barge without Ramp Influence, at 135 Degrees Wave Angle.
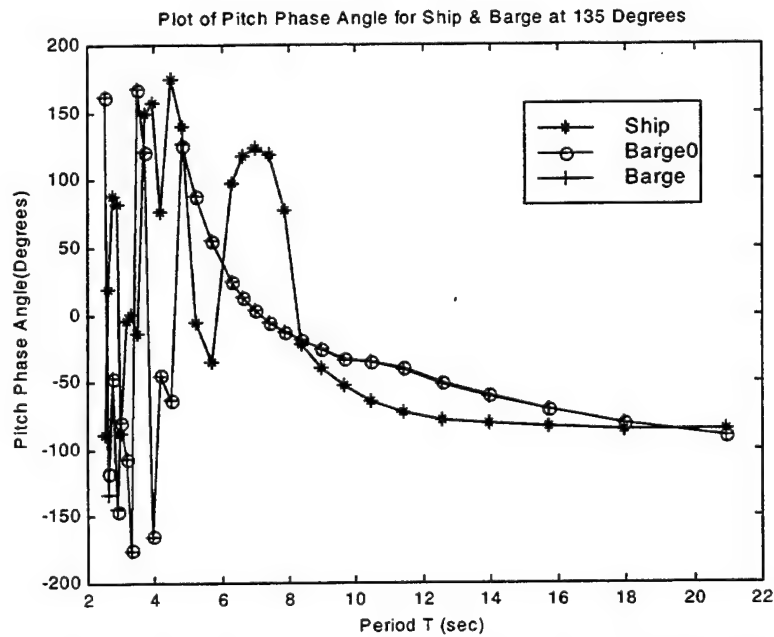
Figure 30. Plot of Pitch Phase Angle for the Ship, Barge without Ship/Ramp Influence, and Barge without Ramp Influence, at 135 Degrees Wave Angle.
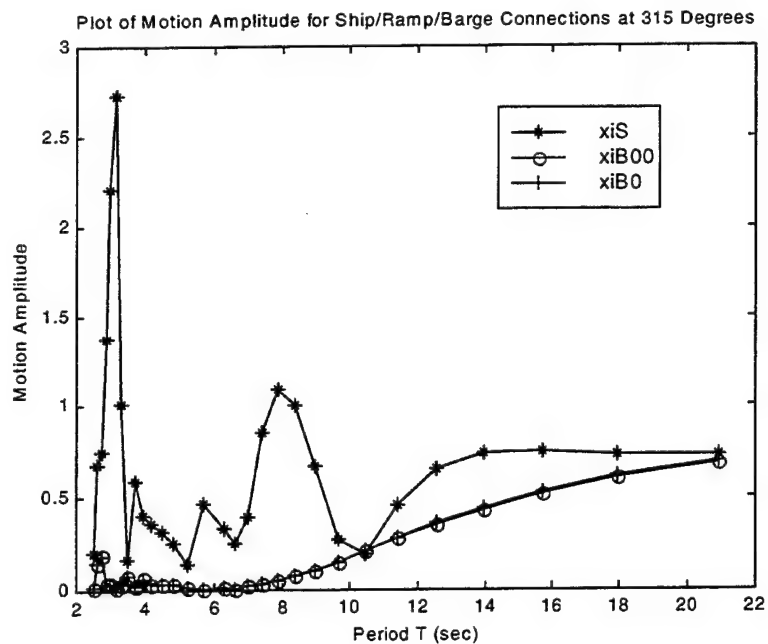
43
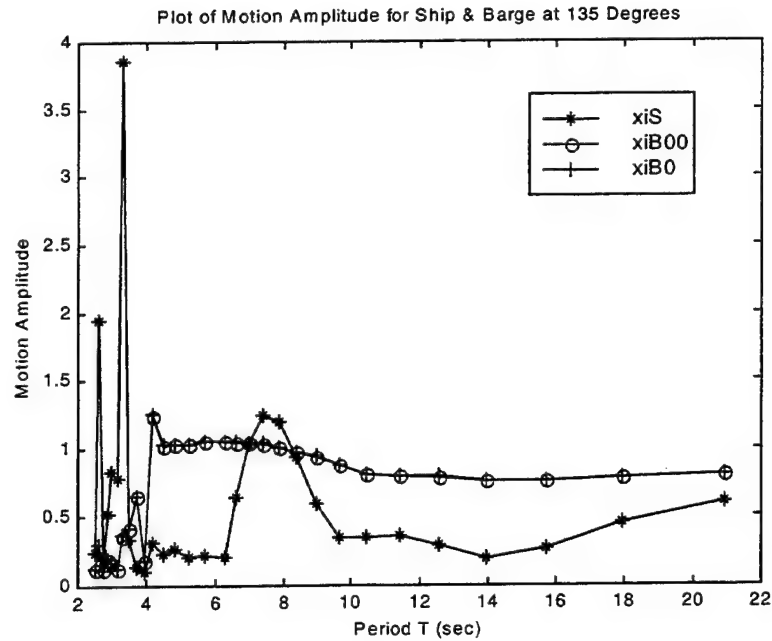
Figure 31. Plot of Vertical Motion Amplitude at the Ship/Ramp/Barge Connection Points, without Ramp Influence for the Barge, at 135 Degrees Wave Angle.
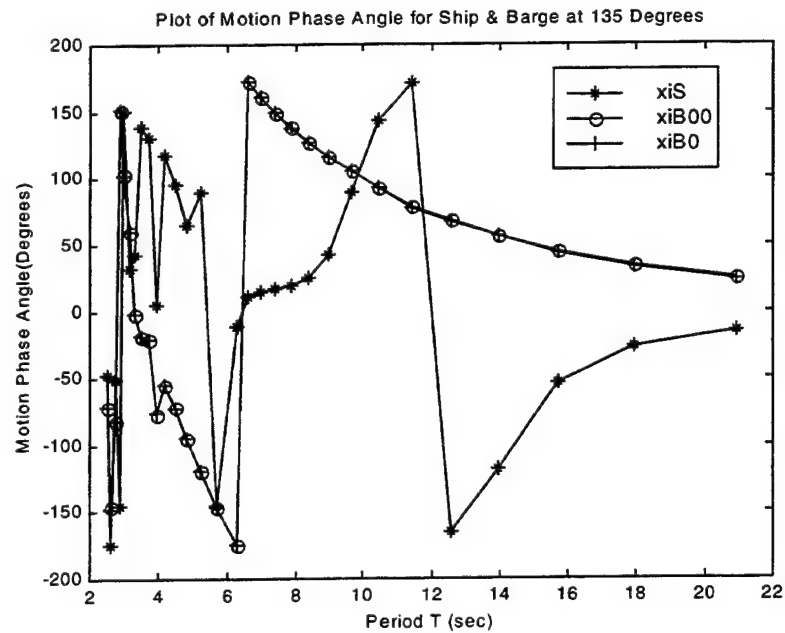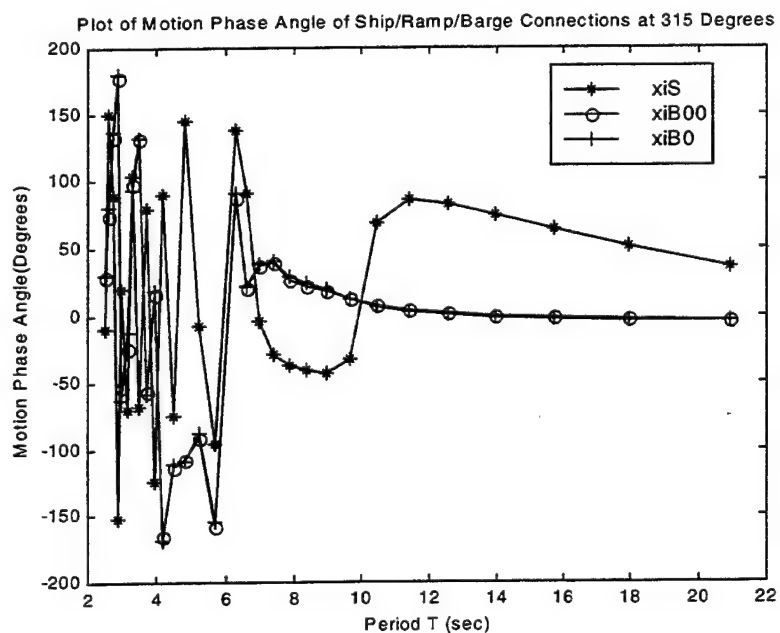

Figure 32. Plot of Vertical Motion Phase Angle at the Ship/Ramp/Barge Connection Points, without Ramp Influence for the Barge, at 135 Degrees Wave Angle.

44
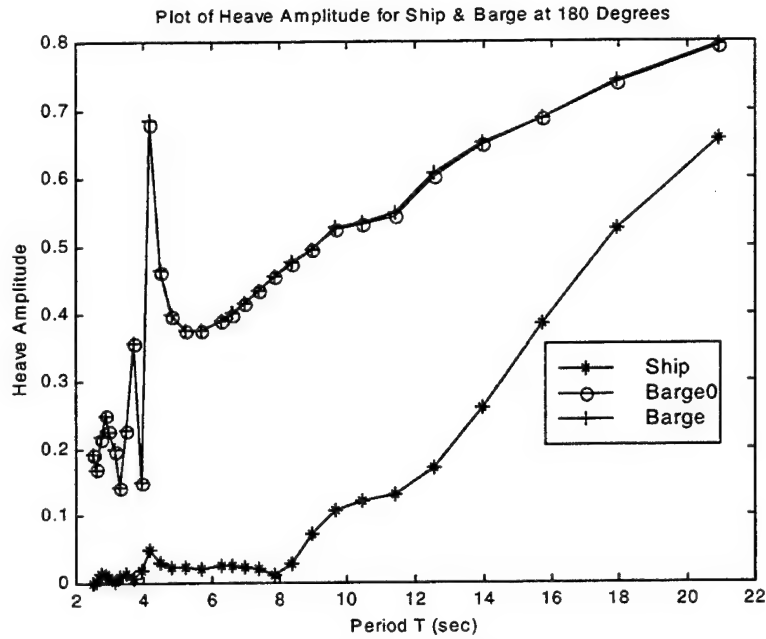
Figure 33. Plot of Heave Amplitude for the Ship, Barge without Ship/Ramp Influence, and Barge without Ramp Influence, at 180 Degrees Wave Angle.
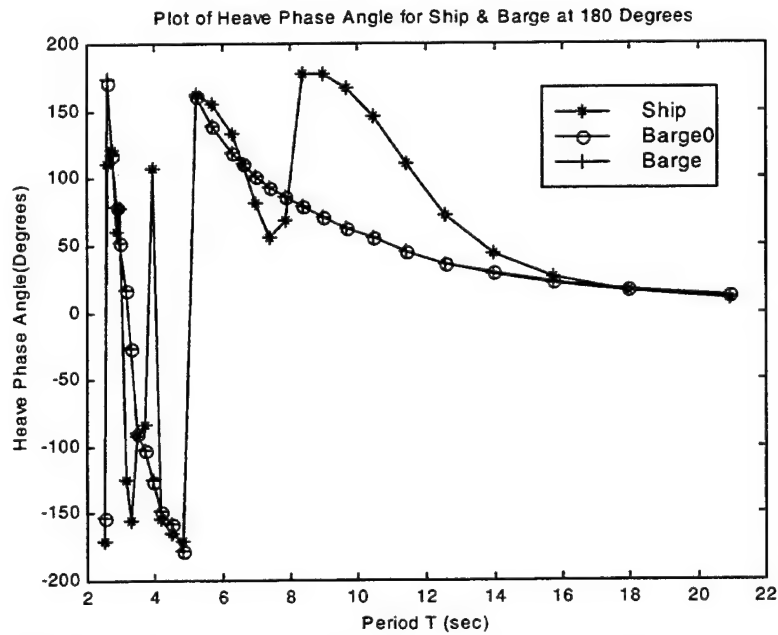
Figure 34. Plot of Heave Phase Angle for the Ship, Barge without Ship/Ramp Influence, and Barge without Ramp Influence, at 180 Degrees Wave Angle.

45
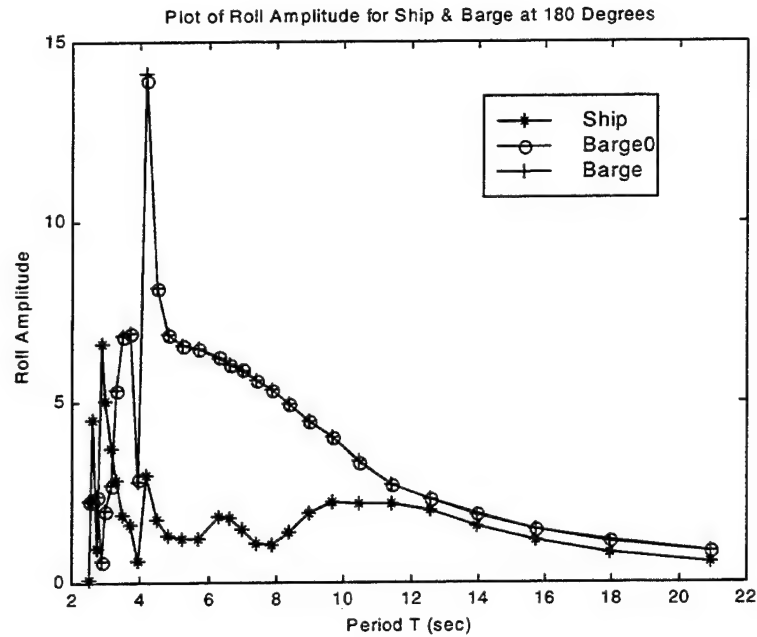
Figure 35. Plot of Roll Amplitude for the Ship, Barge without Ship/Ramp Influence, and Barge without Ramp Influence, at 180 Degrees Wave Angle.
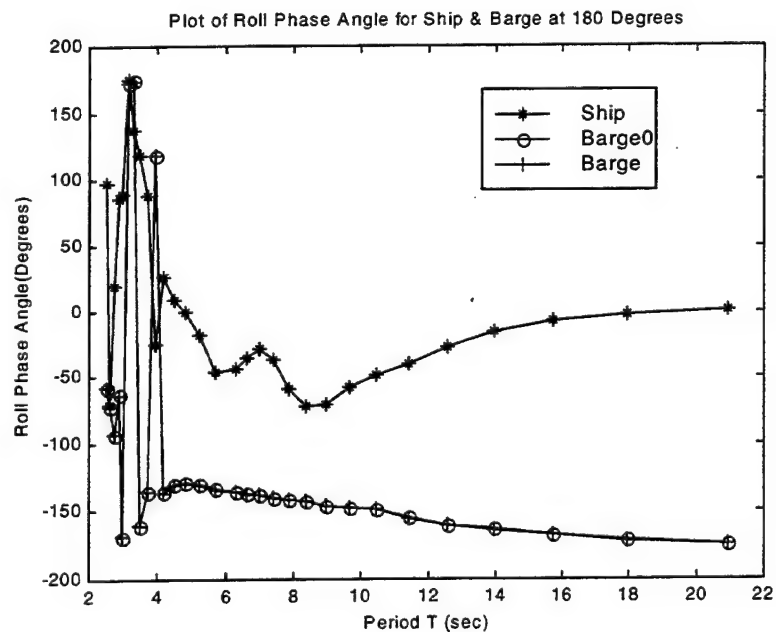
Figure 36. Plot of Roll Phase Angle for the Ship, Barge without Ship/Ramp Influence, and Barge without Ramp Influence, at 180 Degrees Wave Angle.

46
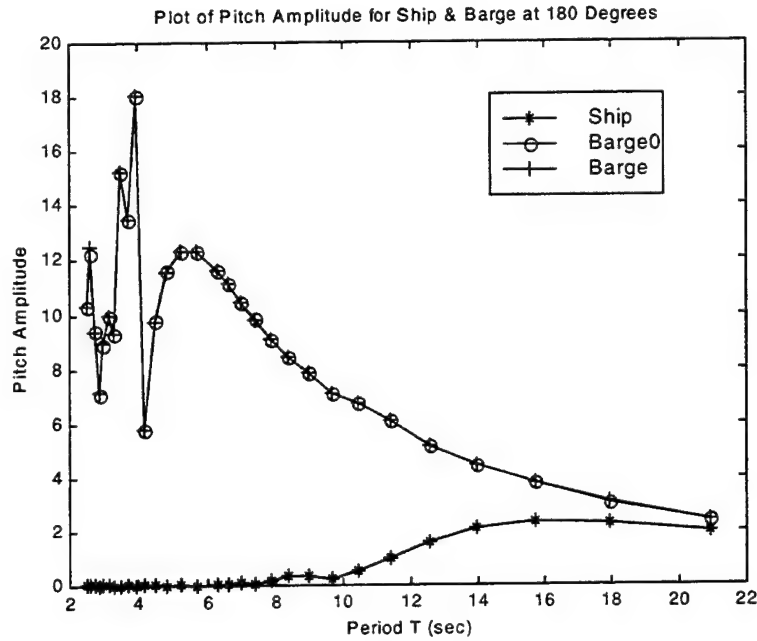
Figure 37. Plot of Pitch Amplitude for the Ship, Barge without Ship/Ramp Influence, and Barge without Ramp Influence, at 180 Degrees Wave Angle.
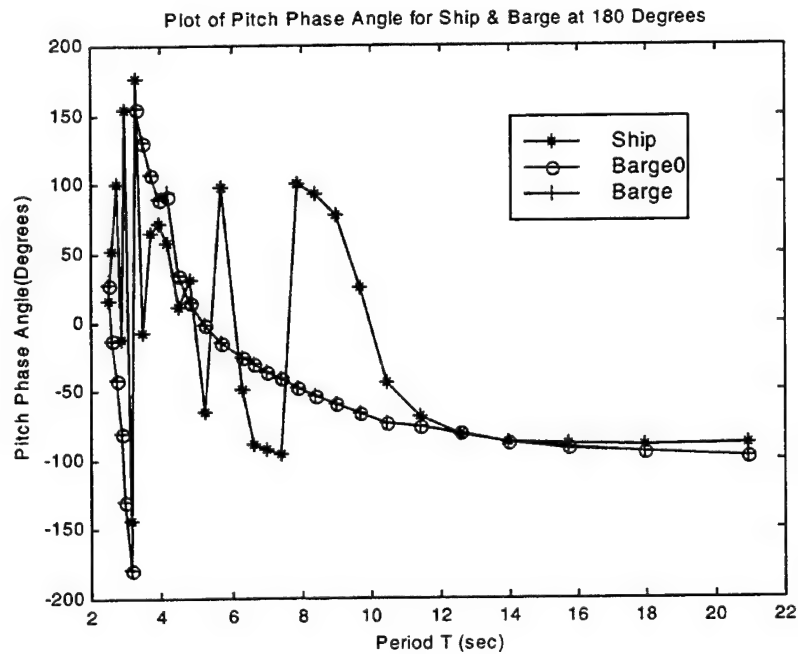
Figure 38. Plot of Pitch Phase Angle for the Ship, Barge without Ship/Ramp Influence, and Barge without Ramp Influence, at 180 Degrees Wave Angle.

47
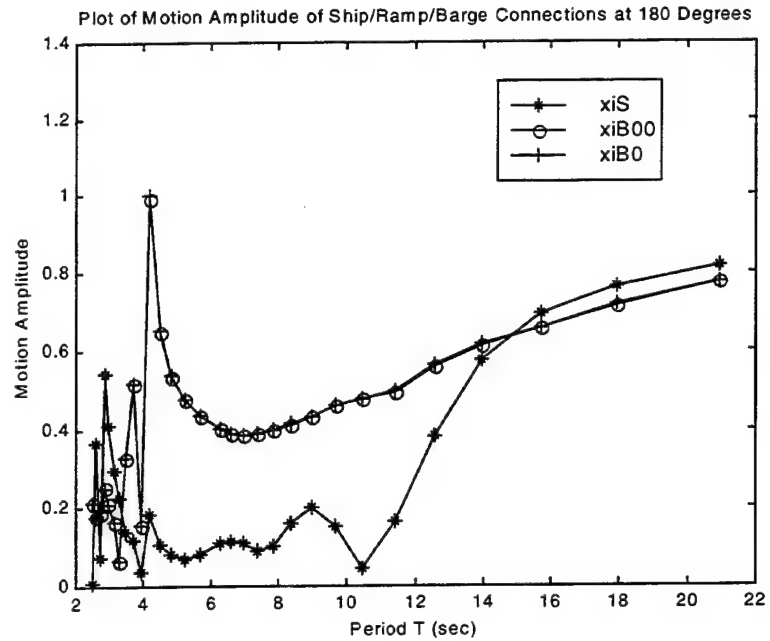
Figure 39. Plot of Vertical Motion Amplitude at the Ship/Ramp/Barge Connection Points, without Ramp Influence for the Barge, at 180 Degrees Wave Angle.
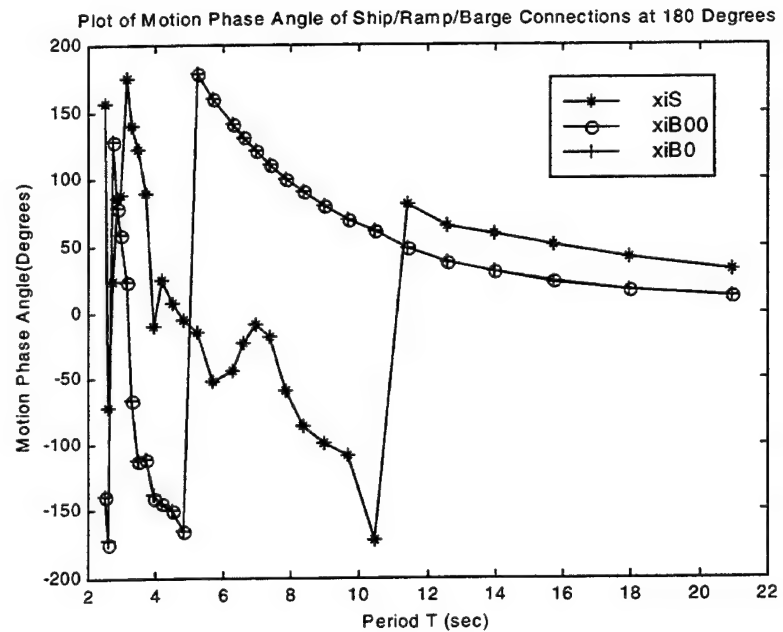
Figure 40. Plot of Vertical Motion Phase Angle at the Ship/Ramp/Barge Connection Points, without Ramp Influence for the Barge, at 180 Degrees Wave Angle.

48
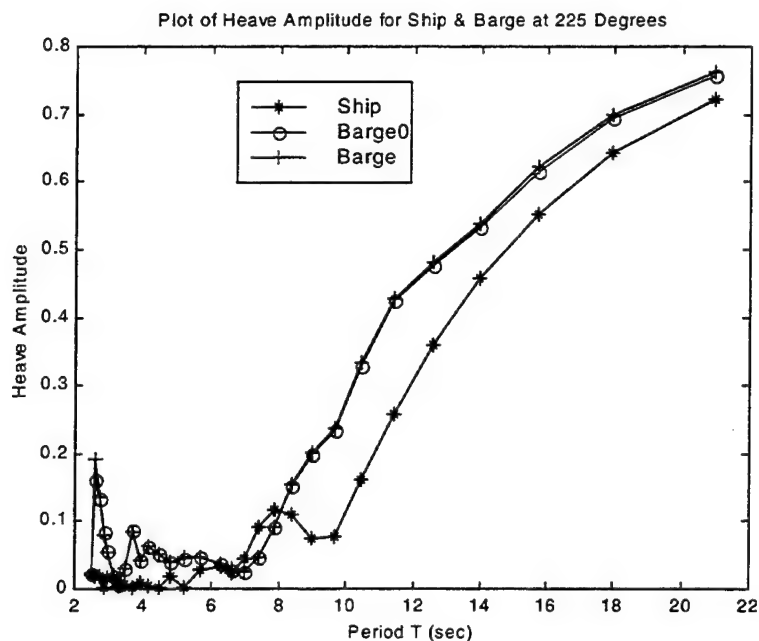
Figure 41. Plot of Heave Amplitude for the Ship, Barge without Ship/Ramp Influence, and Barge without Ramp Influence, at 225 Degrees Wave Angle.
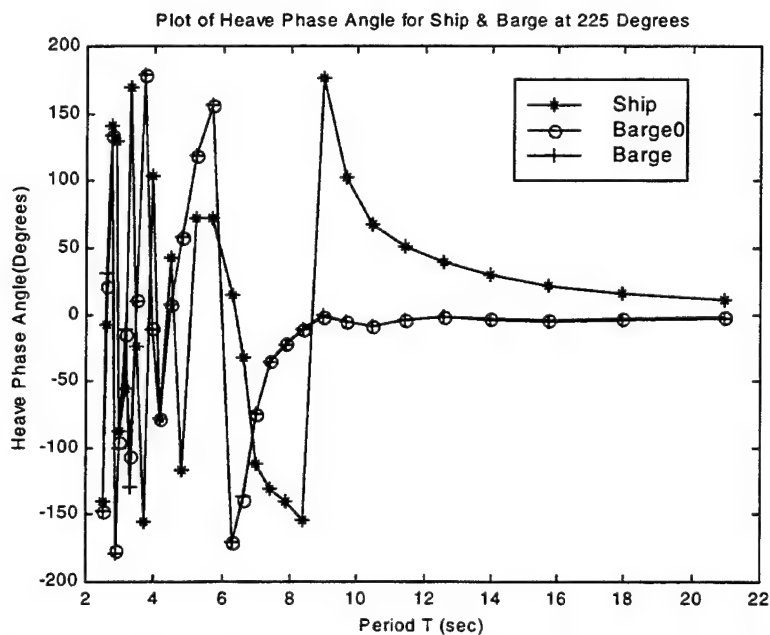
Figure 42. Plot of Heave Phase Angle for the Ship, Barge without Ship/Ramp Influence, and Barge without Ramp Influence, at 225 Degrees Wave Angle.

49

Figure 43. Plot of Roll Amplitude for the Ship, Barge without Ship/Ramp Influence, and Barge without Ramp Influence, at 225 Degrees Wave Angle.

Figure 44. Plot of Roll Phase Angle for the Ship, Barge without Ship/Ramp Influence, and Barge without Ramp Influence, at 225 Degrees Wave Angle.

50

Plot of Pitch Amplitude for Ship & Barge at 225 Degrees

Figure 45. Plot of Pitch Amplitude for the Ship, Barge without Ship/Ramp Influence, and Barge without Ramp Influence, at 225 Degrees Wave Angle.

Plot of Pitch Phase Angle for Ship & Barge at 225 Degrees

Figure 46. Plot of Pitch Phase Angle for the Ship, Barge without Ship/Ramp Influence, and Barge without Ramp Influence, at 225 Degrees Wave Angle.

51

Figure 47. Plot of Vertical Motion Amplitude at the Ship/Ramp/Barge Connection Points, without Ramp Influence for the Barge, at 225 Degrees Wave Angle.

Figure 48. Plot of Vertical Motion Phase Angle at the Ship/Ramp/Barge Connection Points, without Ramp Influence for the Barge, at 225 Degrees Wave Angle.

52

Figure 49. Plot of Heave Amplitude for the Ship, Barge without Ship/Ramp Influence, and Barge without Ramp Influence, at 270 Degrees Wave Angle.

Figure 50. Plot of Heave Phase Angle for the Ship, Barge without Ship/Ramp Influence, and Barge without Ramp Influence, at 270 Degrees Wave Angle.

Figure 51. Plot of Roll Amplitude for the Ship, Barge without Ship/Ramp Influence, and Barge without Ramp Influence, at 270 Degrees Wave Angle.

Figure 52. Plot of Roll Phase Angle for the Ship, Barge without Ship/Ramp Influence, and Barge without Ramp Influence, at 270 Degrees Wave Angle.

54

Figure 53. Plot of Pitch Amplitude for the Ship, Barge without Ship/Ramp Influence, and Barge without Ramp Influence, at 270 Degrees Wave Angle.

Figure 54. Plot of Pitch Phase Angle for the Ship, Barge without Ship/Ramp Influence, and Barge without Ramp Influence, at 270 Degrees Wave Angle.

55

Figure 55. Plot of Vertical Motion Amplitude at the Ship/Ramp/Barge Connection Points, without Ramp Influence for the Barge, at 270 Degrees Wave Angle.

Figure 56. Plot of Vertical Motion Phase Angle at the Ship/Ramp/Barge Connection Points, without Ramp Influence for the Barge, at 270 Degrees Wave Angle.

56

Figure 57. Plot of Heave Amplitude for the Ship, Barge without Ship/Ramp Influence, and Barge without Ramp Influence, at 315 Degrees Wave Angle.

Figure 58. Plot of Heave Phase Angle for the Ship, Barge without Ship/Ramp Influence, and Barge without Ramp Influence, at 315 Degrees Wave Angle.

57

Figure 59. Plot of Roll Amplitude for the Ship, Barge without Ship/Ramp Influence, and Barge without Ramp Influence, at 315 Degrees Wave Angle.

Figure 60. Plot of Roll Phase Angle for the Ship, Barge without Ship/Ramp Influence, and Barge without Ramp Influence, at 315 Degrees Wave Angle.

Figure 61. Plot of Pitch Amplitude for the Ship, Barge without Ship/Ramp Influence, and Barge without Ramp Influence, at 315 Degrees Wave Angle.

Figure 62. Plot of Pitch Phase Angle for the Ship, Barge without Ship/Ramp Influence, and Barge without Ramp Influence, at 315 Degrees Wave Angle.

59

Figure 63. Plot of Vertical Motion Amplitude at the Ship/Ramp/Barge Connection Points, without Ramp Influence for the Barge, at 315 Degrees Wave Angle.

Figure 64. Plot of Vertical Motion Phase Angle at the Ship/Ramp/Barge Connection Points, without Ramp Influence for the Barge, at 315 Degrees Wave Angle.

C.   RAMP ANALYSIS

The Ramp is assumed to be a simply supported beam with a simple hinge connection on the ship, while the connection on the barge is modeled as a spring-damper connection. Table 4 shows the dimensions of the ramp.

Description	Dimensions
Ramp Length (Pivot to Pivot)	165 ft (50.29 m)
Ramp Width	20 ft (5.48 m)
Ramp Weight	96.94 LT
Young's Modulus	2.7e+11 N/m2
Moment of Inertia	0.01 m4

Table 4. Ramp (beam) Dimensions

Figures 65 through 96 display the results for the Ship/Ramp/Barge Connection Points Responses (Vertical Motion Amplitudes) for various values of the stiffness and damping of the Ramp/Barge Spring-Damper Connection Model, ranging again from zero degrees through 315 degrees Wave Angle at 45-degree intervals. For comparison purposes, the Vertical Motion Amplitude of the Ramp/Barge Connection without Ramp Influence (xiB0), is also included in the above figures.

The results for the Ramp Excitation Force on the Ramp/Barge Connection Point, as well as the corresponding Motion Amplitude of the Connection, for different values of the isolator stiffness (k) and damping (c), and Incident Wave Angle ranging from zero through 315 degrees, are presented in Figures 97 through 112.

Figures 113 through 116 display, for comparison purposes, the Ramp Excitation Force on the Ramp/Barge Connection Point, each time for specific values of stiffness (k)

61

and damping (c), but at Various Wave Angles.

The frequency response characteristics for the ramp in the above results were obtained after assuming that the ramp rigidity is described by equations (50), (51), and (52). The natural frequency ω_n that was used here corresponds to the fundamental frequency of a system of a simply supported beam having a total mass m_b, and a concentrated mass M at mid-span, as described in pages 24,25 of [Ref 6], and it is given by equation (52). The above consideration corresponds to an envisioned worse case scenario of one tank breaking down in the middle of the ramp and a second one providing assistance during a military equipment and machinery transfer from the ship to the barge through the connected ramp system.

The results of the following figures demonstrate the influence of the assumed isolator properties on motions, and consequently ramp stresses. Note that this influence is not monotonic throughout the frequency range, which suggests that optimization of isolator properties is, in principle, possible. Such optimization will be performed in random seas in the following chapter.
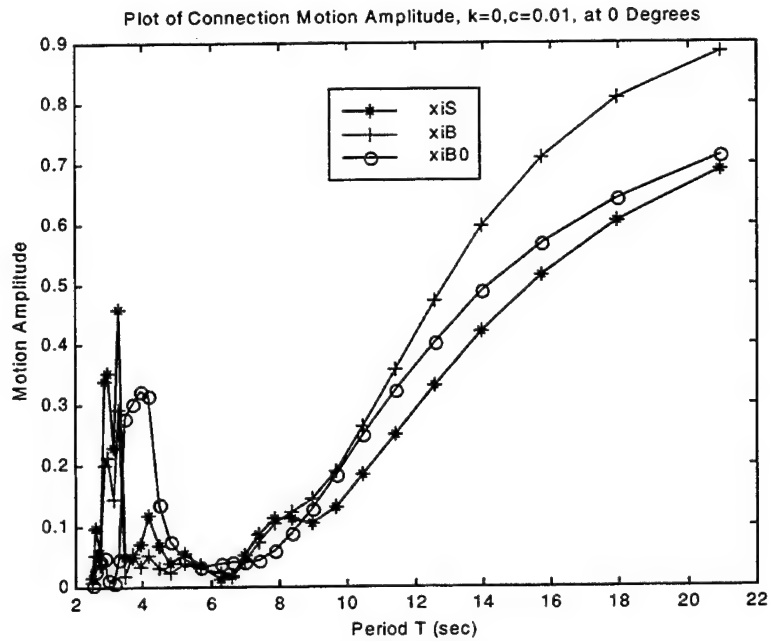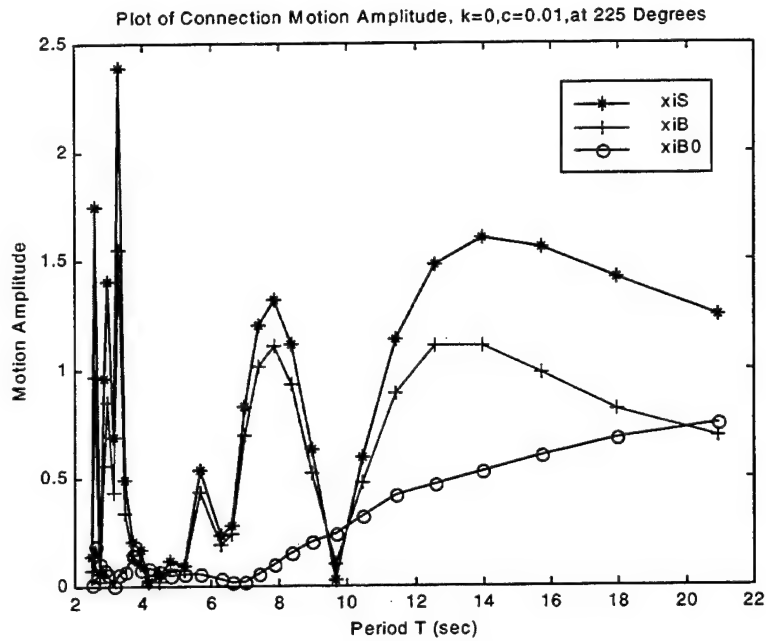
Figure 65. Plot of Vertical Motion Amplitude for the Ship/Ramp/Barge Connection Points, for k = 0, c = 0.01, at 0 Degrees Wave Angle.
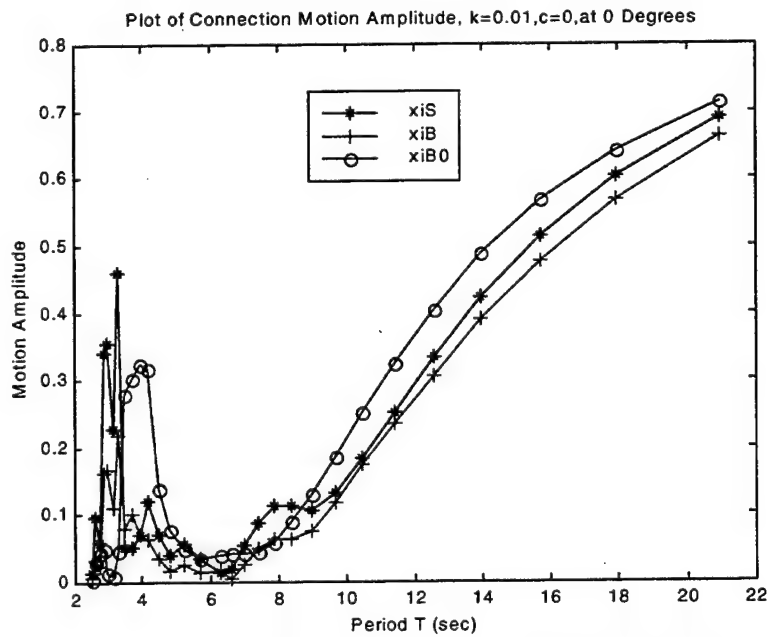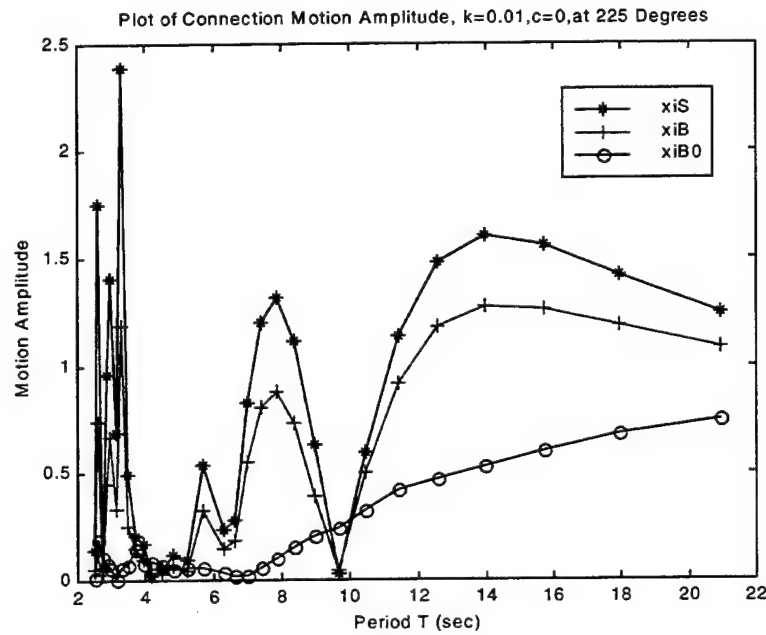

Figure 66. Plot of Vertical Motion Amplitude for the Ship/Ramp/Barge Connection Points, for k = 0.01, c = 0, at 0 Degrees Wave Angle.
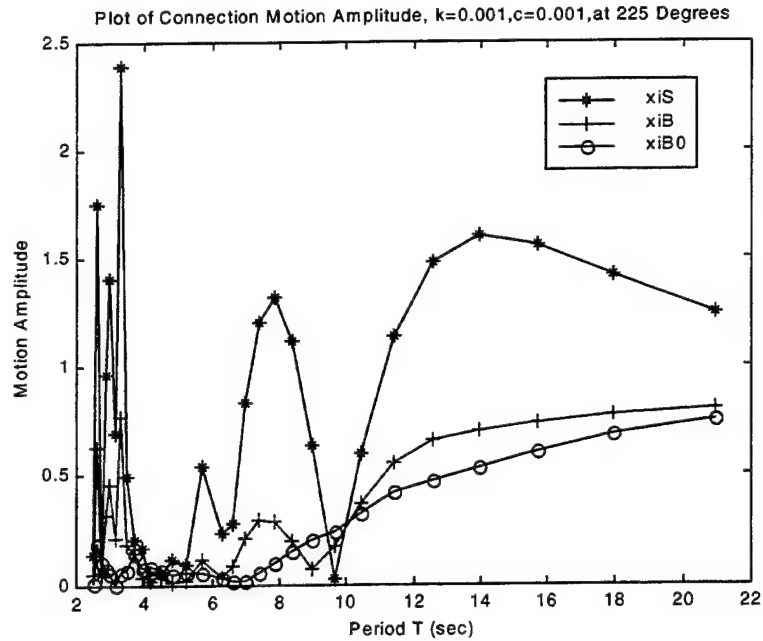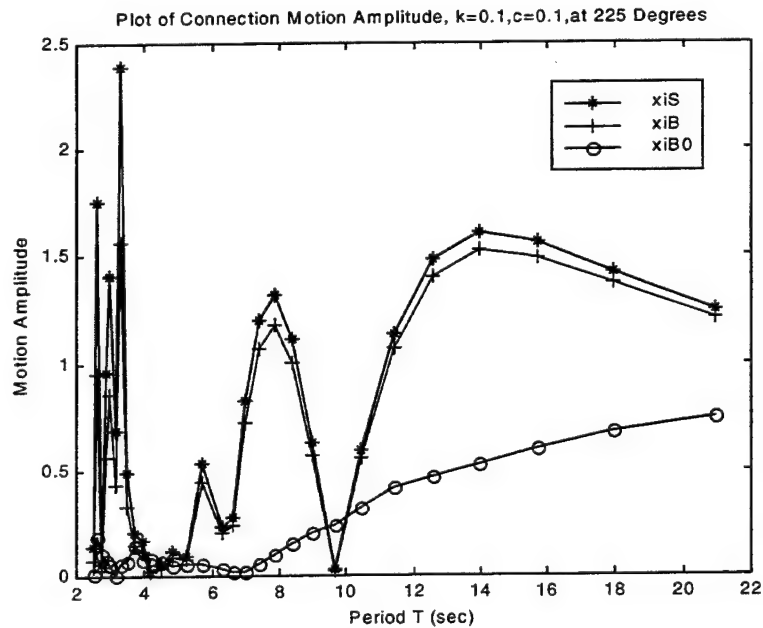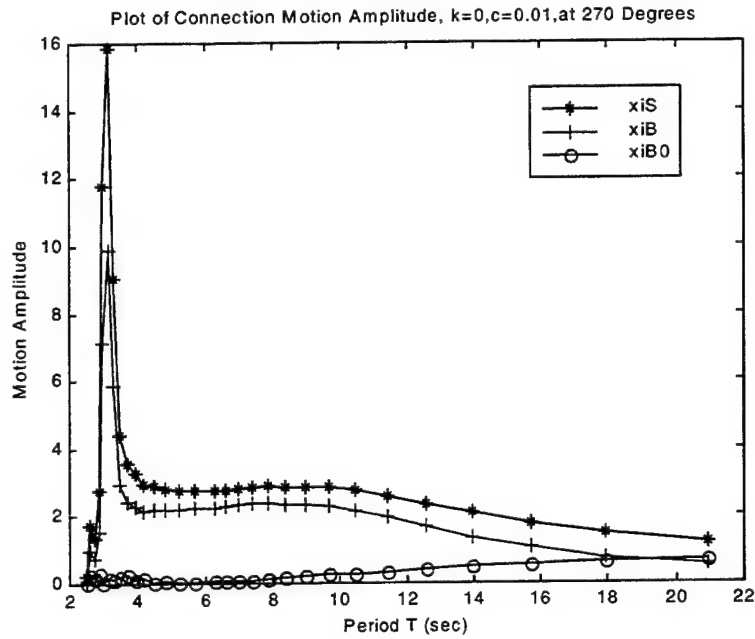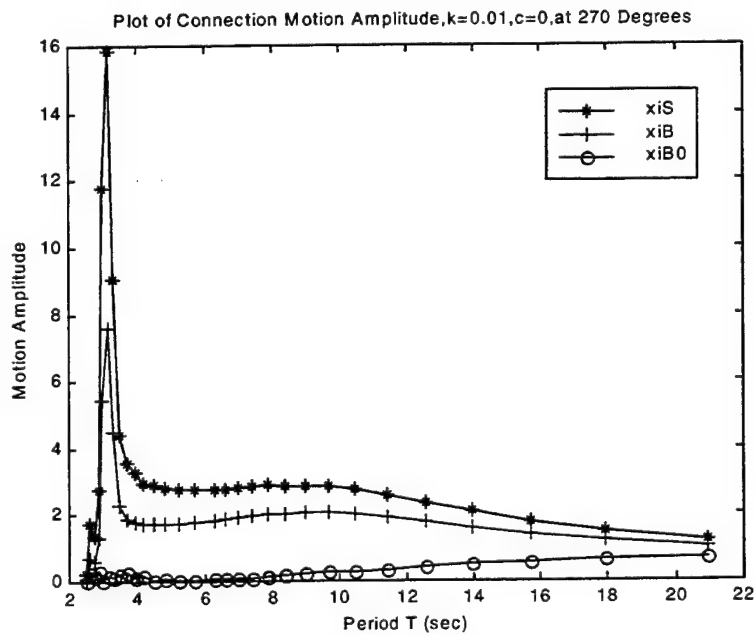
63
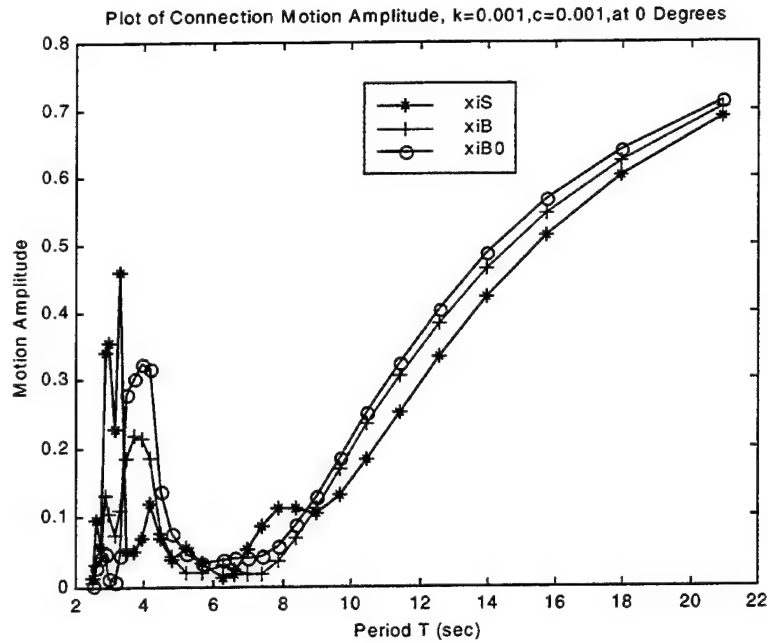
Figure 67. Plot of Vertical Motion Amplitude for the Ship/Ramp/Barge
Connection Points, for k = 0.001, c = 0.001, at 0 Degrees Wave Angle.
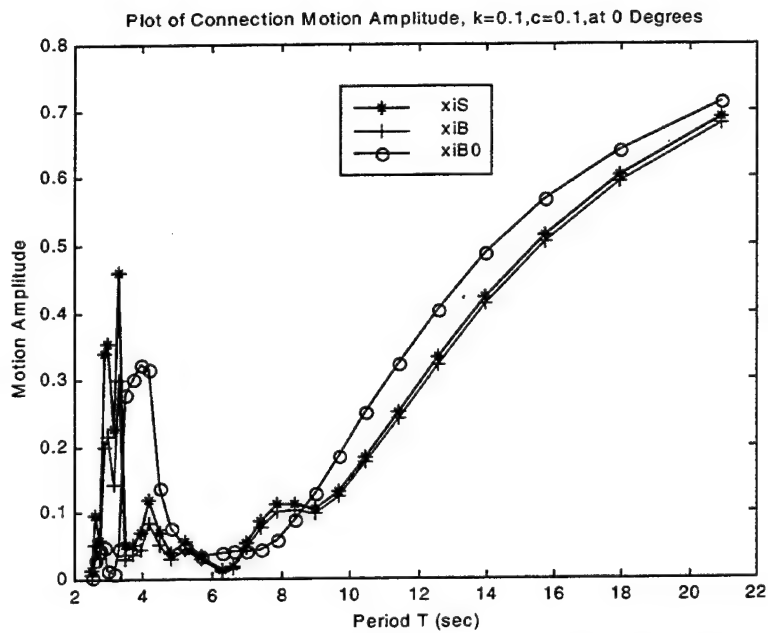
Figure 68. Plot of Vertical Motion Amplitude for the Ship/Ramp/Barge
Connection Points, for k = 0.1, c = 0.1, at 0 Degrees Wave Angle.
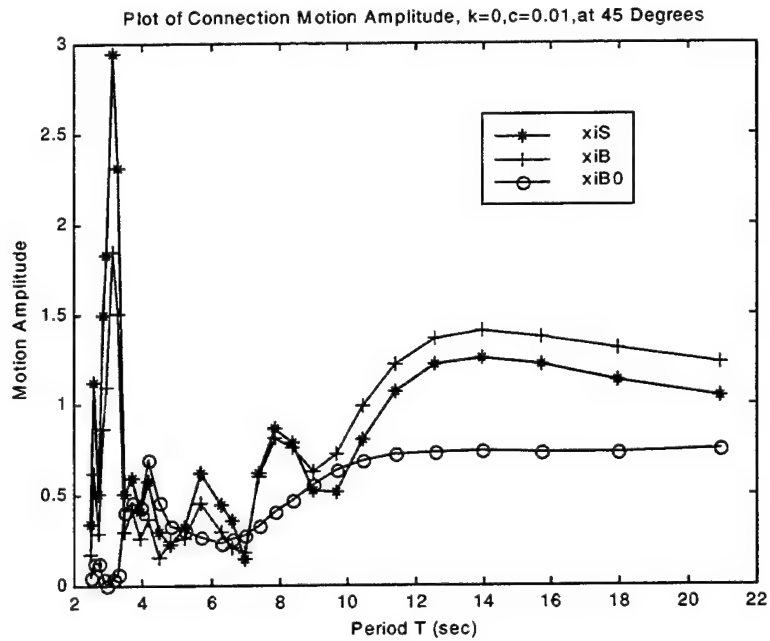
Figure 69. Plot of Vertical Motion Amplitude for the Ship/Ramp/Barge
Connection Points, for k = 0, c = 0.01, at 45 Degrees Wave Angle.
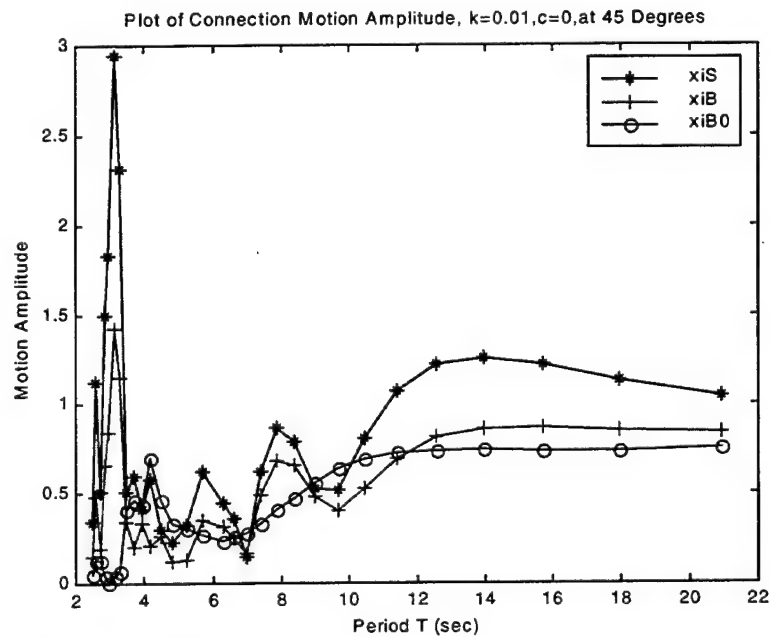
Figure 70. Plot of Vertical Motion Amplitude for the Ship/Ramp/Barge
Connection Points, for k = 0.01, c = 0, at 45 Degrees Wave Angle.

65
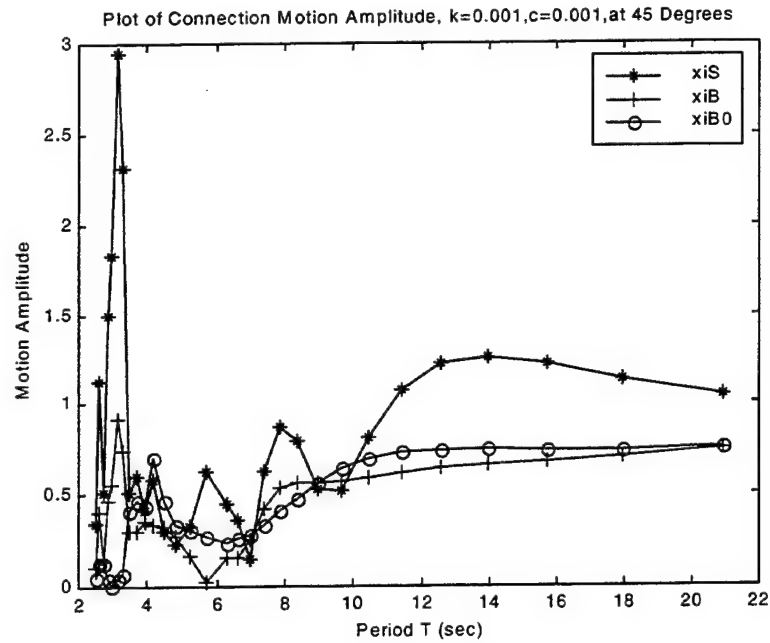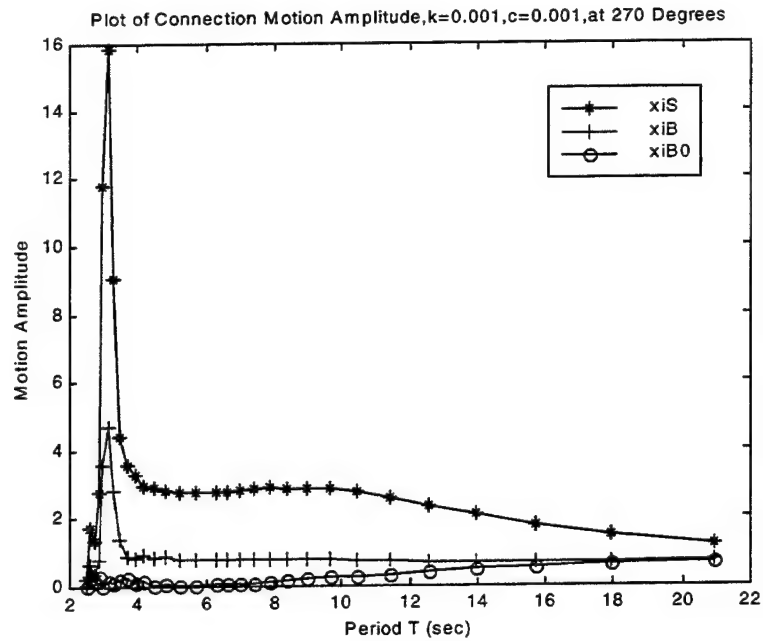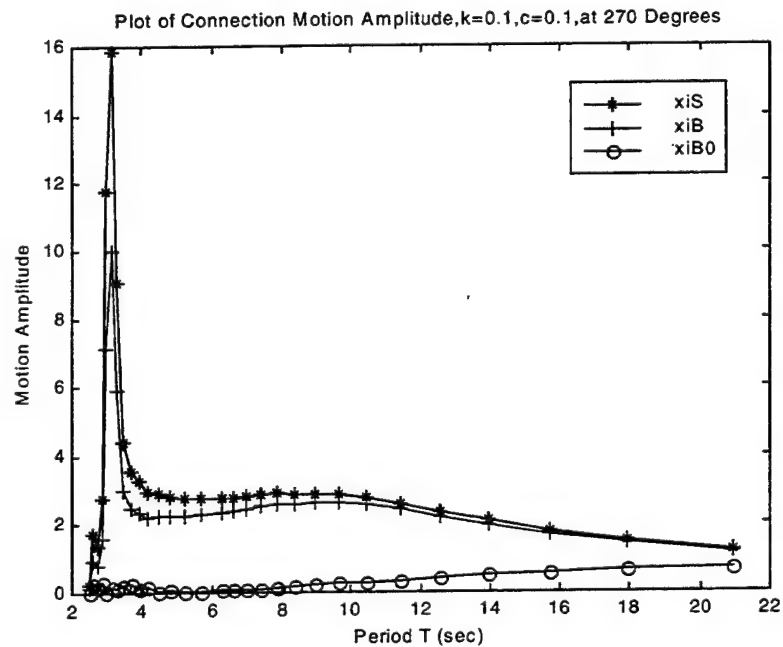
Figure 71. Plot of Vertical Motion Amplitude for the Ship/Ramp/Barge Connection Points, for k = 0.001, c = 0.001, at 45 Degrees Wave Angle.
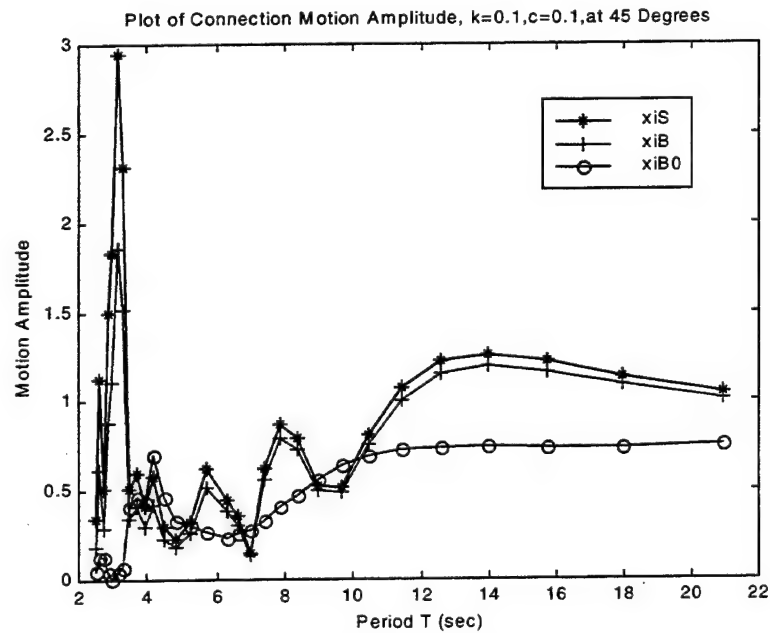
Figure 72. Plot of Vertical Motion Amplitude for the Ship/Ramp/Barge Connection Points, for k = 0.1, c = 0.1, at 45 Degrees Wave Angle.
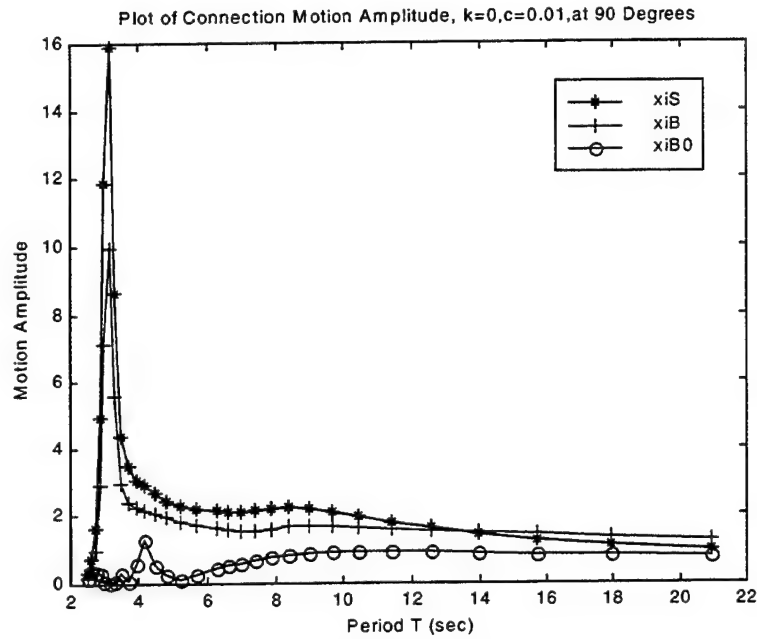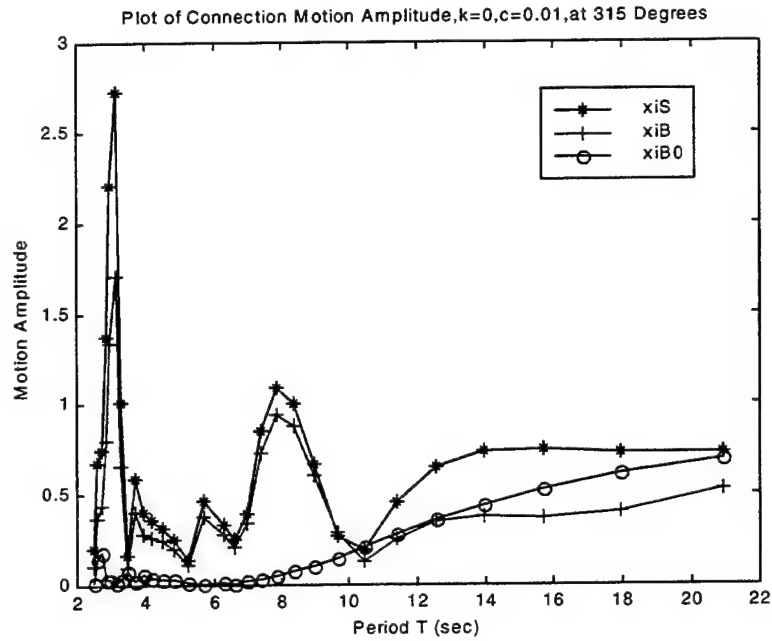
Figure 73. Plot of Vertical Motion Amplitude for the Ship/Ramp/Barge Connection Points, for k = 0, c = 0.01, at 90 Degrees Wave Angle.
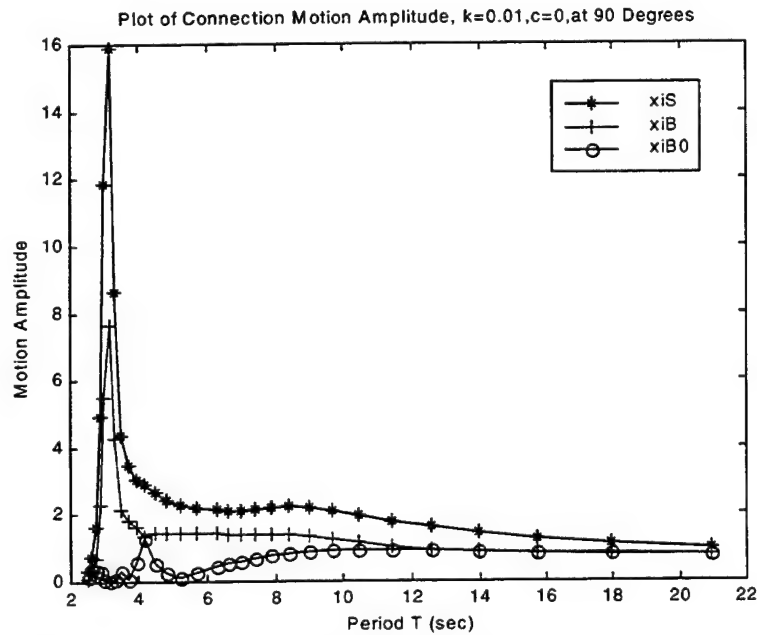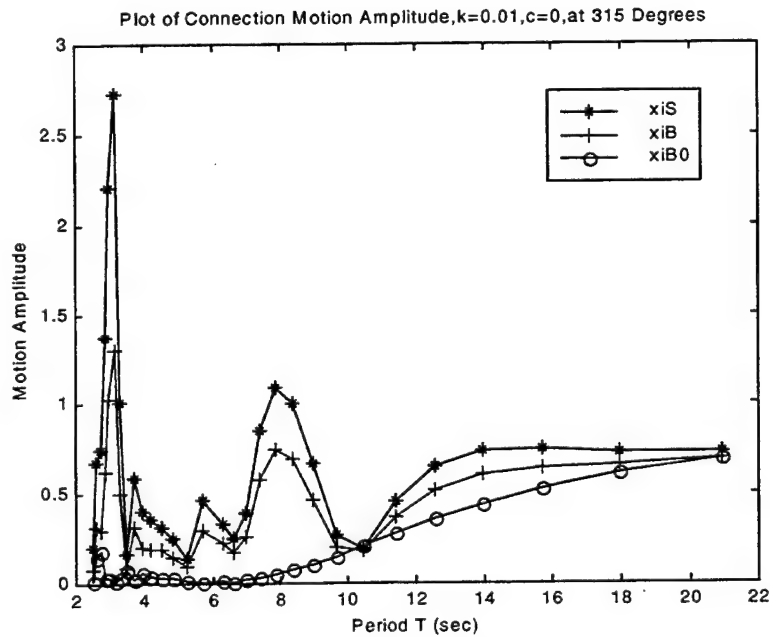

Figure 74. Plot of Vertical Motion Amplitude for the Ship/Ramp/Barge Connection Points, for k = 0.01, c = 0, at 90 Degrees Wave Angle.
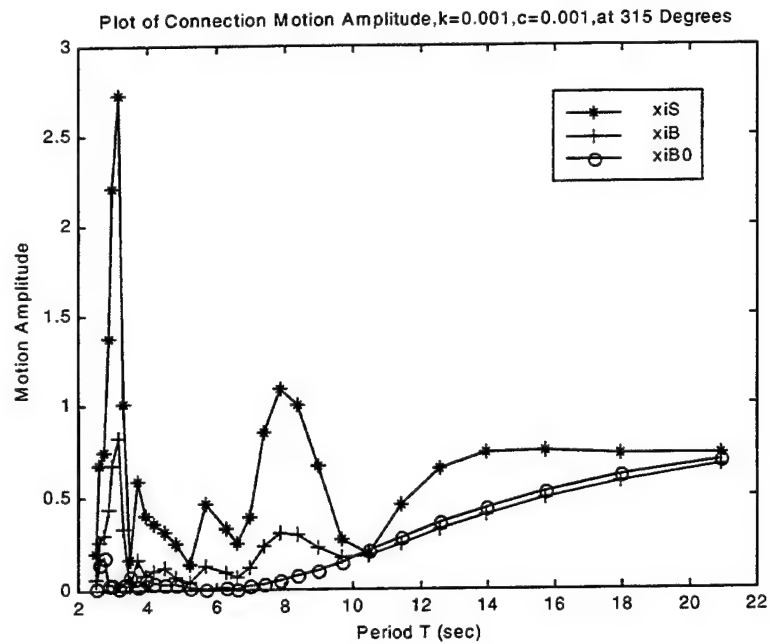
67
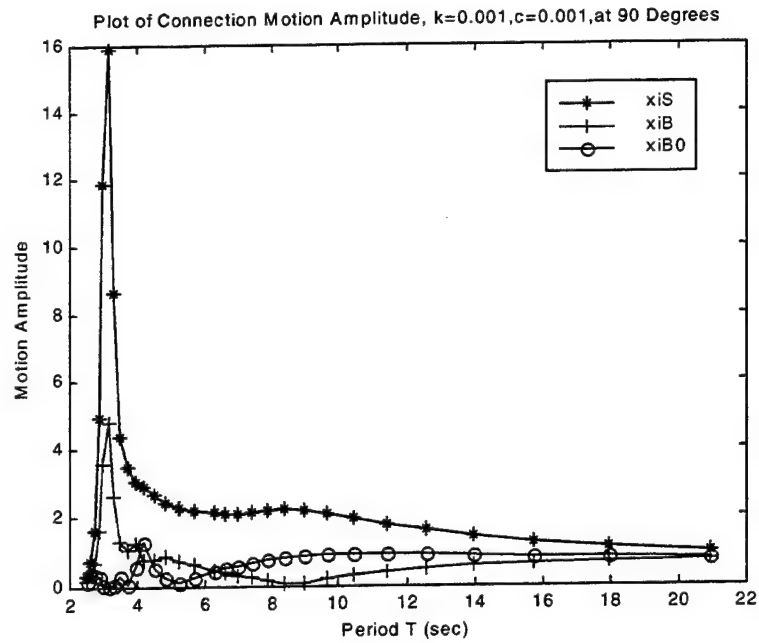
Figure 75. Plot of Vertical Motion Amplitude for the Ship/Ramp/Barge Connection Points, for k = 0.001, c = 0.001, at 90 Degrees Wave Angle.
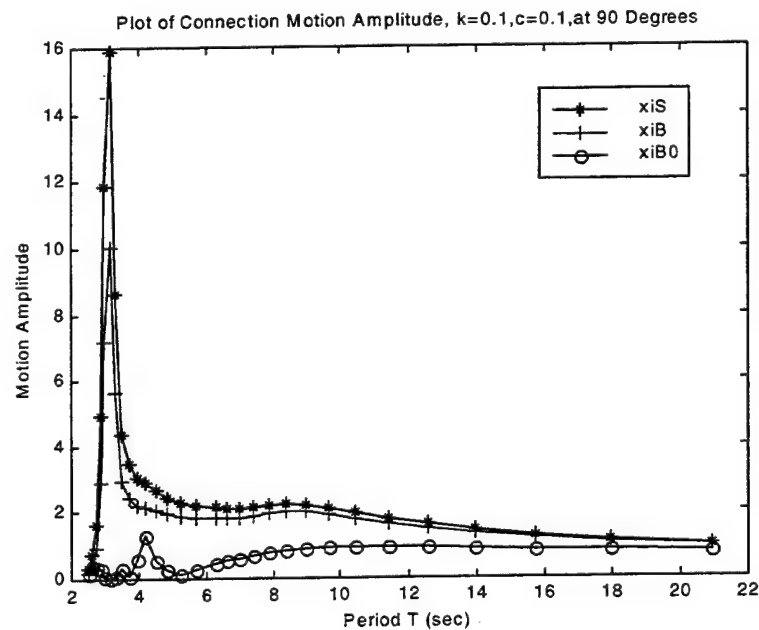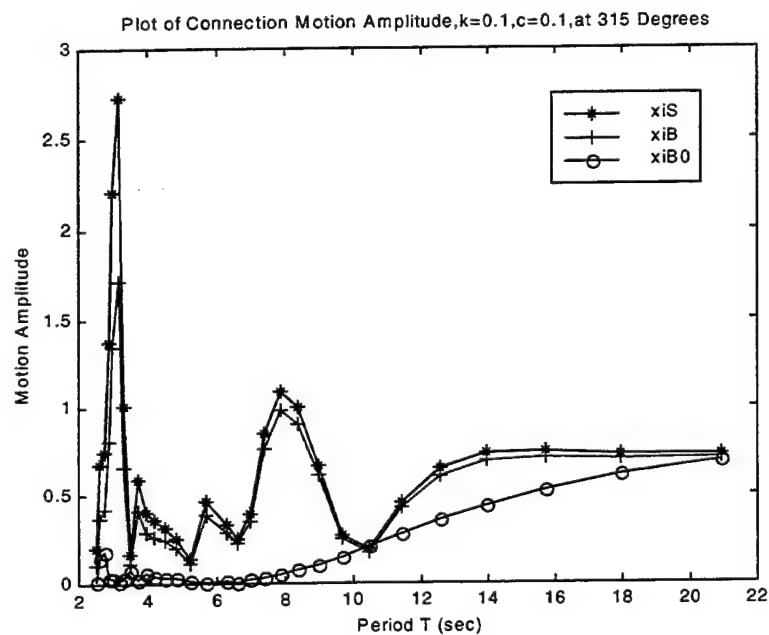

Figure 76. Plot of Vertical Motion Amplitude for the Ship/Ramp/Barge Connection Points, for k = 0.1, c = 0.1, at 90 Degrees Wave Angle.

68
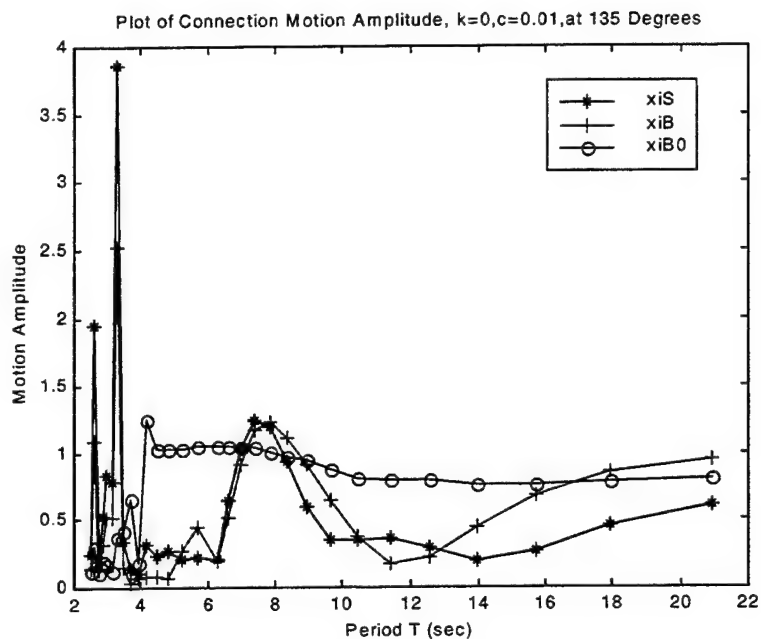
Figure 77. Plot of Vertical Motion Amplitude for the Ship/Ramp/Barge
Connection Points, for k = 0, c = 0.01, at 135 Degrees Wave Angle.
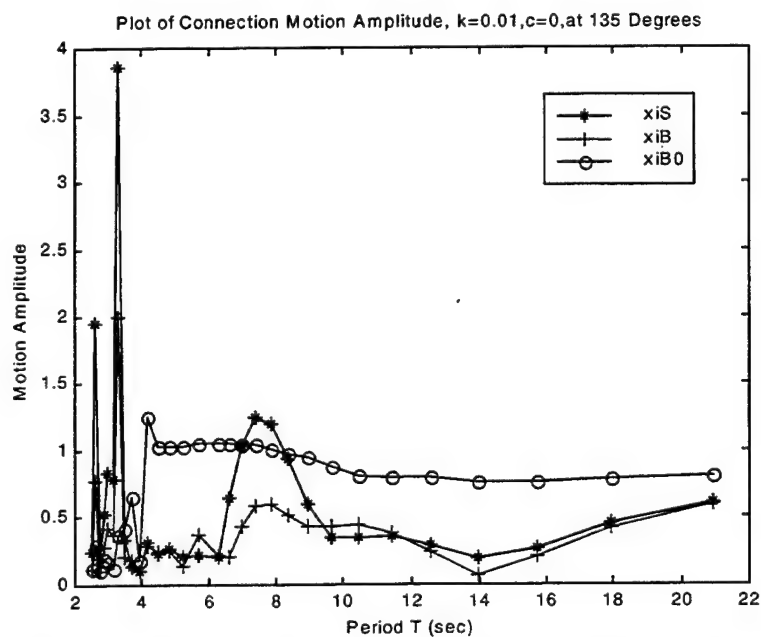

Figure 78. Plot of Vertical Motion Amplitude for the Ship/Ramp/Barge
Connection Points, for k = 0.01, c = 0, at 135 Degrees Wave Angle.

69
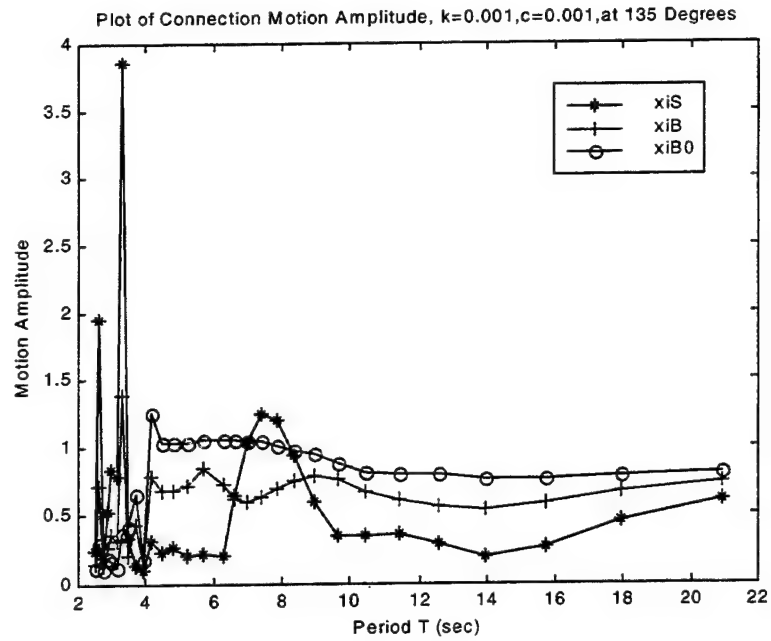
Figure 79. Plot of Vertical Motion Amplitude for the Ship/Ramp/Barge
Connection Points, for k = 0.001, c = 0.001, at 135 Degrees Wave Angle.
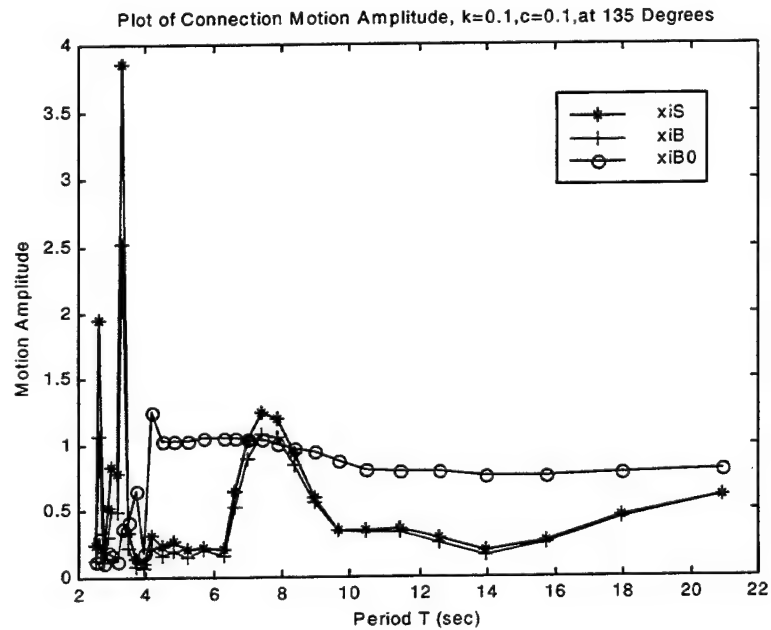
Figure 80. Plot of Vertical Motion Amplitude for the Ship/Ramp/Barge
Connection Points, for k = 0.1, c = 0.1, at 135 Degrees Wave Angle.

70

Plot of Connection Motion Amplitude, k=0,c=0.01,at 180 Degrees
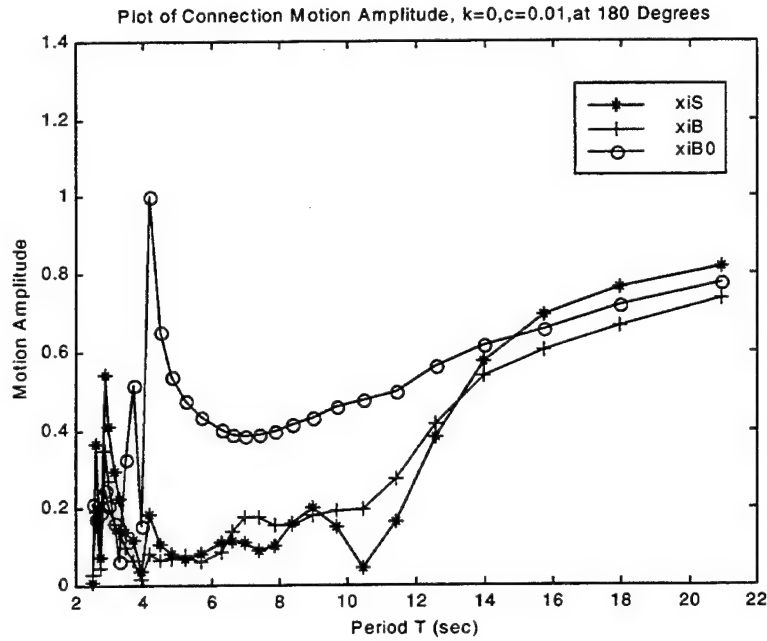
Figure 81. Plot of Vertical Motion Amplitude for the Ship/Ramp/Barge Connection Points, for k = 0, c = 0.01, at 180 Degrees Wave Angle.

Plot of Connection Motion Amplitude, k=0.01,c=0,at 180 Degrees
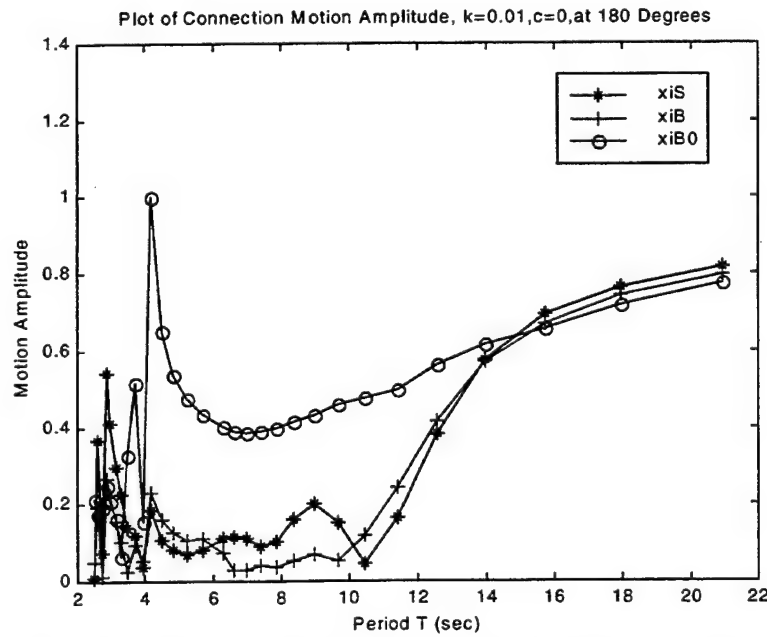
Figure 82. Plot of Vertical Motion Amplitude for the Ship/Ramp/Barge Connection Points, for k = 0.01, c = 0, at 180 Degrees Wave Angle.

71

Plot of Connection Motion Amplitude, k=0.001,c=0.001,at 180 Degrees
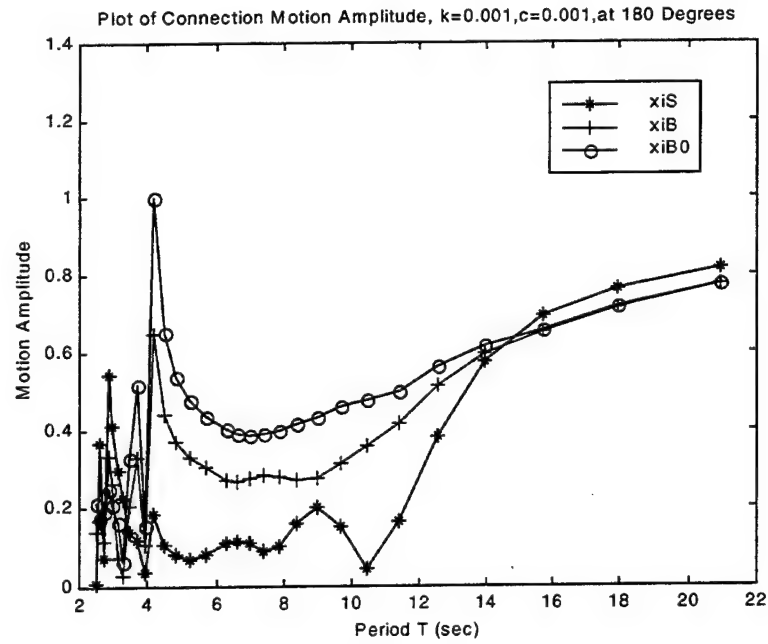
Figure 83. Plot of Vertical Motion Amplitude for the Ship/Ramp/Barge Connection Points, for k = 0.001, c = 0.001, at 180 Degrees Wave Angle.

Plot of Connection Motion Amplitude, k=0.1,c=0.1,at 180 Degrees
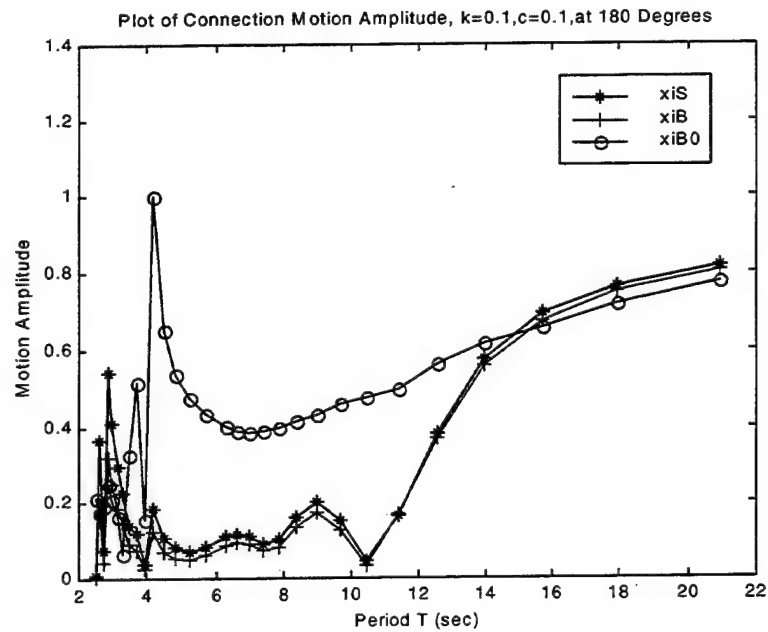
Figure 84. Plot of Vertical Motion Amplitude for the Ship/Ramp/Barge Connection Points, for k = 0.1, c = 0.1, at 180 Degrees Wave Angle.

Figure 85. Plot of Vertical Motion Amplitude for the Ship/Ramp/Barge
Connection Points, for k = 0, c = 0.01, at 225 Degrees Wave Angle.

Figure 86. Plot of Vertical Motion Amplitude for the Ship/Ramp/Barge
Connection Points, for k = 0.01, c = 0, at 225 Degrees Wave Angle.

73

Figure 87. Plot of Vertical Motion Amplitude for the Ship/Ramp/Barge
Connection Points, for k = 0.001, c = 0.001, at 225 Degrees Wave Angle.

Figure 88. Plot of Vertical Motion Amplitude for the Ship/Ramp/Barge
Connection Points, for k = 0.1, c = 0.1, at 225 Degrees Wave Angle.

74

Figure 89. Plot of Vertical Motion Amplitude for the Ship/Ramp/Barge
Connection Points, for k = 0, c = 0.01, at 270 Degrees Wave Angle.

Figure 90. Plot of Vertical Motion Amplitude for the Ship/Ramp/Barge
Connection Points, for k = 0.01, c = 0, at 270 Degrees Wave Angle.

75

Plot of Connection Motion Amplitude,k=0.001,c=0.001,at 270 Degrees

Figure 91. Plot of Vertical Motion Amplitude for the Ship/Ramp/Barge Connection Points, for k = 0.001, c = 0.001, at 270 Degrees Wave Angle.

Plot of Connection Motion Amplitude,k=0.1,c=0.1,at 270 Degrees

Figure 92. Plot of Vertical Motion Amplitude for the Ship/Ramp/Barge Connection Points, for k = 0.1, c = 0.1, at 270 Degrees Wave Angle.

Figure 93. Plot of Vertical Motion Amplitude for the Ship/Ramp/Barge Connection Points, for k = 0, c = 0.01, at 315 Degrees Wave Angle.

Figure 94. Plot of Vertical Motion Amplitude for the Ship/Ramp/Barge Connection Points, for k = 0.01, c = 0, at 315 Degrees Wave Angle.

77

Figure 95. Plot of Vertical Motion Amplitude for the Ship/Ramp/Barge
Connection Points, for k = 0.001, c = 0.001, at 315 Degrees Wave Angle.

Figure 96. Plot of Vertical Motion Amplitude for the Ship/Ramp/Barge
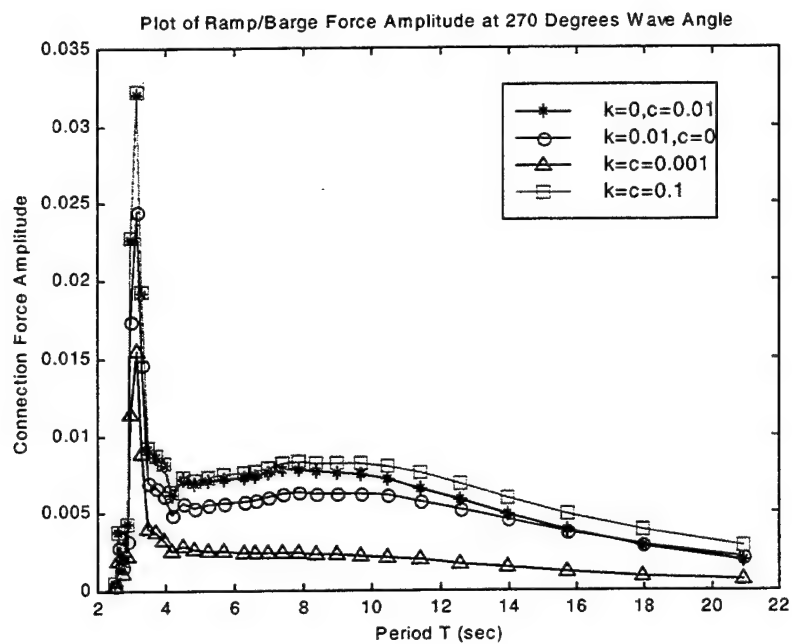Connection Points, for k = 0.1, c = 0.1, at 315 Degrees Wave Angle.
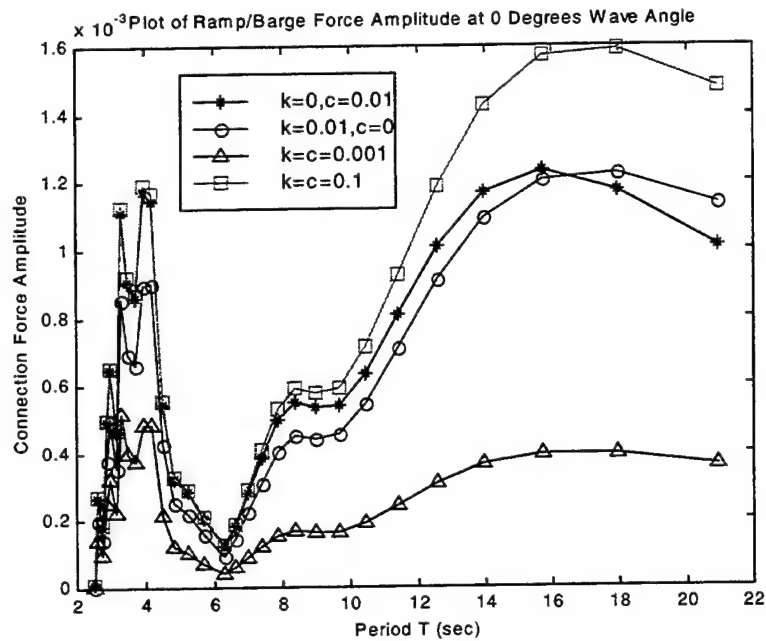
Figure 97. Plot of Ramp Excitation Force on the Ramp/Barge Connection
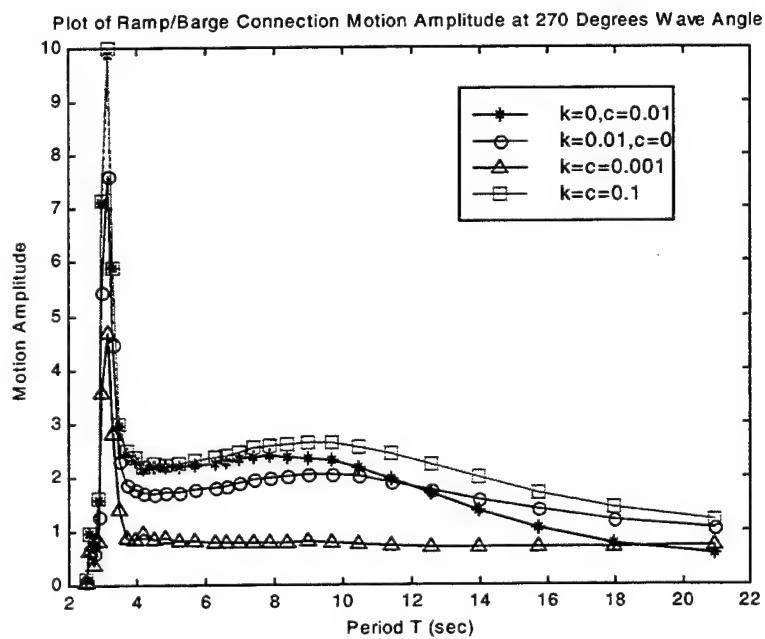for various values of k and c, at a Wave Angle of 0 Degrees.
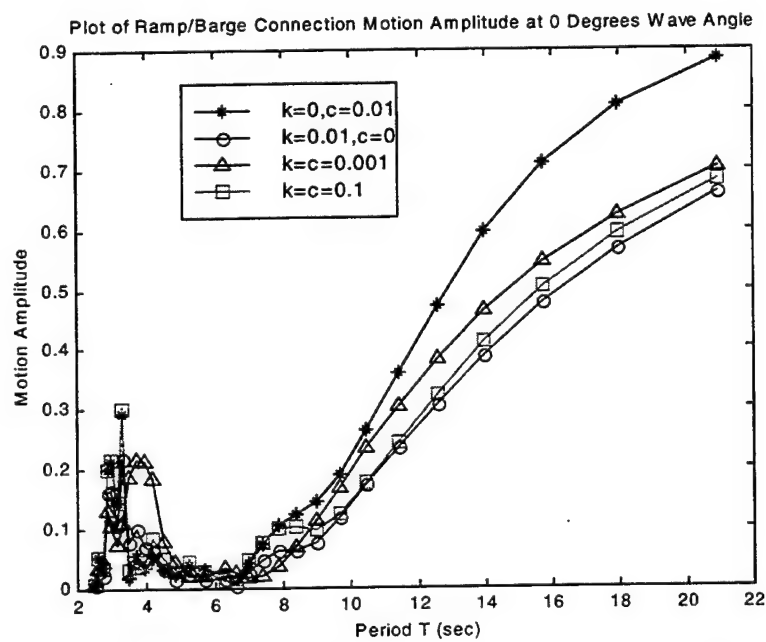
Figure 98. Plot of Ramp/Barge Connection Motion Amplitude
for various values of k and c, at a Wave Angle of 0 Degrees.

79
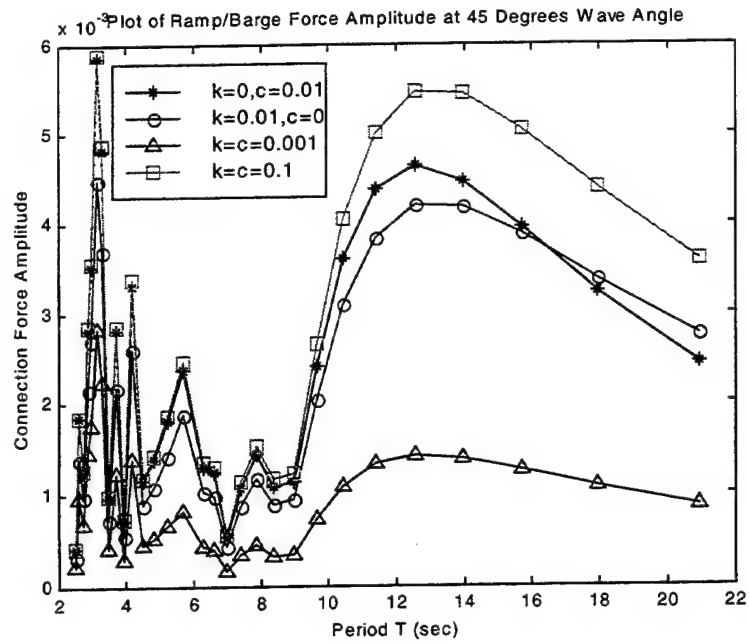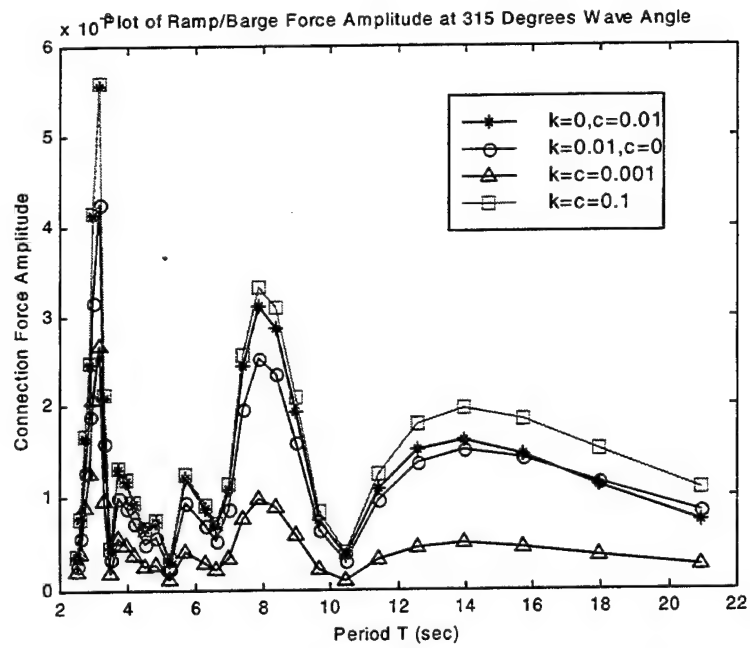
Figure 99. Plot of Ramp Excitation Force on the Ramp/Barge Connection
for various values of k and c, at a Wave Angle of 45 Degrees.
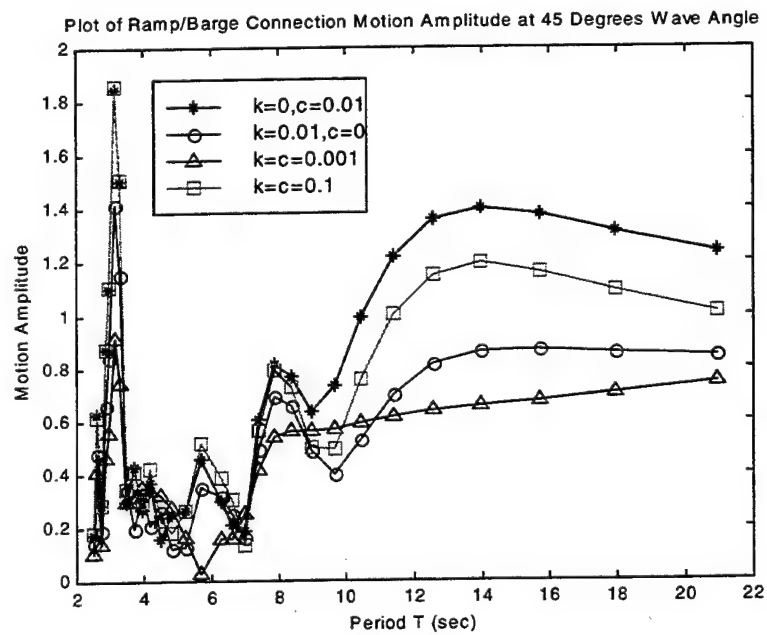
Figure 100. Plot of Ramp/Barge Connection Motion Amplitude
for various values of k and c, at a Wave Angle of 45 Degrees.
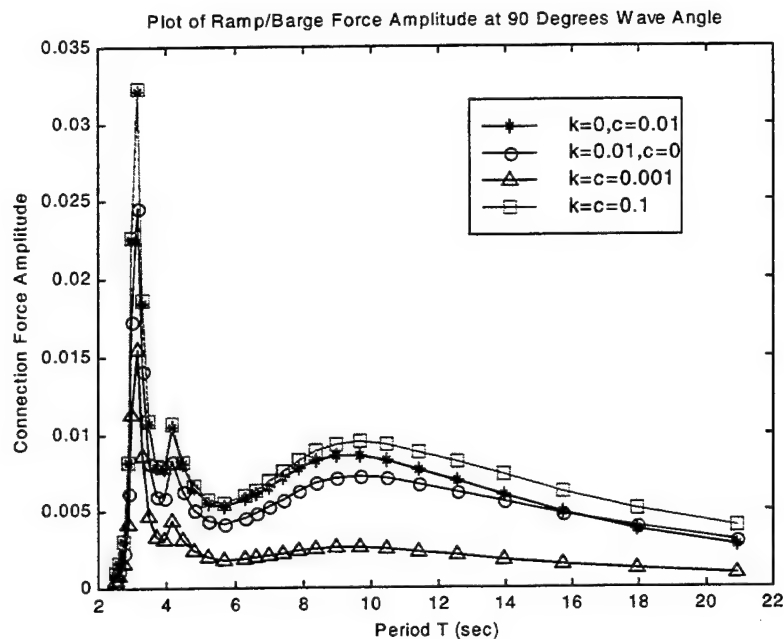
Figure 101. Plot of Ramp Excitation Force on the Ramp/Barge Connection
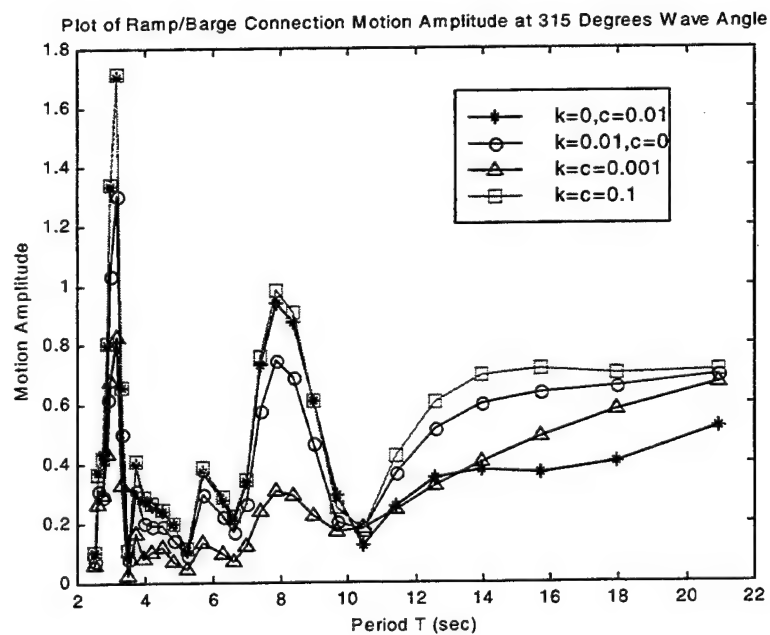for various values of k and c, at a Wave Angle of 90 Degrees.
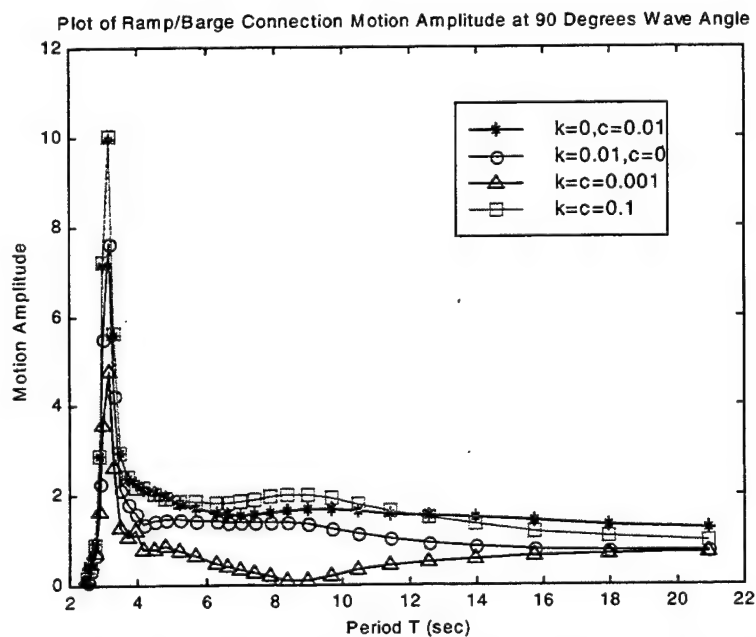
Figure 102. Plot of Ramp/Barge Connection Motion Amplitude
for various values of k and c, at a Wave Angle of 90 Degrees.

81
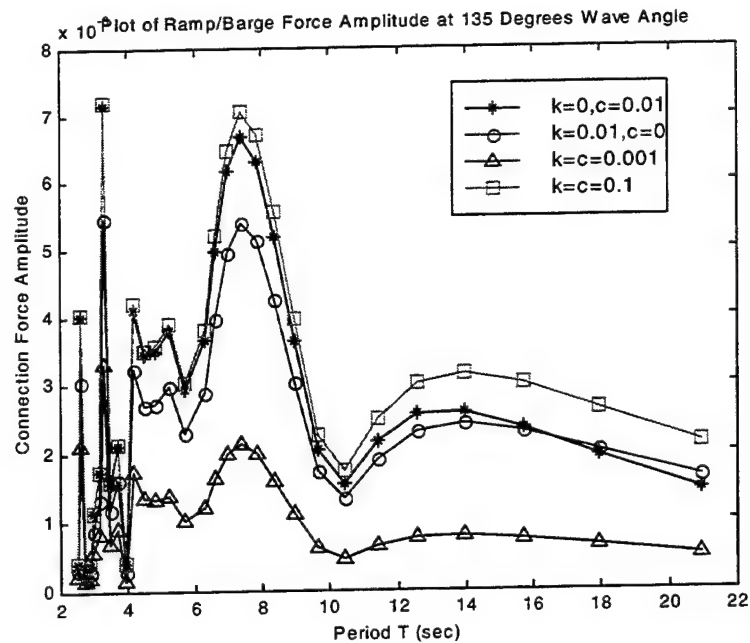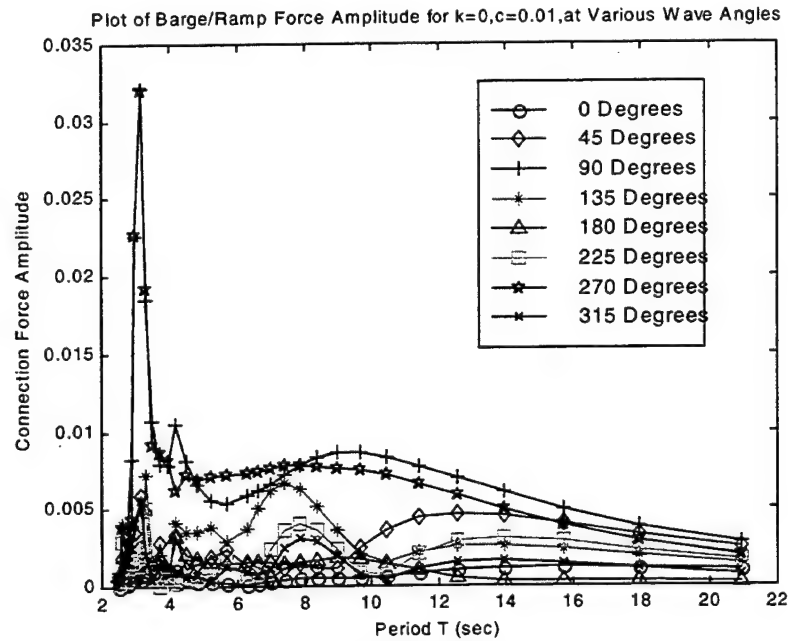
Figure 103. Plot of Ramp Excitation Force on the Ramp/Barge Connection
for various values of k and c, at a Wave Angle of 135 Degrees.
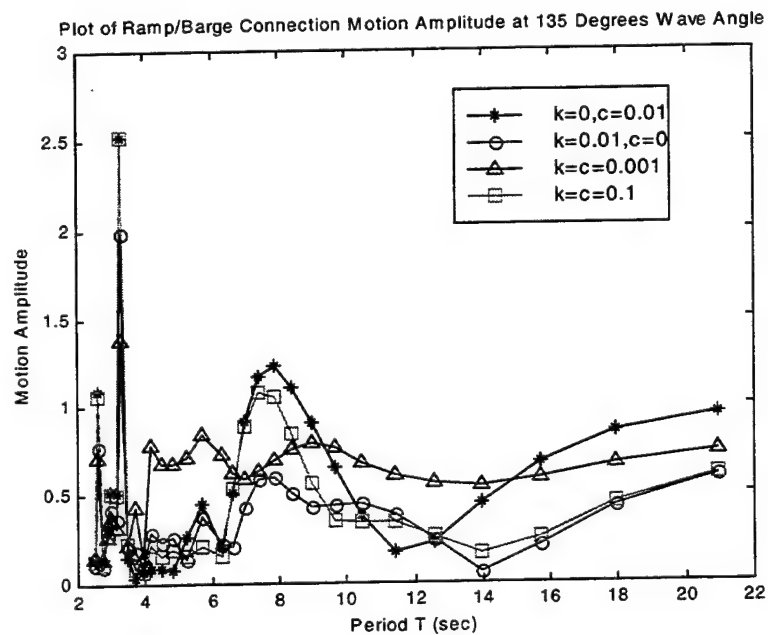
Figure 104. Plot of Ramp/Barge Connection Motion Amplitude
for various values of k and c, at a Wave Angle of 135 Degrees.

82
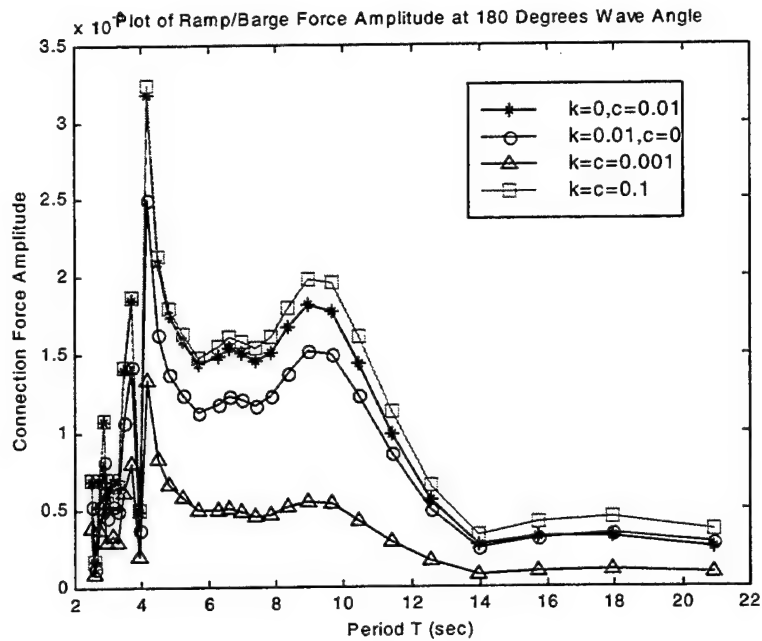
Figure 105. Plot of Ramp Excitation Force on the Ramp/Barge Connection
for various values of k and c, at a Wave Angle of 180 Degrees.
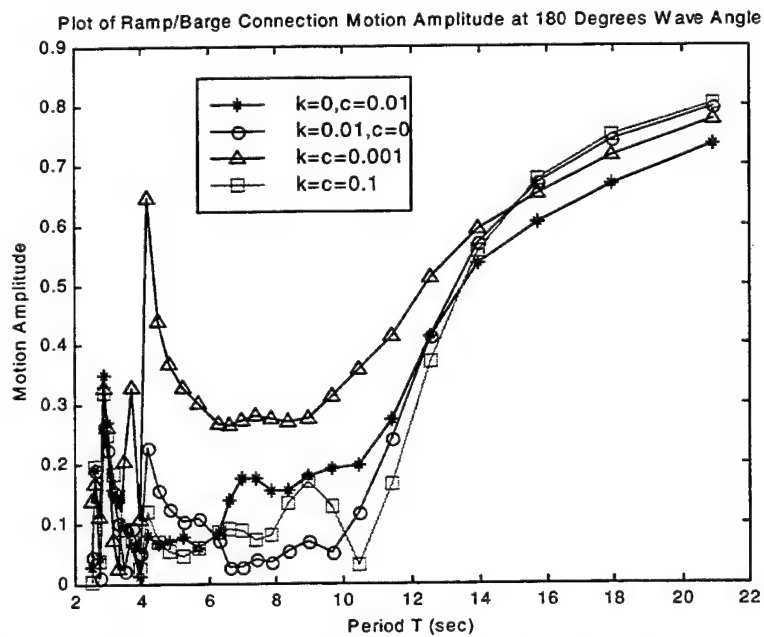
Figure 106. Plot of Ramp/Barge Connection Motion Amplitude
for various values of k and c, at a Wave Angle of 180 Degrees.

83
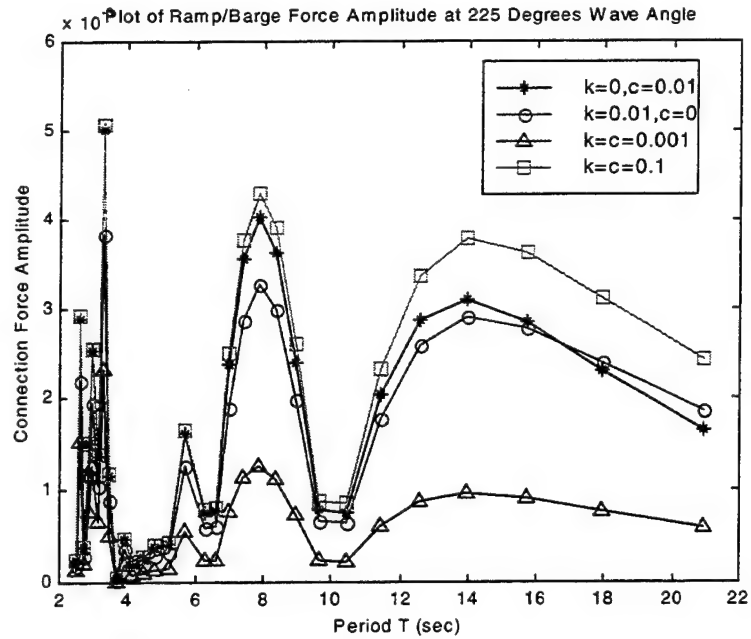
Figure 107. Plot of Ramp Excitation Force on the Ramp/Barge Connection
for various values of k and c, at a Wave Angle of 225 Degrees.
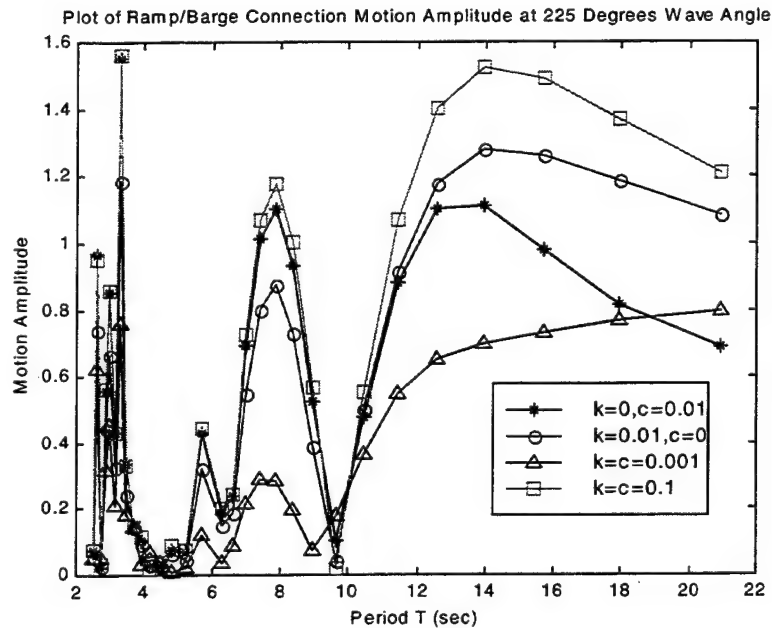
Figure 108. Plot of Ramp/Barge Connection Motion Amplitude
for various values of k and c, at a Wave Angle of 225 Degrees.

84

Figure 109. Plot of Ramp Excitation Force on the Ramp/Barge Connection
for various values of k and c, at a Wave Angle of 270 Degrees.

Figure 110. Plot of Ramp/Barge Connection Motion Amplitude
for various values of k and c, at a Wave Angle of 225 Degrees.

85

Figure 111. Plot of Ramp Excitation Force on the Ramp/Barge Connection
for various values of k and c, at a Wave Angle of 315 Degrees.

Figure 112. Plot of Ramp/Barge Connection Motion Amplitude
for various values of k and c, at a Wave Angle of 315 Degrees.

86

Figure 113. Plot of Ramp Excitation Force on the Barge/Ramp Connection for k=0, c=0.01, at Various Wave Angles.
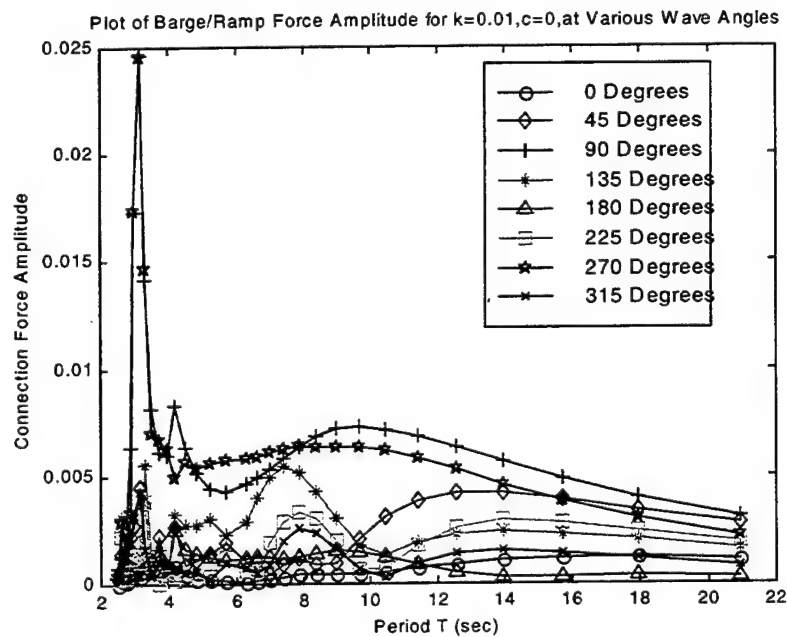
Figure 114. Plot of Ramp Excitation Force on the Barge/Ramp Connection for k=0.01, c=0, at Various Wave Angles.

87
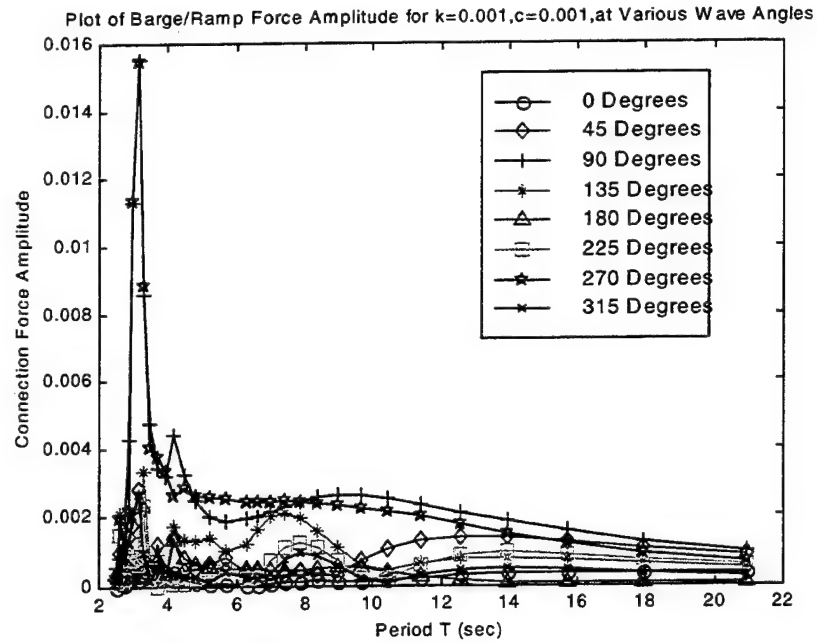
Figure 115. Plot of Ramp Excitation Force on the Barge/Ramp Connection
for k=0.001, c=0.001, at Various Wave Angles.
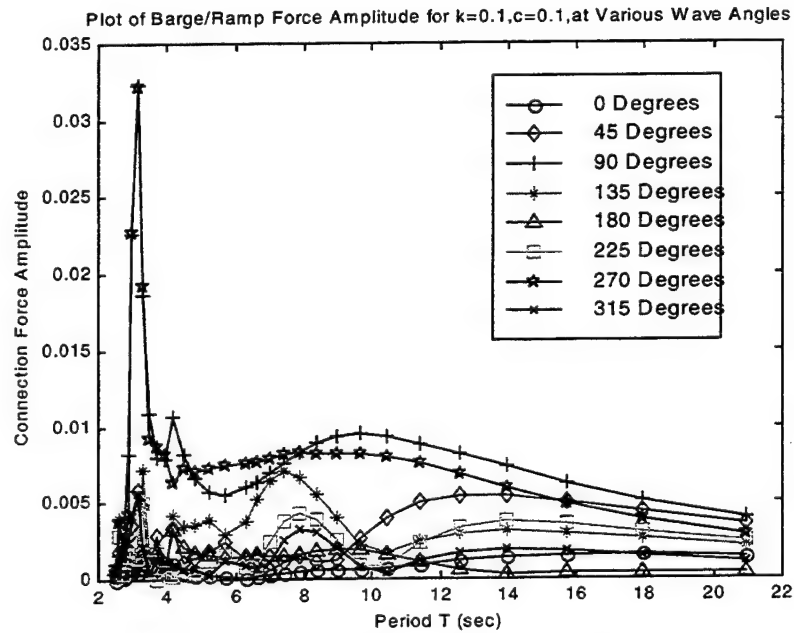
Figure 116. Plot of Ramp Excitation Force on the Barge/Ramp Connection
for k=0.1, c=0.1, at Various Wave Angles.

88

IV. RANDOM WAVE RESULTS

A. DESCRIPTION OF THE SEAWAY

Wave patterns in an open sea are ever changing with time and space, in a manner that appears to defy analysis be it linear or second order Stokes. Ambient waves on the surface of the sea are dispersive as well as random. The generating mechanism is, predominantly, the effect upon the water surface of wind in the atmosphere. The wind is itself random, especially when viewed from the standpoint of the turbulent fluctuations and eddies which are important in generating waves. The randomness of sea waves is subsequently enhanced by their propagation over large distances in space and time and their exposure to the random nonuniformities of the water and air.

According to the principle of superposition, we could attempt a description of the seaway deterministically accounting for each one of the individual wave components. Leaving aside the issue of whether such an approach is possible or not (advocates of chaos theory may well argue that it is impossible), it is clearly a highly impractical task. Fortunately, it is not required either. It would suffice to represent sea waves in a probabilistic manner.

Doing so, we have to bear in mind that there exist two possible ways of defining the statistical properties of a random process. We can consider the statistical properties taken "across the ensemble" at fixed values of time $t = t_1$, $t = t_2$, etc., or we may consider the properties of the random process taken "along the ensemble" where t_1, t_2, etc., are assumed to vary. Description of a random process so general would require an enormous amount of information. Fortunately, for certain random processes such as sea waves, it is

89

possible to assume that the process is of a special form: "stationary", "homogeneous", and "ergodic". For sea waves it should be adequate to describe the wave environment over a period of a few hours (or before the next weather report comes in), and to assume that the wave motion is *stationary* (its statistics remain the same over time) during this interval of time. Likewise, we have no interest in describing the wave environment simultaneously throughout the world, a small area of operations is all we need, and we can assume that the wave motion is *homogeneous* (its statistics remain the same in that area) in space over the area in question. These statements have meaning only in a statistical sense, since for a random wave system it would be funny to suggest that the precise wave motion is the same at different points in space or time. Eventually, it is reasonable to assume that the statistical properties of the waves measured over time, should be "typical" of the random process. This means that they should be the same even if we were able to sample all possible realizations of the wave motion at a fixed time. Such random processes are said to be *ergodic*.

One of the most significant parameters we need in order to arrive at a statistical description of the seaway is the total mean energy of the wave system per unit area of the free surface ($\overline{E}$). It can be shown from hydrodynamics that this is equal to:

$$\overline{E} = \rho g \int_0^\infty \int_0^{2\pi} S(\omega,\theta) d\theta d\omega \qquad (97)$$

The function $S(\omega,\theta)$ is called the *spectral density* and more rigorously can be defined as the Fourier transform of the correlation function for the free surface elevation. It is customary to ignore the factor ρg and to refer to the function $S(\omega,\theta)$ as the *spectral energy density* or simply the *energy spectrum*. More specifically, this is a *directional*

90

energy spectrum. It can be integrated over all wave directions to give the *frequency spectrum*:

$$S(\omega) = \int_0^{2\pi} S(\omega,\theta)d\theta \qquad (\ 98\ )$$

Using equations (97) and (98) we can see that:

$$\overline{E} = \int_0^\infty S(\omega)d\omega \qquad (\ 99\ )$$

i.e., the area under the spectrum $S(\omega)$ is equal to (within the constant ρg) the mean energy stored in that particular wave system.

If one attempts to find the sea wave spectrum from measurements of the free surface elevation at a single point in space, for instance by recording the heave motion of a buoy, the directional characteristic of the waves will be lost. Only the frequency spectrum (98) can be determined from such a restricted set of data. A limited amount of directional information follows if one measures the slope of the free surface, for example by measuring the angular response of the buoy as well as its heave. A complete description of the directional wave spectrum requires an extensive array of measurements at several adjacent points in space, and there are practical difficulties associated with this task.

As a simpler alternative, one can assume that the waves are *unidirectional*, with the energy spectrum proportional to a delta function in θ. Wave spectra of this form are called *long crested*, since the fluid motion is two dimensional and the wave crests are parallel, and the frequency spectrum (98) is sufficient to describe the wave environment.

If the waves are generated by a single storm, far removed from the point of observation, it might be presumed that these waves would come from the direction of the

91

storm in a long crested manner. The limitations of this assumption are obvious to anyone who has observed the sea surface. While a preferred direction may exist, especially for long swell that has traveled large distances, even these long waves will be distributed in their direction, and for short steep waves the directional variation is particularly significant Since the superposition of such waves from a range of different directions appears in space as a variation of the free surface elevation in all directions, these waves are known as *short crested* waves.

Usually in the fields of ocean engineering and naval architecture it is customary to assume that the waves are long crested. With such a simplification it is possible to use existing information for the frequency spectrum (98), which is based on a combination of theory and full-scale observations. Sea wave spectra depend on the velocity of the wind as well as its duration in time and the distance over which the wind is acting on the free surface. This distance is known as the *fetch*. Wave spectra that have reached a steady state of equilibrium, independent of the duration and fetch are known as *fully developed*. A semi-empirical expression for the frequency spectrum of fully developed seas is:

$$S(\omega) = \frac{ag^2}{\omega^5} \exp\left[-\beta\left(\frac{g}{U\omega}\right)^4\right] \tag{100}$$

Here α and β are nondimensional parameters defining the spectrum, and U is the wind velocity at a standard height of 19.5 meters above the free surface. This two parameters spectrum is sufficiently general to fit quite a few observations and is consistent with theoretical predictions of the high frequency limit. The most common values for these parameters are:

92

$$a = 8.1 \text{ x } 10^{-3} \quad \text{and} \quad \beta = 0.74 \qquad\qquad (\,101\,)$$

and with these values it is known as the *Pierson - Moscowitz* spectrum.

B.   SHIP/RAMP/BARGE RESPONSE SPECTRAL ANALYSIS

1. Introduction

The ultimate goal of ship motion studies is to be able to predict how the ship will behave in realistic irregular seas such as those represented by a particular sea spectrum. The relationship between motions in regular and irregular waves must be established in order to use either the theoretical equations or the experimental studies to lead to practical predictions of ship behavior in a realistic seaway.

The needed relationship is expressed by the principle of linear superposition, which says that the response of a ship to an irregular sea can be represented by a linear summation of its responses to the component regular waves that comprise the irregular sea. To make use of this principle, a ship response to regular waves, whether it has been determined by calculation or by model measurement, is expressed in a special form often referred to as a *Response Amplitude Operator* (RAO). A response amplitude operator is a measure of the response to a regular wave of unit amplitude.

Like the sea waves themselves, a ship response is a random variable. The statistics of a floating body response are identical to the wave statistics, except that the wave energy spectrum S is multiplied by the square of the RAO (this is a property of linear systems). Thus, if the subscript R represents any body response, we have:

$$S_R(\omega) = |Z_R(\omega)|^2 S(\omega) \qquad\qquad (\,102\,)$$

93

where $Z_R(\omega)$ is the RAO of the response R, and $S(\omega)$ the spectrum of the seaway. Equation (102) can then be utilized to obtain the spectrum of the response R, and after that specific formulas can be used to provide the statistics of this response in a particular sea state.

To a large extent, equation (102) provides the justification for studying regular wave responses. The transfer function $Z_R(\omega)$ is valid not only in regular waves, where it has been derived, but also in a superposition of regular waves, and ultimately in a spectrum of random waves. Generally speaking, a vessel with favorable response characteristics in regular waves will be good in irregular waves, and vice versa. This statement is oversimplified, however, and the relative shape of the energy spectrum and the transfer function is very crucial. For example, a large resonant response of the body will be of importance only if the resonant frequency is located close to the peak of the wave energy spectrum, and vice versa.

Eventually, the statistical predictions of the amplitudes of ship motions may be determined from the variance, or spectral area, of a ship response spectrum given by the equation:

$$\bar{S}_R = \int_0^\infty S_R(\omega)d\omega \qquad (103)$$

2. Results

Figures 117 through 124, display the Spectrum of the Ramp/Barge Connection Force, for the Incident Wave Angle (heading) ranging from zero to 360 degrees at

intervals of 45 degrees. Headings of zero degrees indicate waves coming directly from the stern of the ship and barge, 90 degrees from the starboard beam, 180 degrees from the bow, and 270 degrees from the port beam. These figures clearly show the changes in overall Ramp Excitation Force Spectrum if different values of connection stiffness and damping are assumed to exist.

The Response Spectrum of the Vertical Motion at the Ship/Ramp and Ramp/Barge Connection Points, with and without the Ramp Influence, for various values of Ramp/Barge connection stiffness and damping, at an incident Wave Angle ranging again from zero to 360 degrees, is displayed at Figures 125 through 156.

3. Significant Values

In order to present the random wave results in a more compact manner, we will employ the significant values of the responses. The significant value of a random process is defined as the average of the 1/3 of the highest values of all responses and is frequently used in design to characterize the severity of a particular response. The significant value can be easily computed from the spectrum of the response and is in fact equal to four times the square root of the area under the spectrum of the response, which is the integral of the spectrum function over the frequency range. Figure 157 presents parametric results in terms of the significant value of the normalized ramp motion as a function of the significant wave height. The ramp motion is normalized with respect to the ramp motion in the absence of an isolator, so values less than one designate motion reduction. Although the results are shown for given isolator properties, they are typical for other properties as well. As can be seen, under the assumed criterion of normalized motion less

95

than one, certain sea states (characterized by the significant wave height) and sea directions seem to be worse for the passive isolator than others. Although different criteria and ramp model will yield different results, the methodology is the same.

In order to present the results in a more compact manner, we employ polar diagrams such as the one shown in Figure 158. The radial coordinate is the significant wave height (equivalent to a sea state) and the polar coordinate show the round the clock sea headings. We then mark the points on the graph where the selected criterion (normalized significant ramp motion greater than one) is violated. Red is where the isolator magnifies motions (in terms of significant amplitudes) and green where it reduces them. In the diagram, heading 0 corresponds to following seas and 180 to head seas, 90 is beam seas (RRDF side, exposed side), 270 is beam seas again (ship side, sheltered side). The results are not port/starboard symmetric due to the strong interactions of the ship to the RRDF. Typical results of this kind are presented in figure 159, for different isolator properties. It can be seen that for most sea state and sea directions, it is possible to select a passive isolator in order to reduce the motions at the end of the ramp. Most cases where motion magnification occurs are for the RRDF sheltered side, which is less severe during operations.
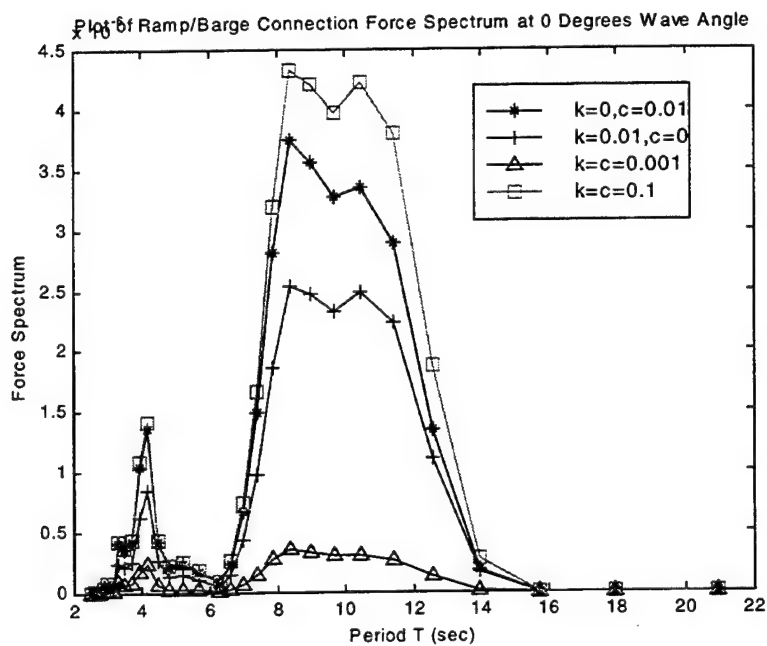
Figure 117. Plot of Ramp Excitation Force Spectrum on the Ramp/Barge Connection, at a Wave Angle of 0 Degrees, with various k and c.
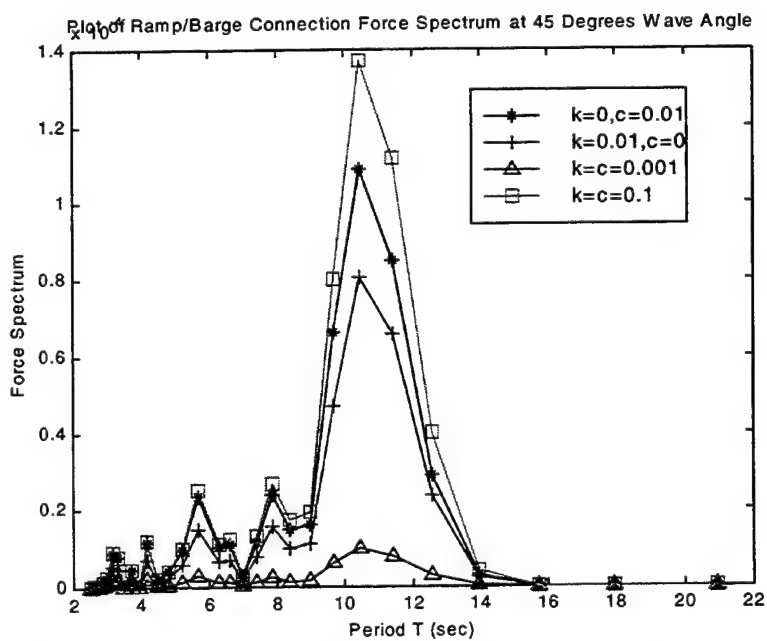
Figure 118. Plot of Ramp Excitation Force Spectrum on the Ramp/Barge Connection, at a Wave Angle of 45 Degrees, with various k and c.

97
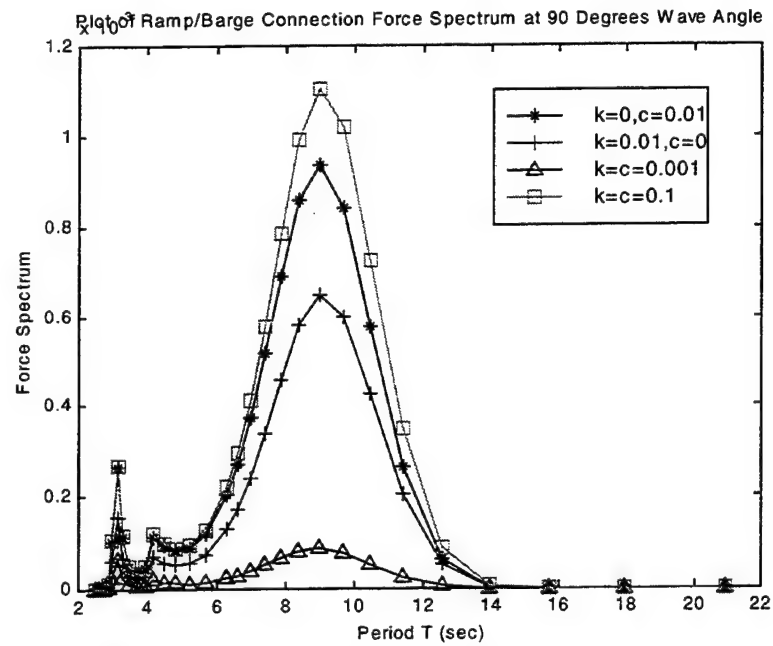
Figure 119. Plot of Ramp Excitation Force Spectrum on the Ramp/Barge Connection, at a Wave Angle of 90 Degrees, with various k and c.
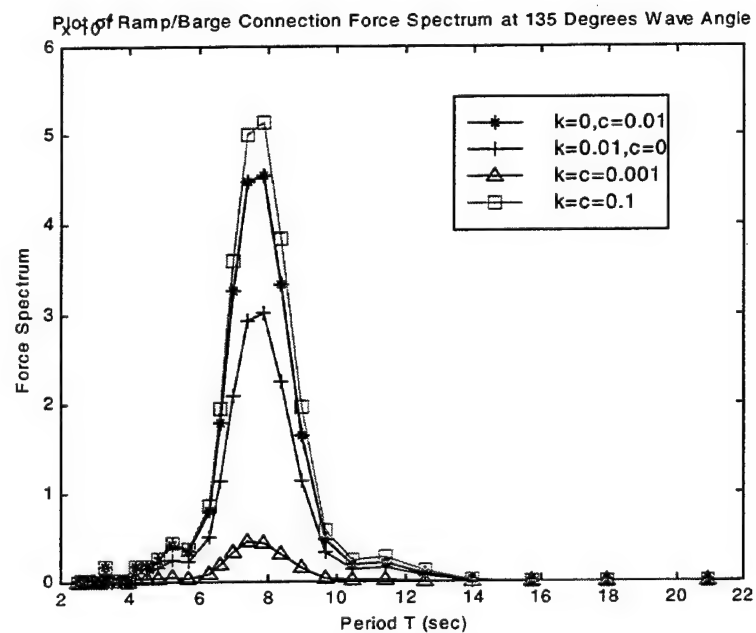
Figure 120. Plot of Ramp Excitation Force Spectrum on the Ramp/Barge Connection, at a Wave Angle of 135 Degrees, with various k and c.

98
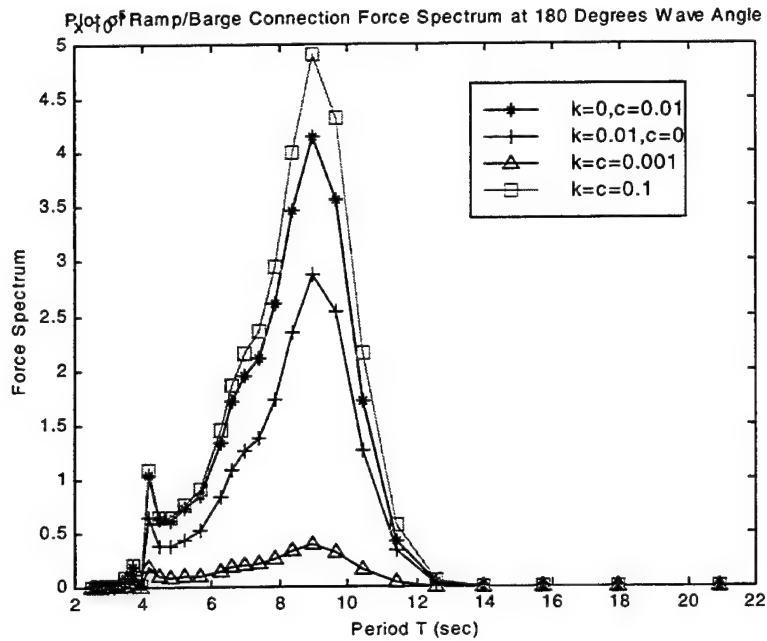
Figure 121. Plot of Ramp Excitation Force Spectrum on the Ramp/Barge
Connection, at a Wave Angle of 180 Degrees, with various k and c.
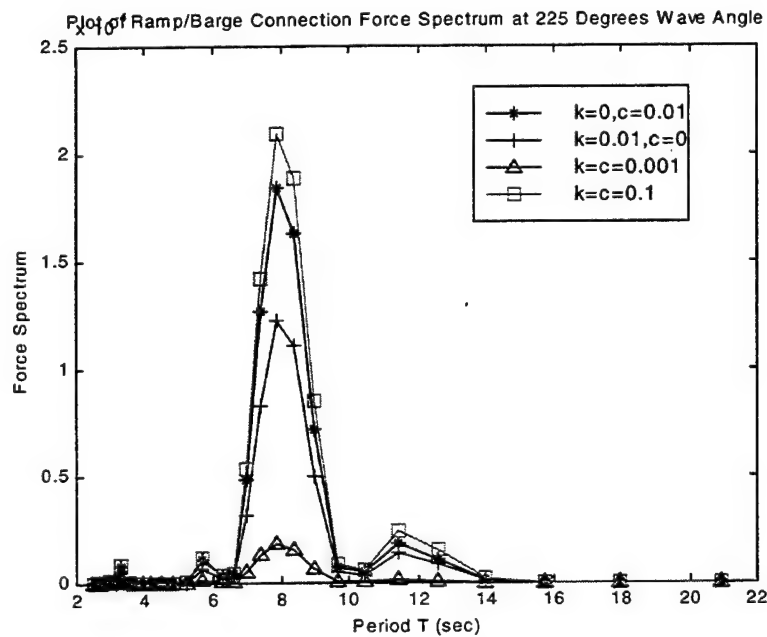
Figure 122. Plot of Ramp Excitation Force Spectrum on the Ramp/Barge
Connection, at a Wave Angle of 225 Degrees, with various k and c.

99
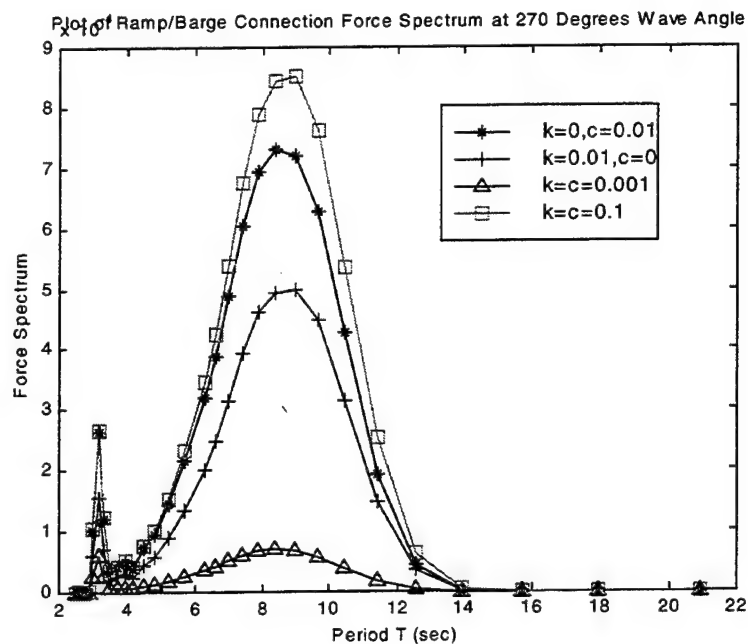
Figure 123. Plot of Ramp Excitation Force Spectrum on the Ramp/Barge Connection, at a Wave Angle of 270 Degrees, with various k and c.
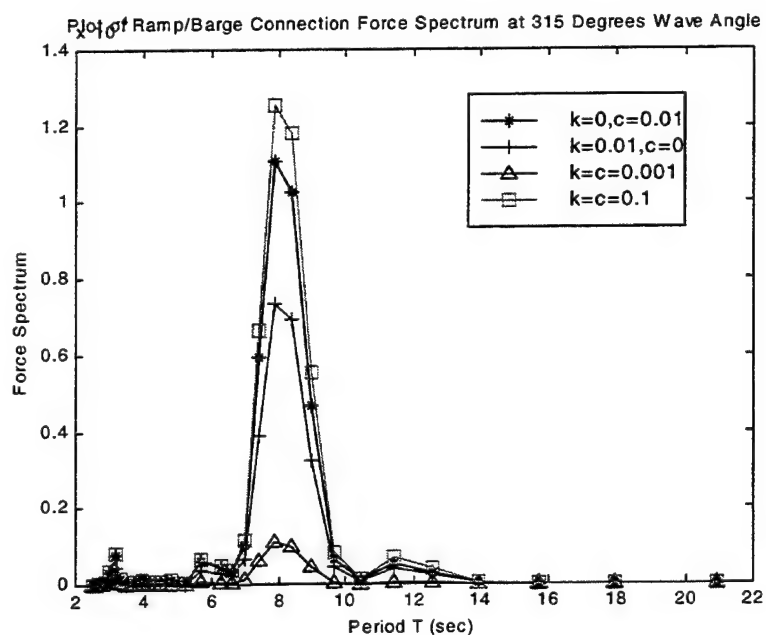
Figure 124. Plot of Ramp Excitation Force Spectrum on the Ramp/Barge Connection, at a Wave Angle of 315 Degrees, with various k and c.
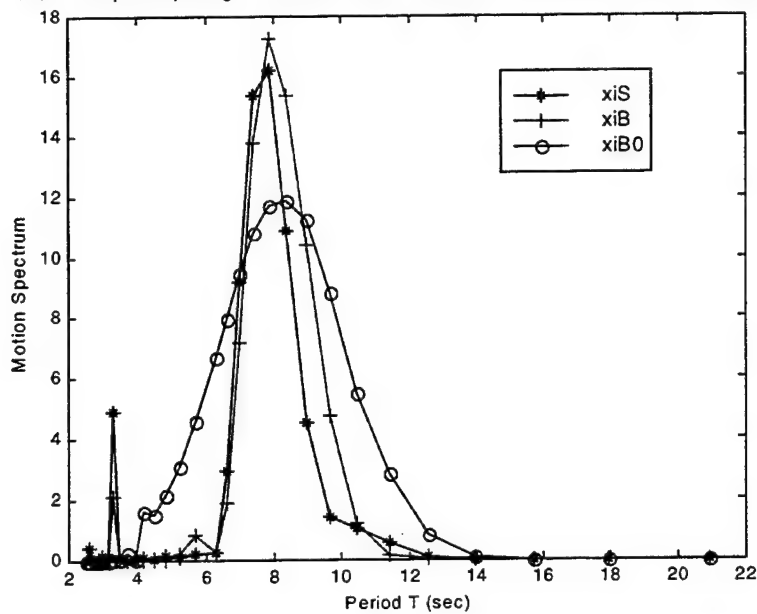
100
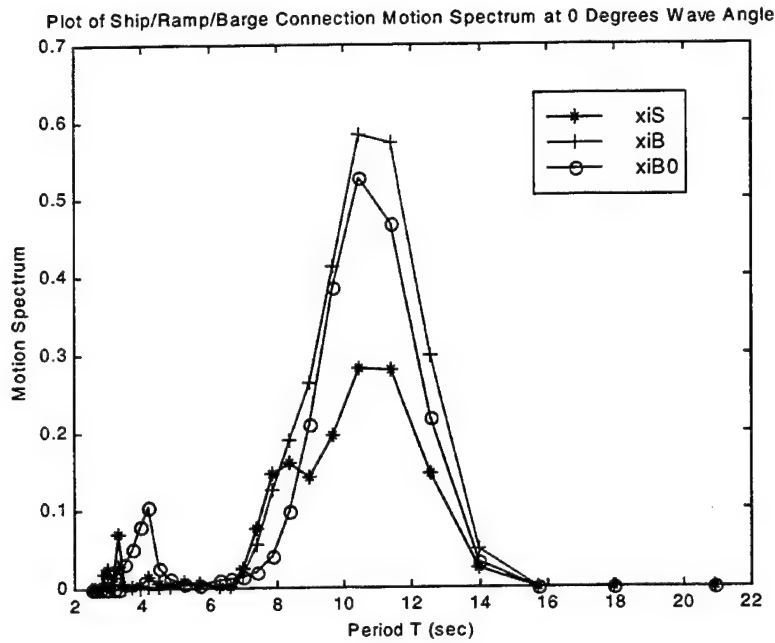
Figure 125. Plot of Vertical Motion Spectrum at the Ship/Ramp/Barge Connections, for k=0 and c=0.01, at a Wave Angle of 0 Degrees.
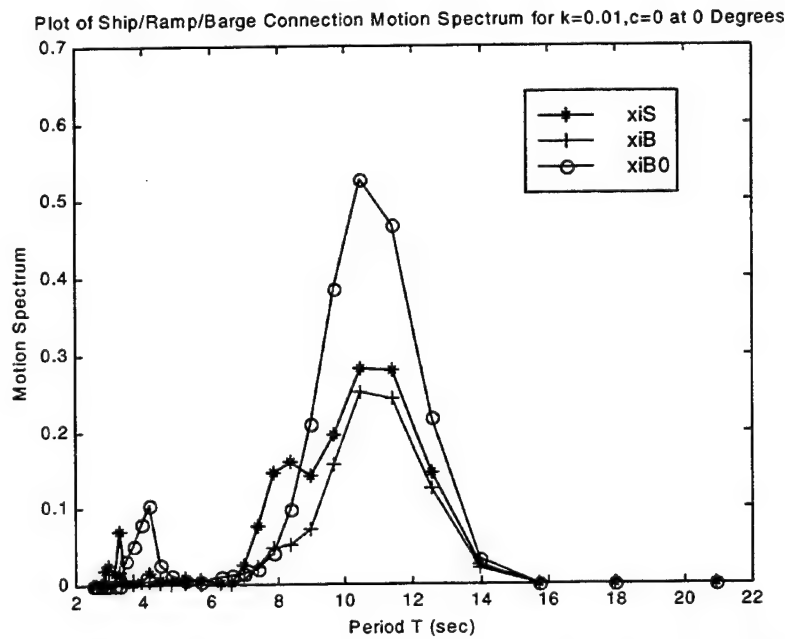
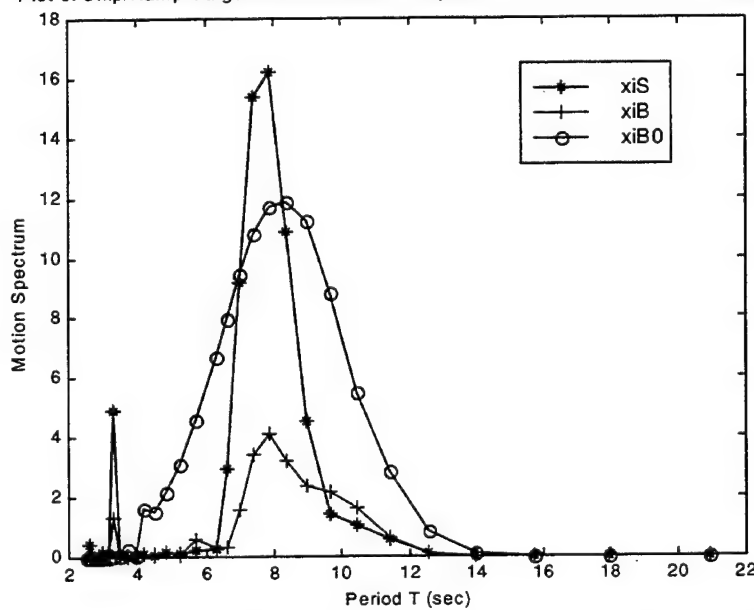

Figure 126. Plot of Vertical Motion Spectrum at the Ship/Ramp/Barge Connections, for k=0.01 and c=0, at a Wave Angle of 0 Degrees.
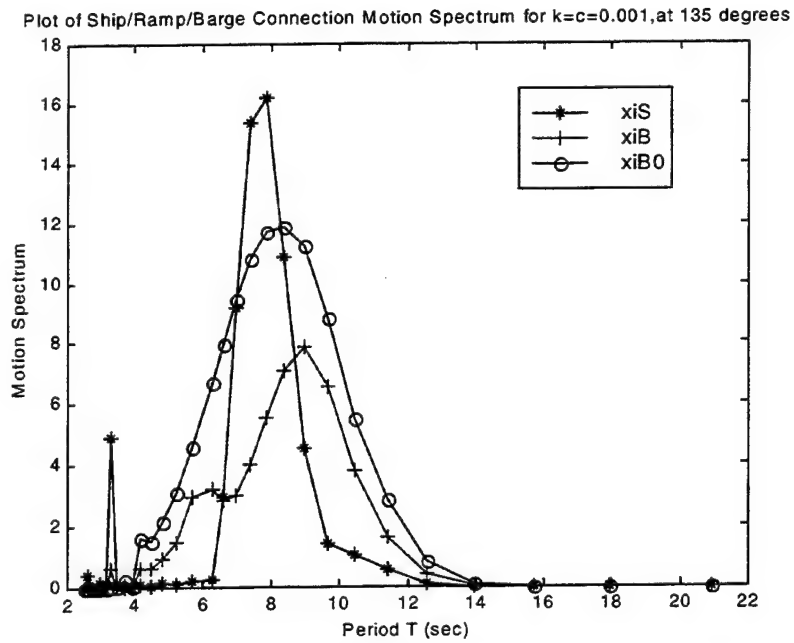
101

Figure 127. Plot of Vertical Motion Spectrum at the Ship/Ramp/Barge Connections, for k=0.001 and c=0.001, at a Wave Angle of 0 Degrees.
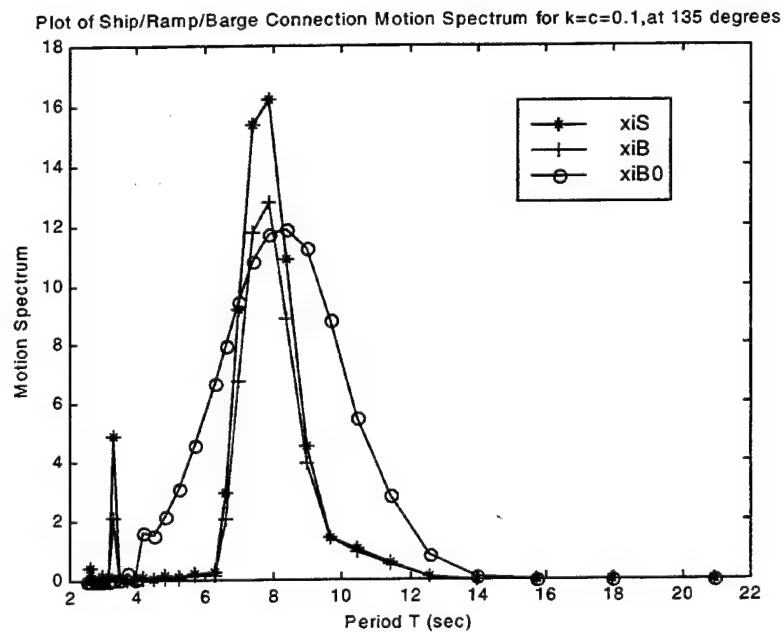

Figure 128. Plot of Vertical Motion Spectrum at the Ship/Ramp/Barge Connections, for k=0.1 and c=0.1, at a Wave Angle of 0 Degrees.

102
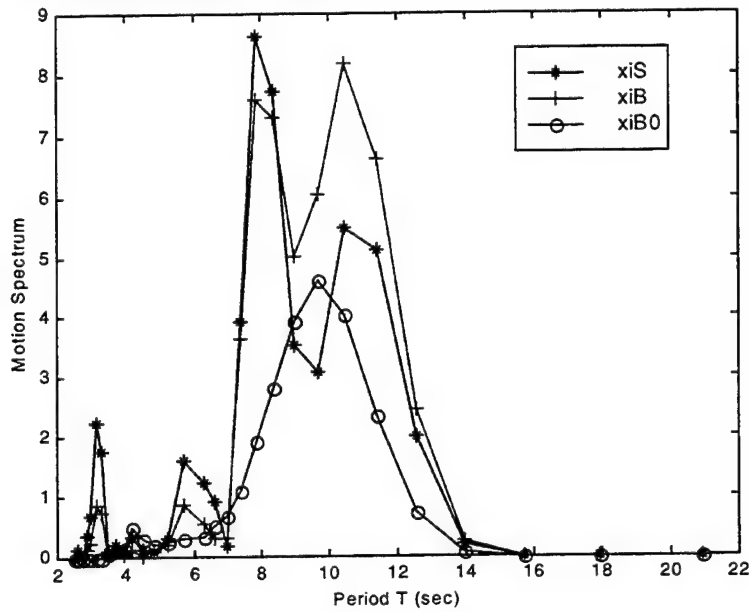
Figure 129. Plot of Vertical Motion Spectrum at the Ship/Ramp/Barge Connections, for k=0 and c=0.01, at a Wave Angle of 45 Degrees.

Figure 130. Plot of Vertical Motion Spectrum at the Ship/Ramp/Barge Connections, for k=0.01 and c=0, at a Wave Angle of 45 Degrees.
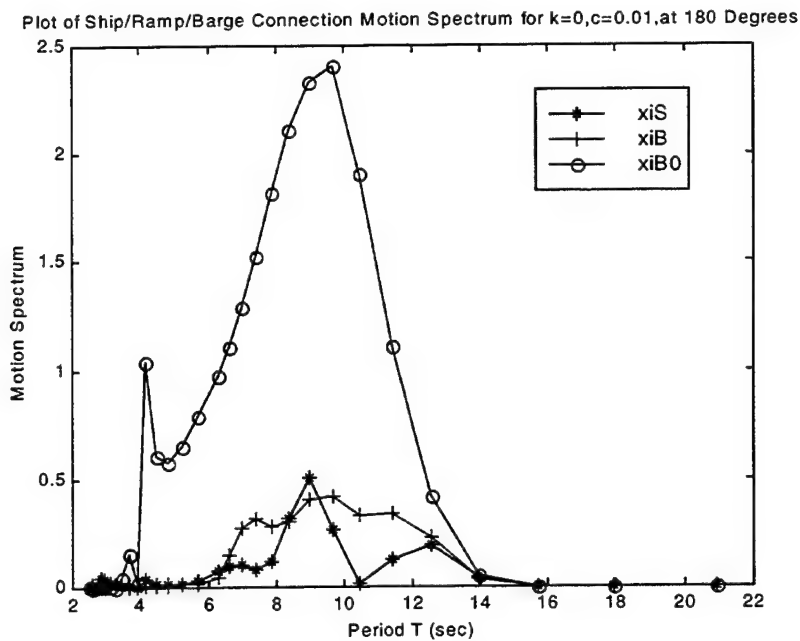
103

Figure 131. Plot of Vertical Motion Spectrum at the Ship/Ramp/Barge Connections, for k=0.001 and c=0.001, at a Wave Angle of 45 Degrees.
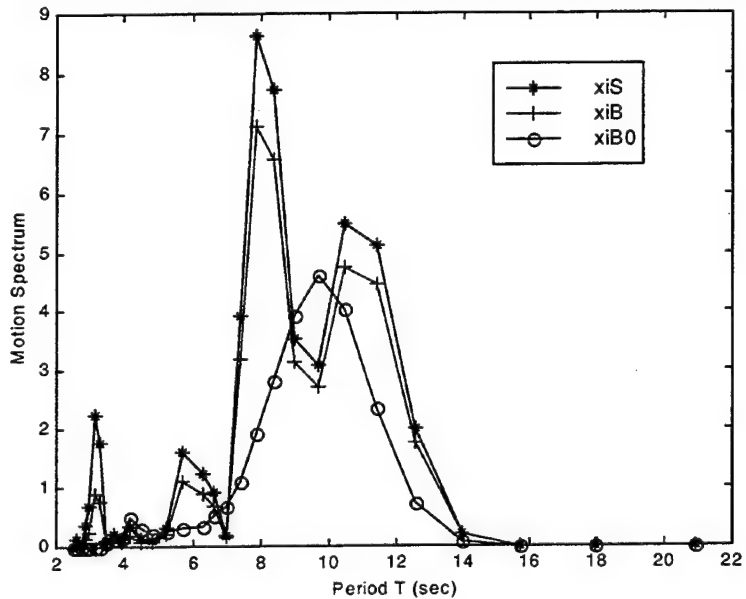
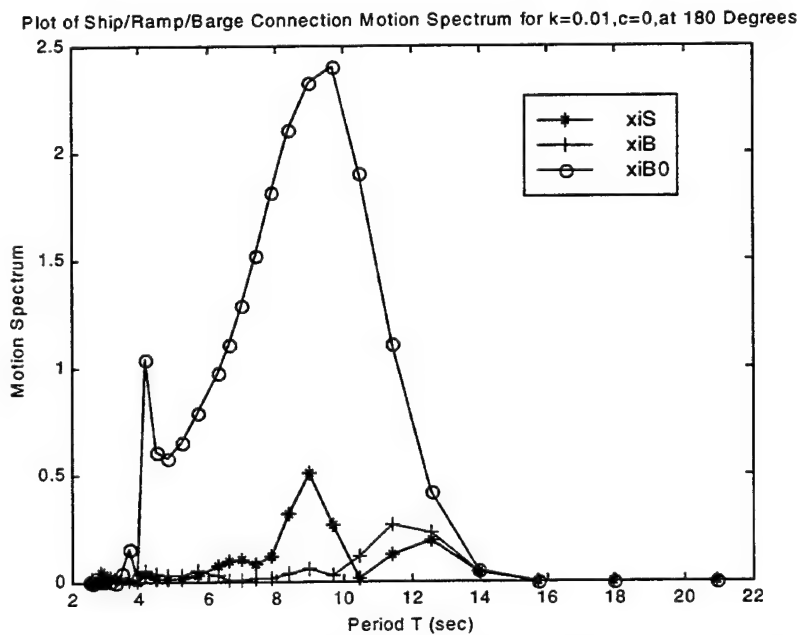Figure 132. Plot of Vertical Motion Spectrum at the Ship/Ramp/Barge Connections, for k=0.1 and c=0.1, at a Wave Angle of 45 Degrees.

104
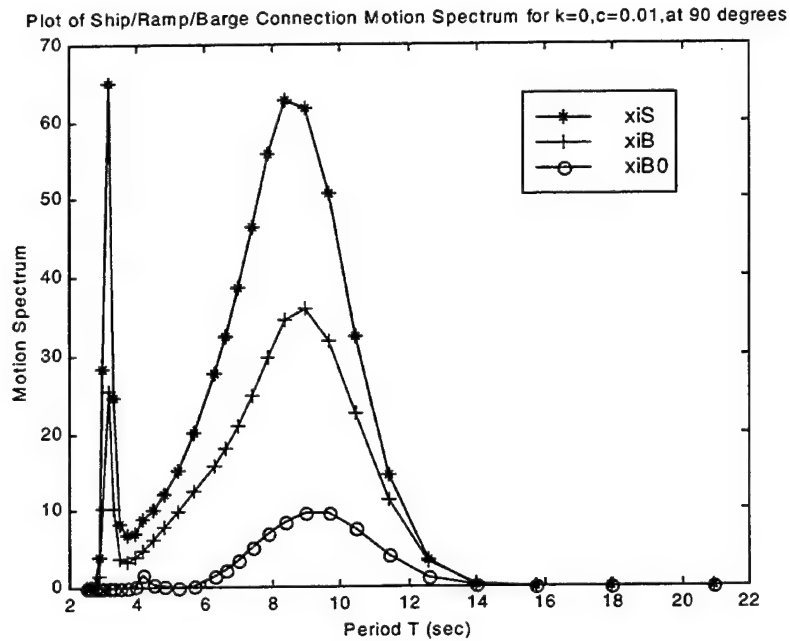
Figure 133. Plot of Vertical Motion Spectrum at the Ship/Ramp/Barge
Connections, for k=0 and c=0.01, at a Wave Angle of 90 Degrees.
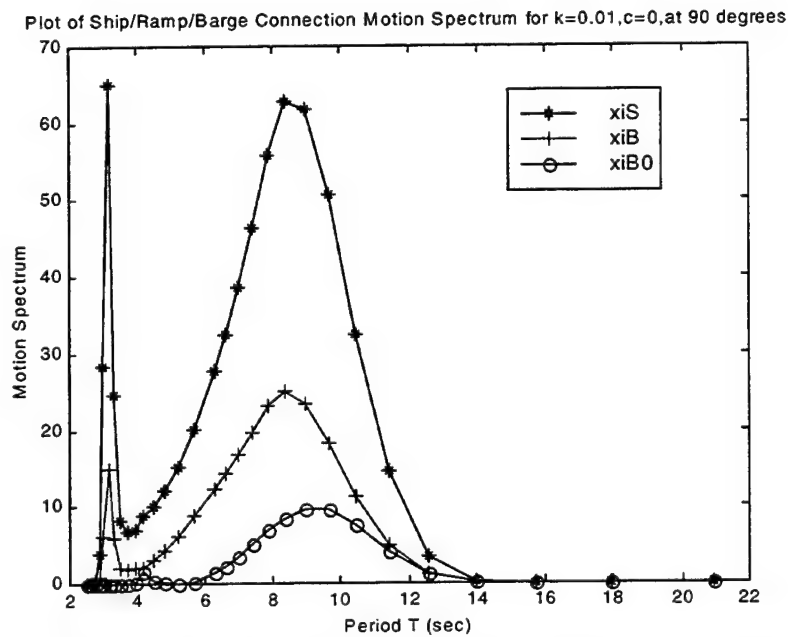
Figure 134. Plot of Vertical Motion Spectrum at the Ship/Ramp/Barge
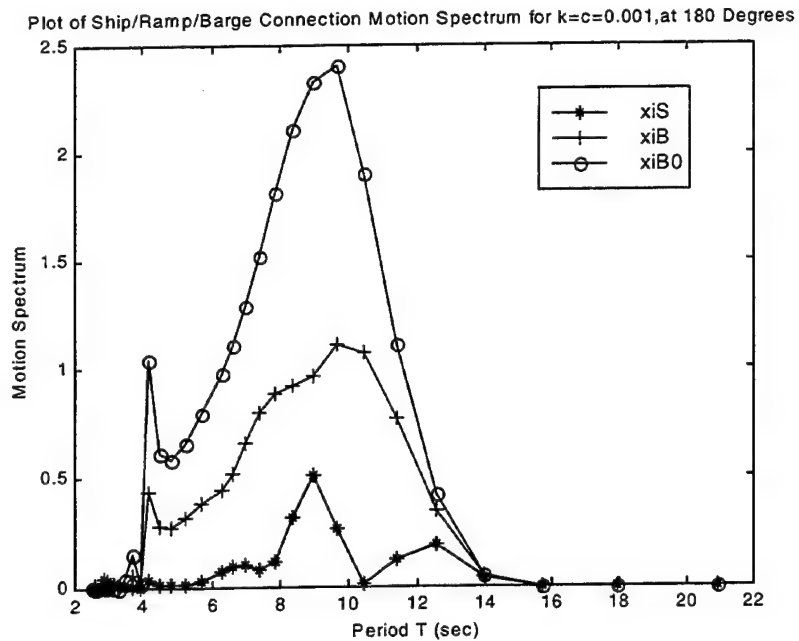Connections, for k=0.01 and c=0, at a Wave Angle of 90 Degrees.

105
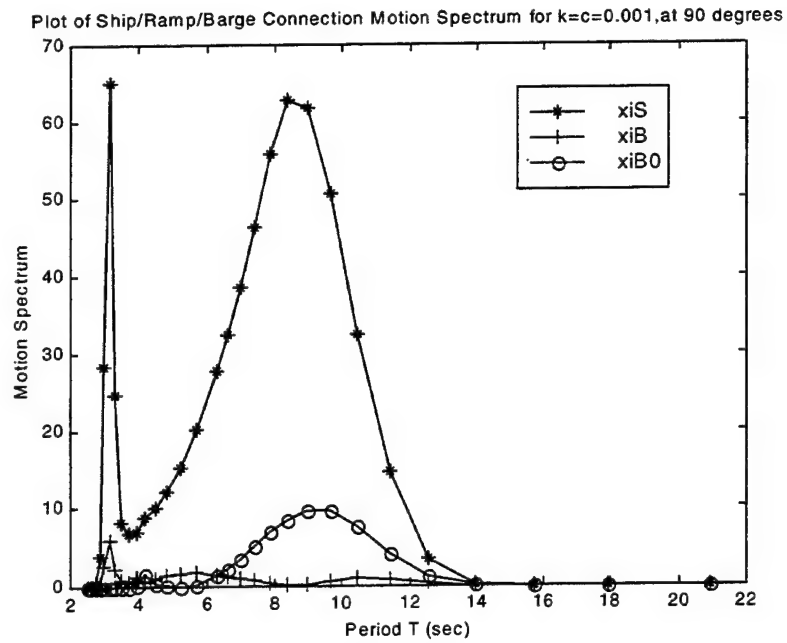
Figure 135. Plot of Vertical Motion Spectrum at the Ship/Ramp/Barge Connections, for k=0.001 and c=0.001, at a Wave Angle of 90 Degrees.
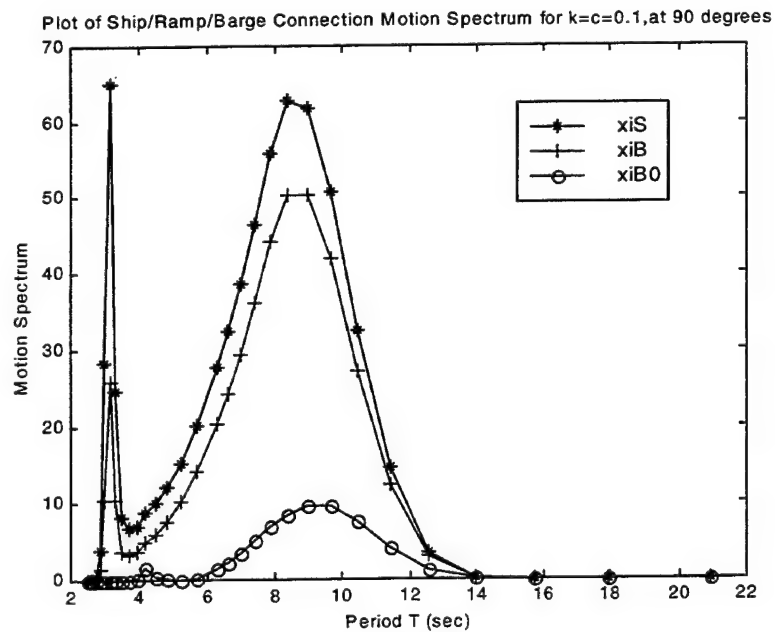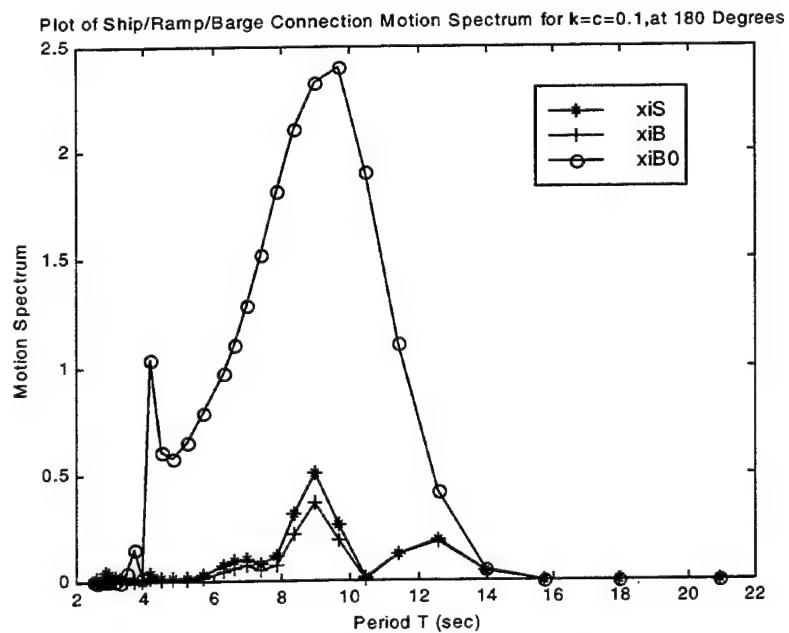

Figure 136. Plot of Vertical Motion Spectrum at the Ship/Ramp/Barge Connections, for k=0.1 and c=0.1, at a Wave Angle of 90 Degrees.
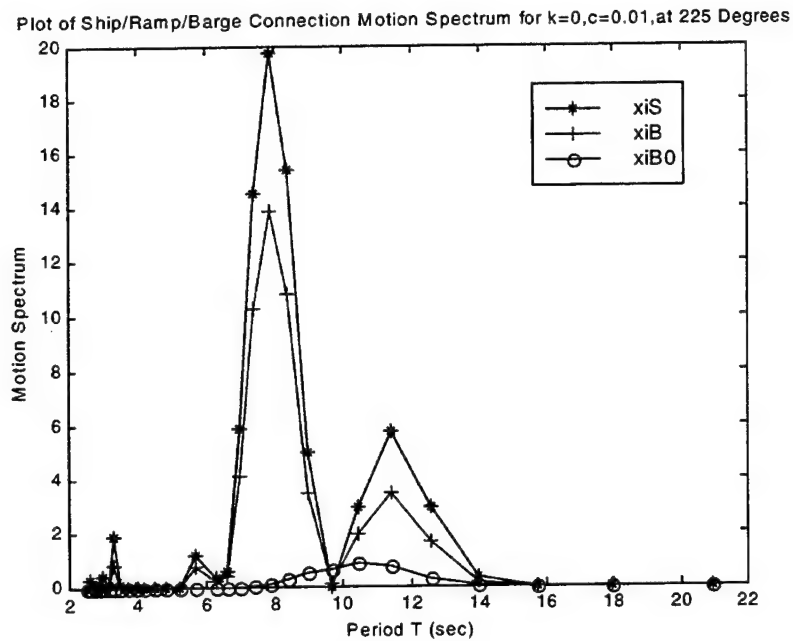
106

Figure 137. Plot of Vertical Motion Spectrum at the Ship/Ramp/Barge Connections, for k=0 and c=0.01, at a Wave Angle of 135 Degrees.
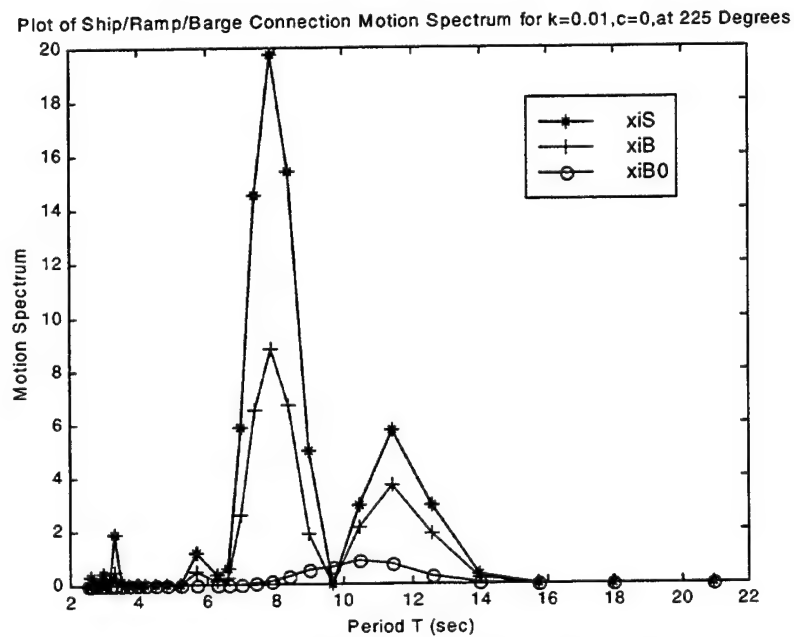

Figure 138. Plot of Vertical Motion Spectrum at the Ship/Ramp/Barge Connections, for k=0.01 and c=0, at a Wave Angle of 135 Degrees.
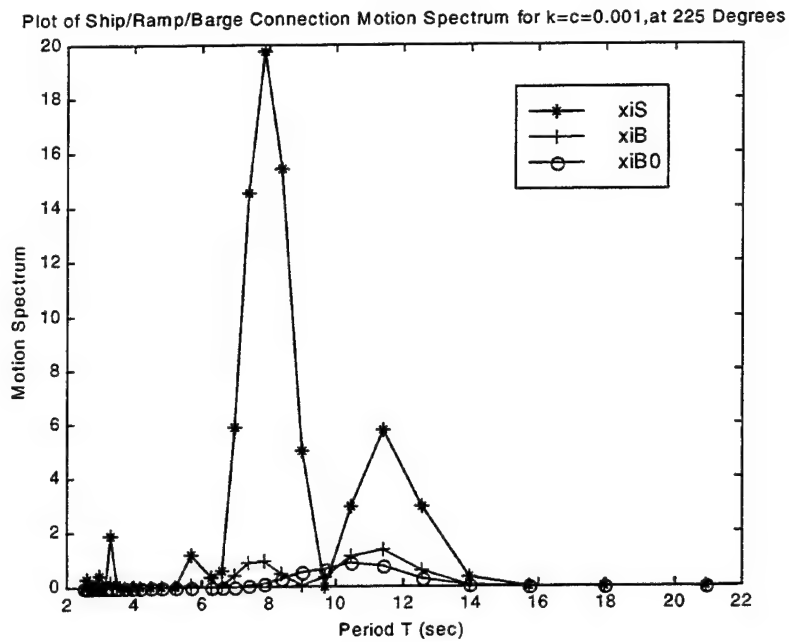
107

Figure 139. Plot of Vertical Motion Spectrum at the Ship/Ramp/Barge
Connections, for k=0.001 and c=0.001, at a Wave Angle of 135 Degrees.

Figure 140. Plot of Vertical Motion Spectrum at the Ship/Ramp/Barge
Connections, for k=0.1 and c=0.1, at a Wave Angle of 135 Degrees.

108

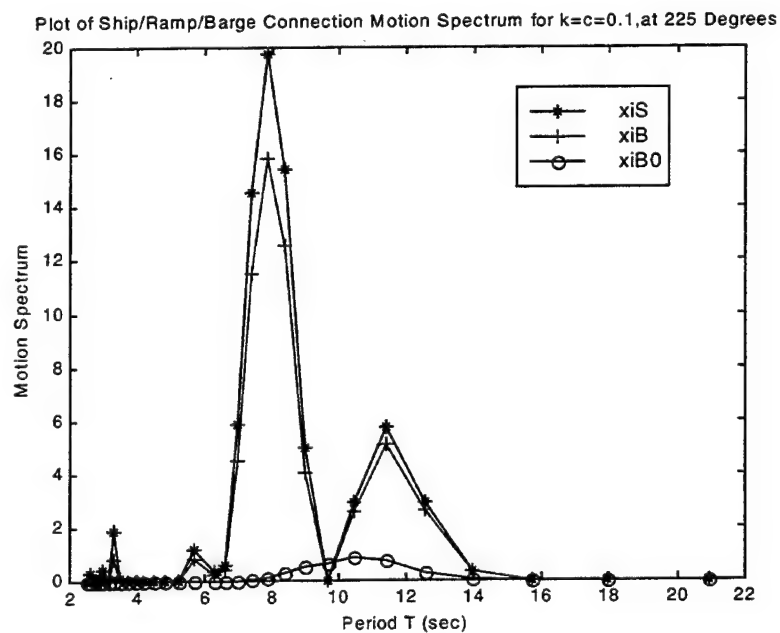Figure 141. Plot of Vertical Motion Spectrum at the Ship/Ramp/Barge
Connections, for k=0 and c=0.01, at a Wave Angle of 180 Degrees.

Figure 142. Plot of Vertical Motion Spectrum at the Ship/Ramp/Barge
Connections, for k=0.01 and c=0, at a Wave Angle of 180 Degrees.

109

Figure 143. Plot of Vertical Motion Spectrum at the Ship/Ramp/Barge Connections, for k=0.001 and c=0.001, at a Wave Angle of 180 Degrees.

Figure 144. Plot of Vertical Motion Spectrum at the Ship/Ramp/Barge Connections, for k=0.1 and c=0.1, at a Wave Angle of 180 Degrees.
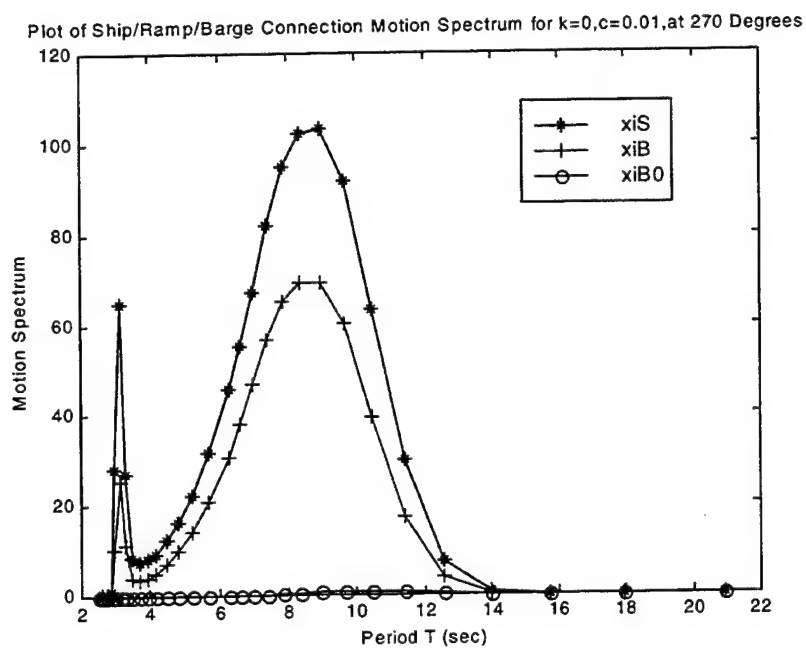
110

Plot of Ship/Ramp/Barge Connection Motion Spectrum for k=0,c=0.01,at 225 Degrees

Figure 145. Plot of Vertical Motion Spectrum at the Ship/Ramp/Barge Connections, for k=0 and c=0.01, at a Wave Angle of 225 Degrees.

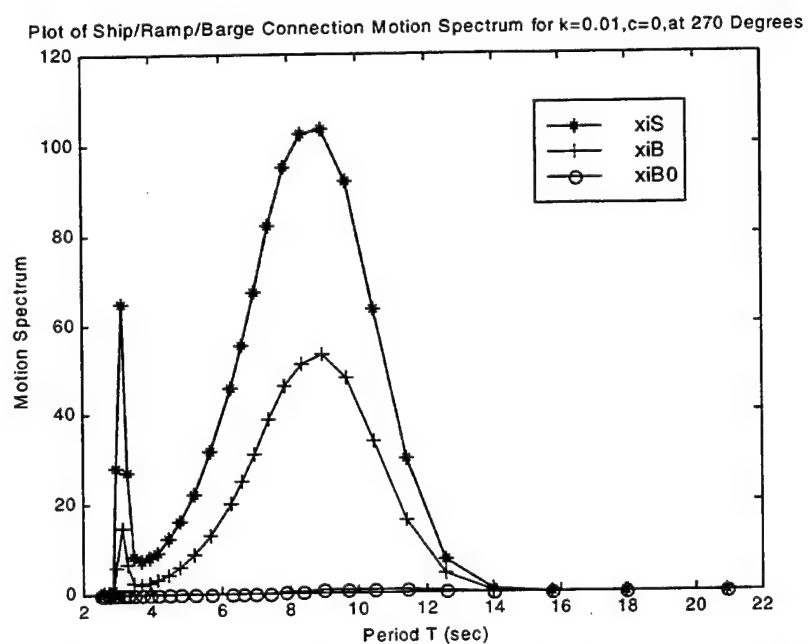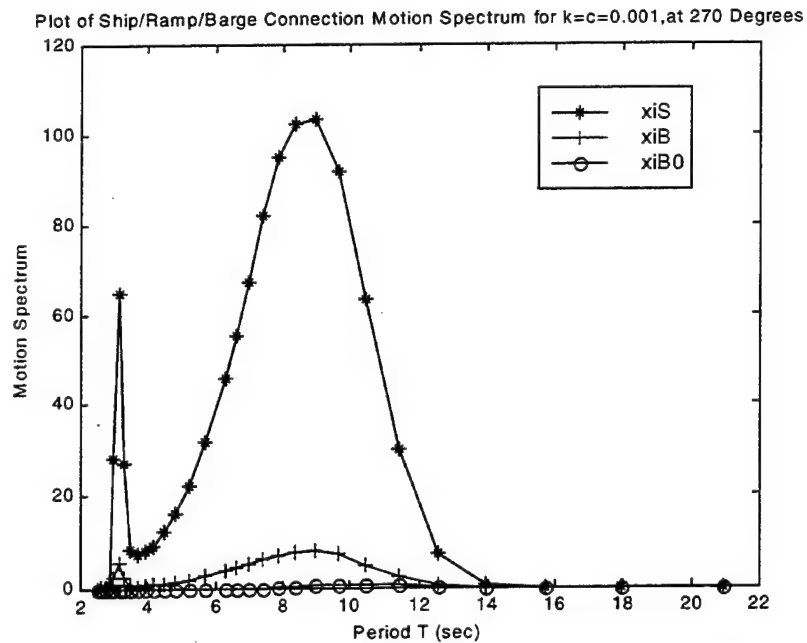Plot of Ship/Ramp/Barge Connection Motion Spectrum for k=0.01,c=0,at 225 Degrees

Figure 146. Plot of Vertical Motion Spectrum at the Ship/Ramp/Barge Connections, for k=0.01 and c=0, at a Wave Angle of 225 Degrees.

111

Figure 147. Plot of Vertical Motion Spectrum at the Ship/Ramp/Barge Connections, for k=0.001 and c=0.001, at a Wave Angle of 225 Degrees.
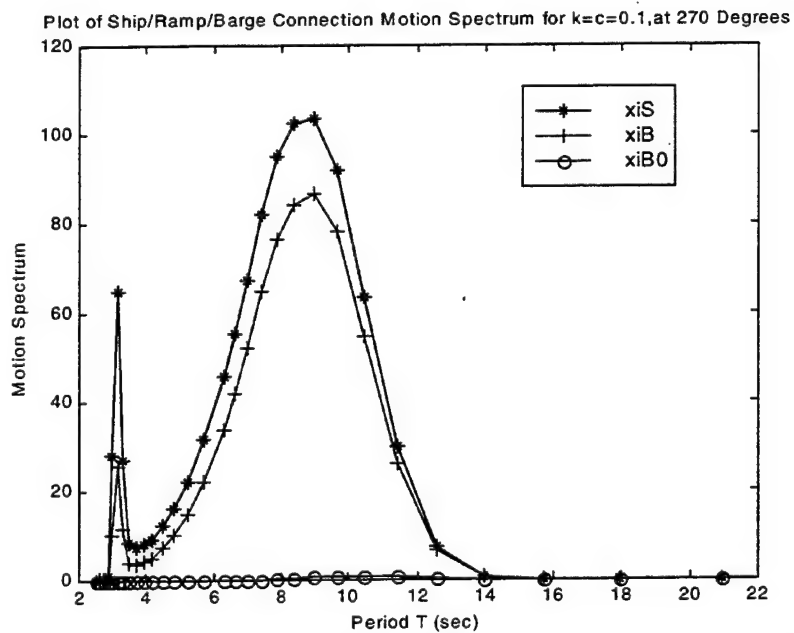

Figure 148. Plot of Vertical Motion Spectrum at the Ship/Ramp/Barge Connections, for k=0.1 and c=0.1, at a Wave Angle of 225 Degrees.

112

Figure 149. Plot of Vertical Motion Spectrum at the Ship/Ramp/Barge Connections, for k=0 and c=0.01, at a Wave Angle of 270 Degrees.

Figure 150. Plot of Vertical Motion Spectrum at the Ship/Ramp/Barge Connections, for k=0.01 and c=0, at a Wave Angle of 270 Degrees.
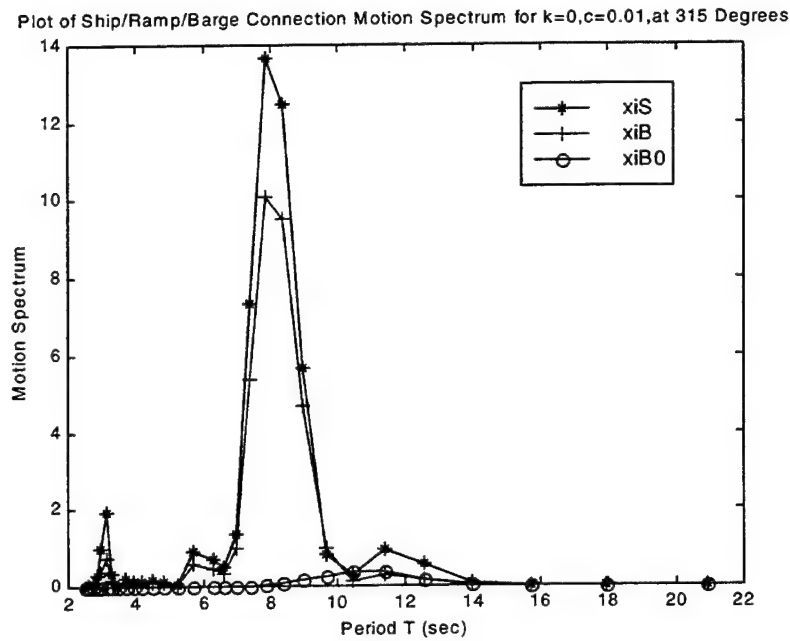
113

Figure 151. Plot of Vertical Motion Spectrum at the Ship/Ramp/Barge Connections, for k=0.001 and c=0.001, at a Wave Angle of 270 Degrees.

Figure 152. Plot of Vertical Motion Spectrum at the Ship/Ramp/Barge Connections, for k=0.1 and c=0.1, at a Wave Angle of 270 Degrees.

114

Figure 153. Plot of Vertical Motion Spectrum at the Ship/Ramp/Barge
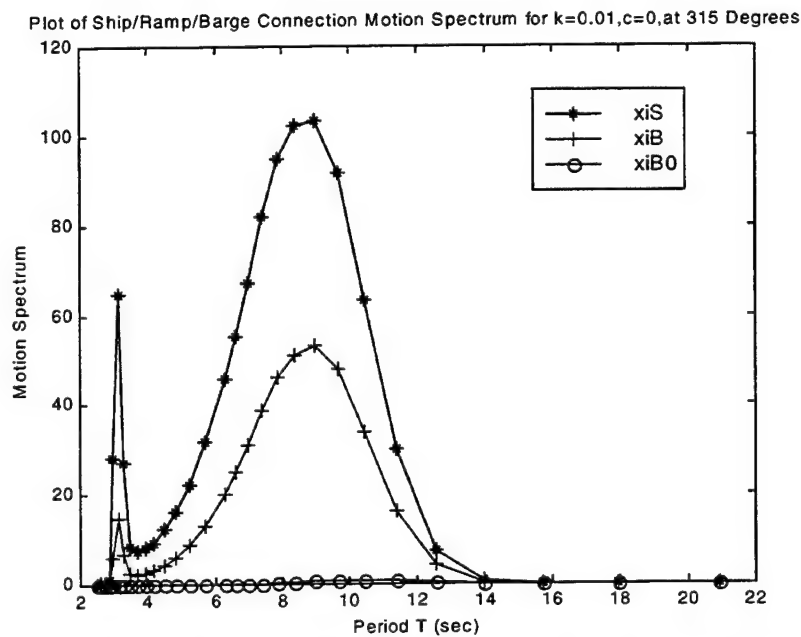Connections, for k=0 and c=0.01, at a Wave Angle of 315 Degrees.

Figure 154. Plot of Vertical Motion Spectrum at the Ship/Ramp/Barge
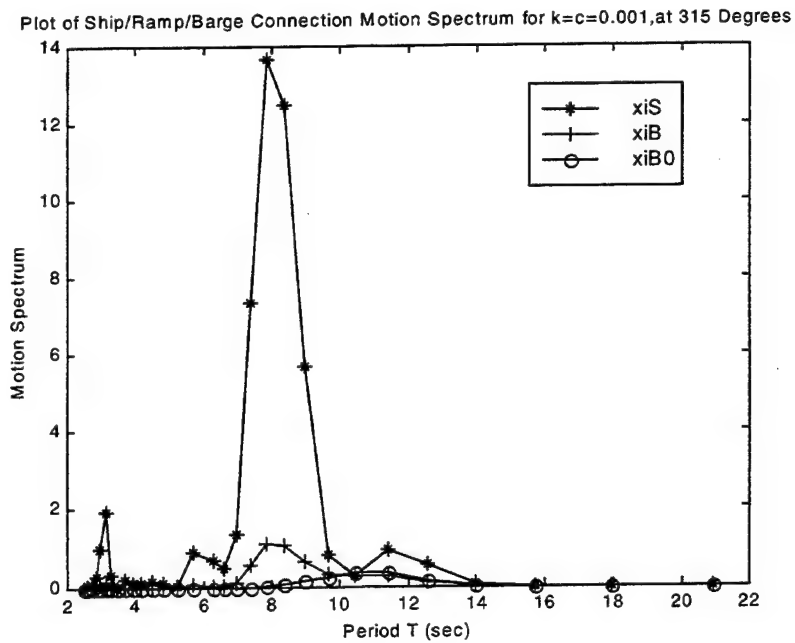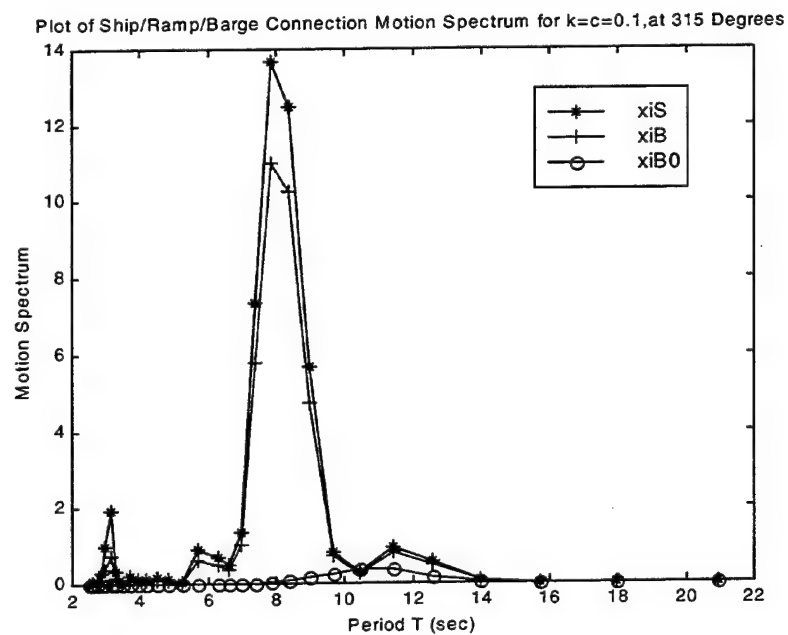Connections, for k=0.01 and c=0, at a Wave Angle of 315 Degrees.

115

Figure 155. Plot of Vertical Motion Spectrum at the Ship/Ramp/Barge Connections, for k=0.001 and c=0.001, at a Wave Angle of 315 Degrees.

Figure 156. Plot of Vertical Motion Spectrum at the Ship/Ramp/Barge Connections, for k=0.1 and c=0.1, at a Wave Angle of 315 Degrees.
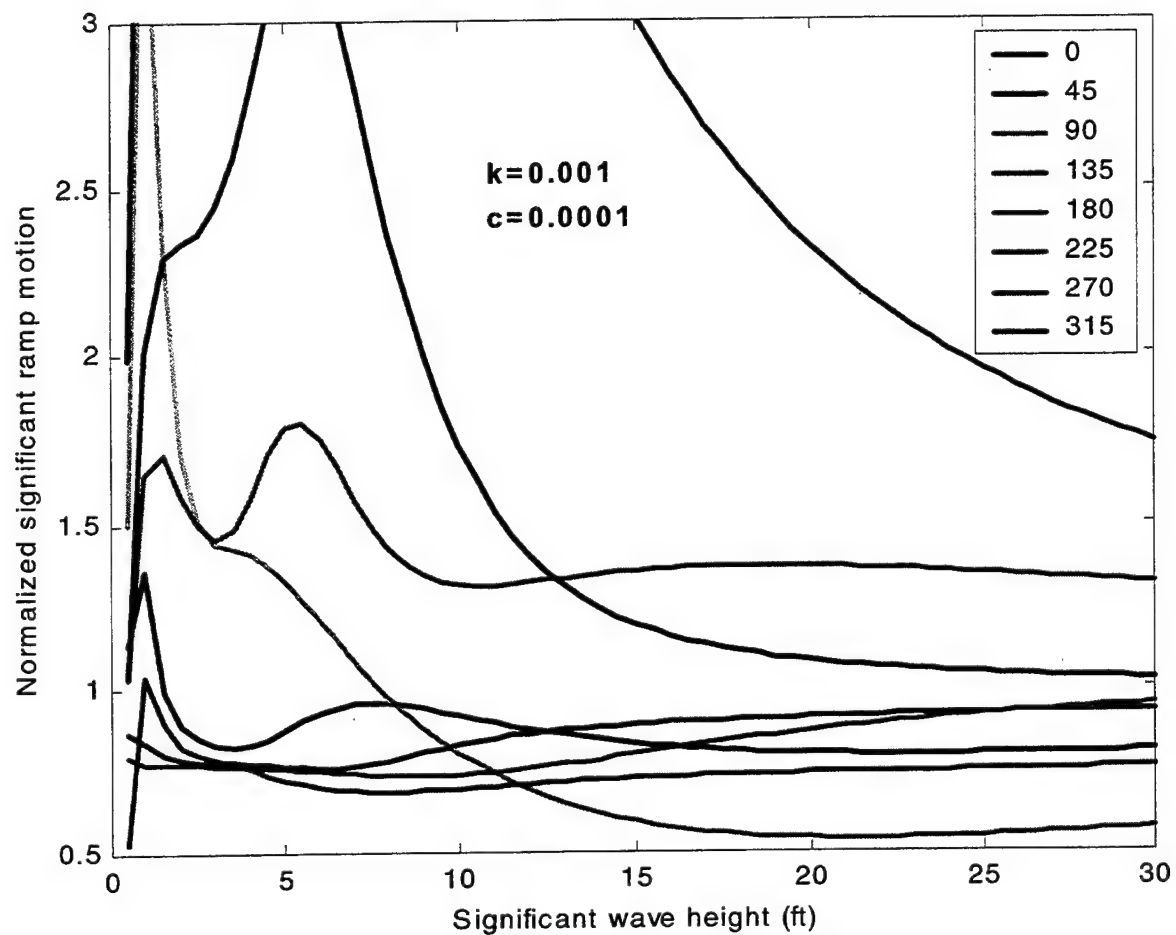
116

Figure 157. Plot of Normalized Significant Ramp Motion versus Significant Wave Height for a variety of Incident Wave Angles ranging from 0 to 315 Degrees.
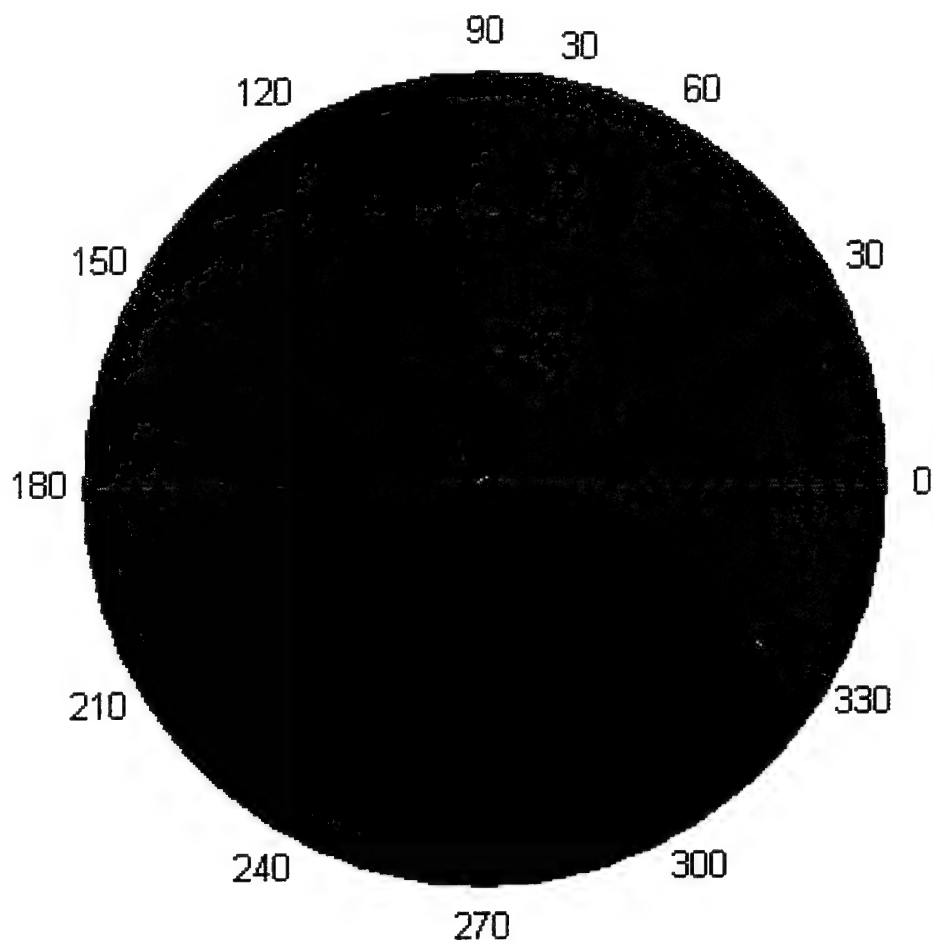
117

Figure 158. Operability Diagram employing standard seakeeping polar plots for
k=0.001, c=0.0001.
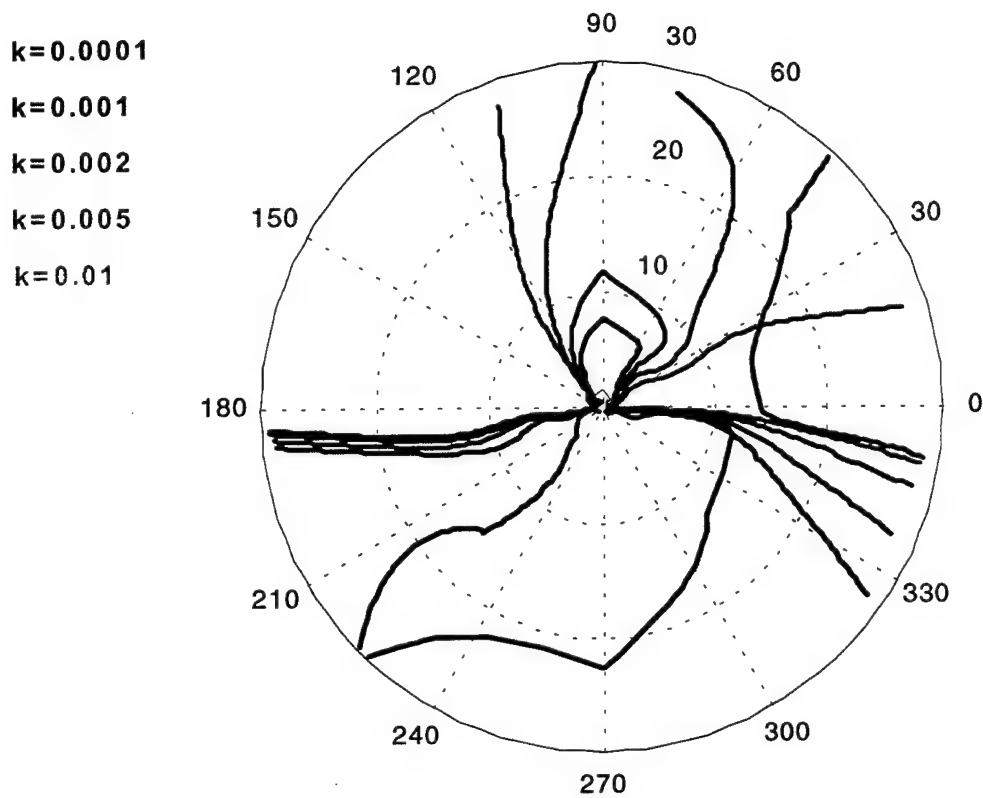
Figure 159. Operability Diagram employing standard seakeeping polar plots for
different isolator spring constants k, and a constant value of damping c.

THIS PAGE INTENTIONALLY LEFT BLANK

V. CONCLUSIONS AND RECOMMENDATIONS

The main conclusions from this work are summarized below:

1. Barge motions are virtually unaffected by the presence of the ship influence coefficients described in Chapter II. In particular, once the RRDF hydrodynamic coefficients have been established, the influence of the ship on the barge can be neglected and therefore one can treat the equations for the RRDF as "uncoupled" from the ship. This is true of course only in a schematic way since the influence of the ship is already reflected into the RRDF added mass and damping terms.

2. The influence of the isolator properties on the ramp motions and stress levels is not monotonic throughout the wave frequency range. This suggests that optimization of the isolator properties is, in principle, feasible for certain conditions.

3. Most cases where motion magnification occurs are for the RRDF sheltered side, which is less severe during operations. Active control should be employed where passive isolation is not feasible

4. Isolator properties can be selected to maximize the operability window for a given range of seas using standard probabilities of occurrence.

Based upon the data and conclusions, the following recommendations are made:

1. Develop an extended state space model for active control studies.

2. Use a realistic ramp model, perform parametric studies and validate experimentally the results.

THIS PAGE INTENTIONALLY LEFT BLANK

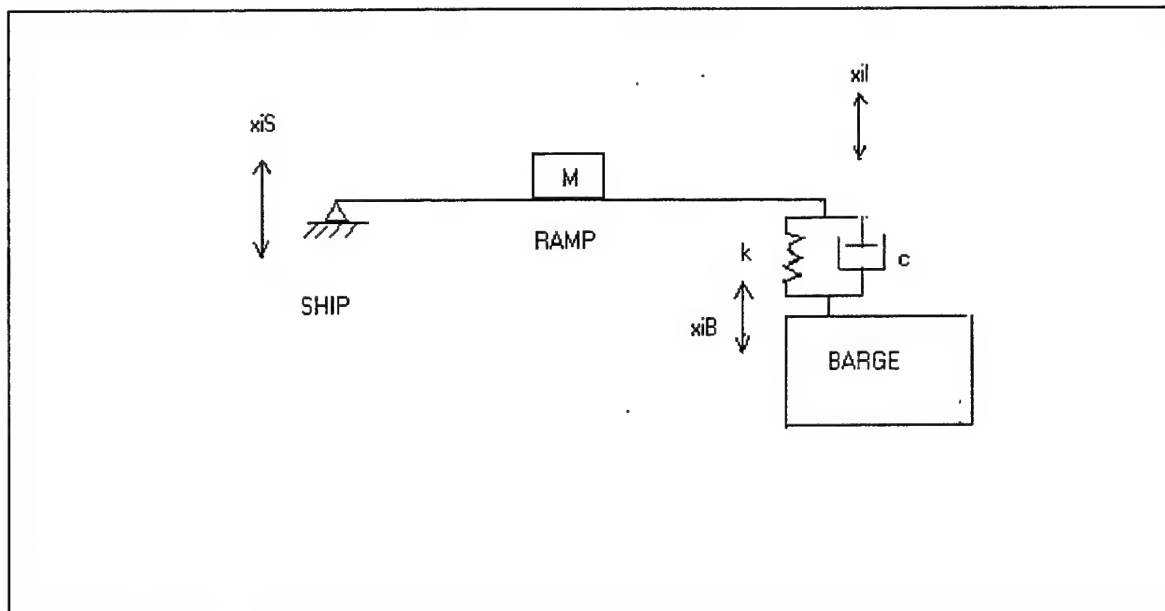# APPENDIX A

FIGURE OF SHIP/RAMP/BARGE CONNECTION:

Figure A. Basic Drawing of Ship/Ramp/Barge Connection Arrangement.

THIS PAGE INTENTIONALLY LEFT BLANK

LIST OF REFERENCES

1. Edward V. Lewis, Editor, *Principles of Naval Architecture, Volume III, Motions in Waves and Controllability,* The Society of Naval Architects and Marine Engineers, 1989, pp. 1-125.

2. Robert B. Zubaly, *Applied Naval Architecture, Ship Dynamics,* Cornell Maritime Press, Inc., 1996, pp. 299-329.

3. Yang, G., Spencer, B.F. Jr., *Reduced Ramp Stress Levels Using "Smart" Damping,* Department of Civil Engineering and Geological Sciences, University of Notre Dame, IN, 1999, pp. 1-28.

4. John J. McMullen Associates, Inc., *Stern Ramp Study Final Report,* Naval Sea Systems Command, Department of the Navy, Arlington, VA, 1997, pp. 1-48.

5. Barry R. Scott, *A Methodology for Design of Passive Isolation for Ship/Barge Connection,* Master Thesis, Naval Postgraduate School, 1999.

6. William T. Thomson and Marie Dillon Dahleh, *Theory of Vibration with Applications,* University of California at Santa Barbara, Fifth Edition, 1998, pp. 24-25.

THIS PAGE INTENTIONALLY LEFT BLANK

INITIAL DISTRIBUTION LIST